

Dissecting the Neuronal Basis of Threat Responding in Mice

Dissertation der Fakultät für Biologie
der Ludwig-Maximilians-Universität München



vorgelegt von

Julia Ruat

Eingereicht im November 2021

München

Erster Gutachter:	PD Dr. Carsten T. Wotjak
Zweite Gutachterin:	Prof. Dr. Laura Busse
Tag der Abgabe:	4. November 2021
Tag der mündlichen Prüfung:	7. April 2022

Eidesstattliche Erklärung

Ich versichere hiermit an Eides statt, dass die vorgelegte Dissertation von mir selbständig und ohne unerlaubte Hilfe angefertigt ist.

München, den 23.05.2022

.....
Julia Ruat

Erklärung

Hiermit erkläre ich, *

- dass die Dissertation nicht ganz oder in wesentlichen Teilen einer anderen Prüfungskommission vorgelegt worden ist.
- dass ich mich anderweitig einer Doktorprüfung ohne Erfolg **nicht** unterzogen habe.
- ~~dass ich mich mit Erfolg der Doktorprüfung im Hauptfach.....
und in den Nebenfächern.....
bei der Fakultät für der
(Hochschule/Universität)
unterzogen habe.~~
- ~~dass ich ohne Erfolg versucht habe, eine Dissertation einzureichen oder mich der Doktorprüfung zu unterziehen.~~

München, den 23.05.2022

.....
Julia Ruat

*) Nichtzutreffendes streichen

Table of Contents

Table of Contents	i
List of Publications.....	ii
Abbreviations	iii
Abstract	1
Zusammenfassung.....	3
1. Introduction	5
1.1. Disorders of Fear, Anxiety and Panic	5
1.2. The Predator Imminence Continuum	6
1.3. Defensive Behaviors in Rodents.....	8
1.4. Neuronal Circuits of Defensive Responses.....	13
1.5. Potential Regulatory Systems	16
1.6. Aims of the Thesis	22
2. Results.....	23
2.1. CB1 Receptors in Corticotropin-Releasing Factor Neurons Selectively Control the Acoustic Startle Response in Male Mice.....	23
2.2. Structural Correlates of Trauma-Induced Hyperarousal in Mice	35
2.3. Why Do Mice Squeak?	46
3. Discussion	82
Declaration of Contribution as a Co-Author	90
Bibliography.....	92
Acknowledgements	106
Curriculum Vitae	107

List of Publications

Ruat J, Hartmann A, Heinz DE, Nemcova P, Stoffel R, Deussing JM, Chen A, Wotjak CT (2021) CB1 receptors in corticotropin-releasing factor neurons selectively control the acoustic startle response in male mice. *Genes Brain Behav.* 2021;e12775

Ruat, J, Heinz DE, Binder FP, Stark T, Neuner R, Hartmann A, Kaplick PM, Chen A, Czisch M, Wotjak CT (2021) Structural correlates of trauma-induced hyperarousal in mice. *Prog Neuro-Psychopharmacology Biol Psychiatry.* 111, 110404.

Ruat J, Genewsky AJ, Heinz DE, Kaltwasser SF, Canteras NS, Czisch M, Chen A, Wotjak CT. Why do mice squeak? [Manuscript under revision]

Abbreviations

2-AG	2-Arachidonoylglycerol
ACTH	Adrenocorticotrophic hormone
AEA	Anandamide
ANOVA	Analysis of variance
ANS	Autonomic nervous system
ASR	Acoustic Startle Response
BL	Baseline
BLA	Basolateral amygdala
BMT	Beetle Mania Task
BNST	Bed nucleus of the stria terminalis
Ca²⁺	Calcium ions
CB1	Cannabinoid type 1 receptor
CB2	Cannabinoid type 2 receptor
CCK	Cholecystokinin
CeA	Central amygdala
CNO	Clozapine N-oxide
CORT	Corticosterone
CRF	Corticotropin-releasing factor
CRFR1	Corticotropin-releasing factor receptor 1
CRFR2	Corticotropin-releasing factor receptor 2
CSF	Cerebrospinal fluid
DAGLα	Diacylglycerol lipase- α
DBM	Deformation-based morphometry
DIG	Digoxigenin
dIPAG	Dorsolateral periaqueductal grey
dmPAG	Dorsomedial periaqueductal grey
dPAG	Dorsal periaqueductal grey
DREADDs	Designer Receptors Exclusively Activated by Designer Drugs
DSE	Depolarization-induced suppression of excitation
DSI	Depolarization-induced suppression of inhibition

Abbreviations

DSM-5	Diagnostic and Statistic Manual of Mental Disorders 5 th Edition
eCB	Endocannabinoid
EPM	Elevated plus maze
FAAH	Fatty acid amide hydrolase
FG	Fluoro-Gold
FID	Flight initiation distance
GABA	γ -aminobutyric acid
GAD	Generalized Anxiety Disorder
GCs	Glucocorticoids
GM	Grey matter
GPCR	G protein-coupled receptor
GR	Glucocorticoid receptor
HAB	High anxiety-related behavior
HPA axis	Hypothalamic-pituitary-adrenal axis
ICD-10	International Classification of Disease 10th Edition
K⁺	Potassium ions
LDB	Light dark box
LD	Looming disk
IPAG	Lateral periaqueductal grey
MAGL	Monoacylglycerol lipase
MEMRI	Manganese-enhanced magnetic resonance imaging
mPFC	Medial prefrontal cortex
MR	Mineralocorticoid receptor
MRI	Magnetic resonance imaging
NAB	Normal anxiety-related behavior
NAPE-PLD	N-acyl phosphatidyl ethanolamine-phospholipase D
OFT	Open field test
PAG	Periaqueductal grey
PB	Playback
PB+S	Playback+Stimulus
PnC	Pontine reticular nucleus
PTSD	Posttraumatic Stress Disorder

Abbreviations

PV	Parvalbumin
PVN	Paraventricular nucleus of the hypothalamus
SC	Superior colliculus
SAP	Stretch-attend posture
SD	Sweeping dot
SEM	Standard error of the mean
TMT	2,5-dihydro-2,4,5-trimethylthiazoline
TST	Tail suspension test
USV	Ultrasonic vocalization
vIPAG	Ventrolateral periaqueductal grey
VMH	Ventromedial nucleus of the hypothalamus
VTT	Visual Threat Task
WM	White matter
Δ9-THC	Δ 9-tetrahydrocannabinol

Abstract

Environmental threats demand adaptive defensive responses of an organism that ensure its survival. Extreme stressors, however, can unbalance stress homeostasis and lead to long-term changes that impair appropriate defensive behaviors and emotional responses. In my thesis, I assessed (1) the interaction of two stress-related neuromodulatory systems, (2) the effects of a traumatic incident on brain volume and hyperarousal, and (3) sonic vocalization as a defensive behavior in mice, and discussed the topics in three independent studies.

In the first study, I evaluated the interaction of two regulatory systems with respect to fear, anxiety, and trauma-related behaviors. Although the endocannabinoid and the corticotropin-releasing factor (CRF) systems are well described in modulating stress-related responses, the direct interaction of both systems remained poorly understood. The generation of a new conditional knockout mouse line that selectively lacked the expression of the cannabinoid type 1 (CB1) receptor in CRF-positive neurons presented no differences in various tests of fear and anxiety-related behaviors under basal conditions or after a traumatic event. Also stress hormone levels were unaffected. However, male knockout animals exhibited a significantly increased acoustic startle response thus suggesting a specific involvement of CB1-CRF interactions in controlling arousal.

In the second study, I assessed the consequences of a traumatic experience on behavior and grey matter volume in mice. Whole-brain deformation-based morphometry (DBM) by means of magnetic resonance imaging (MRI) after incubation of a traumatic incident showed changes in the dorsal hippocampus and the reticular nucleus. Using the severity of hyperarousal as regressor for cross-sectional volumetric differences between traumatized mice and controls revealed a negative correlation with the dorsal hippocampus. Further, longitudinal analysis including volumetric measurements before and after the traumatic incident showed that volume reductions in the globus pallidus reflect trauma-related changes in hyperarousal severity.

In the third study, I characterized sonic vocalization as a defensive behavior in mice. Mice bred for high anxiety-related behavior (HAB) were found to have a high disposition to emit audible squeaks when taken by the tail which was not the case for any of the other five mouse lines tested. The calls emitted had a fundamental frequency of 3.8 kHz and were shown to be sensitive to anxiolytic but not panicolytic compounds. Manganese-enhanced

MRI (MEMRI) scans pointed towards an increased tonic activity, among others, in the periaqueductal grey (PAG). Inhibition of the dorsal PAG by muscimol not only completely abolished sonic vocalization, but also reduced anxiety-like behavior. This suggests that sonic vocalization of mice is related to anxiety and controlled by the PAG. To explore the ecological relevance of defensive vocalization, I performed playback experiments with conspecifics and putative predators. Squeaks turned out to be aversive to HAB mice but became appetitive to both mice and rats when a stimulus mouse was present during playback.

Collectively, the results of this thesis provide novel insights into fear and anxiety-related behaviors and shine light onto their mechanistic basis and ecological relevance.

Zusammenfassung

Gefahren aus der Umwelt erfordern von einem Organismus angepasste defensive Reaktionen, die dessen Überleben sicherstellen. Extreme Stressfaktoren können die Stresshomöostase aus dem Gleichgewicht bringen und zu Langzeitveränderungen führen, die adaptives defensives Verhalten und emotionale Reaktionen beeinträchtigen. In meiner Dissertation habe ich (1) die Interaktion von zwei stressabhängigen neuromodulatorischen Systemen, (2) die Auswirkungen eines traumatischen Ereignisses auf das Hirnvolumen und das individuelle Erregungsniveau und (3) hörbare Vokalisierung als ein defensives Verhalten bei Mäusen untersucht und in drei unabhängigen Studien diskutiert.

In der ersten Studie habe ich die Interaktion zweier regulatorischer Systeme in Bezug auf Furcht, Angst und traumabedingte Verhaltensänderungen untersucht. Obwohl das Endocannabinoid- und das Corticotropin-releasing factor (CRF)-System weitreichend in Bezug auf die Modulation von Stressantworten beschrieben sind, ist über die direkte Interaktion der beiden Systeme wenig bekannt. Die Züchtung einer neuen konditionalen Knockout-Mauslinie, bei der die Expression des Cannabinoid-Rezeptors Typ 1 (CB1) spezifisch auf CRF-positiven Neuronen fehlte, zeigte keine Unterschiede in verschiedenen Tests für Angst- und Furchtverhalten, weder unter basalen Bedingungen noch nach einem traumatischen Ereignis. Auch die Stresshormonkonzentrationen blieben vom Knockout unbeeinflusst. Männliche Knockout-Mäuse zeigten jedoch eine signifikant erhöhte Schreckreaktion, was auf eine Mitwirkung der CB1-CRF-Interaktion bei der Kontrolle der Erregung hindeutet.

In einer zweiten Studie habe ich die Konsequenzen einer traumatischen Erfahrung auf das Erregungsverhalten und das Volumen der grauen Substanz von Mäusen untersucht. Deformation-Based Morphometry (DBM) mithilfe von Magnetresonanztomografie (MRT) nach der Inkubation eines traumatischen Ereignisses zeigte Veränderungen im dorsalen Hippocampus und dem Nucleus reticularis auf. Durch die Anwendung des individuellen Erregungsniveaus als Regressor konnte eine negative Korrelation zwischen Erregungsniveau und dem Volumen des dorsalen Hippocampus im Vergleich von traumatisierten Mäusen und Kontrollen gefunden werden. Des Weiteren zeigte eine longitudinale Analyse mit Volumenmessungen vor und nach dem traumatischen Ereignis, dass eine Volumenabnahme im Globus Pallidus mit traumabedingten Veränderungen in der Schwere der Übererregbarkeit koinzidiert.

In der dritten Studie habe ich die hörbare Vokalisierung als defensives Verhalten von Mäusen charakterisiert. Eine Mauslinie, die auf erhöhtes Angstverhalten gezüchtet wurde (HAB-Mäuse), zeigt eine hohe Tendenz, hörbare Quiek-Laute auszustoßen, wenn sie an der Schwanzwurzel hochgehoben wurde. Dies konnte bei fünf weiteren getesteten Mauslinien nicht beobachtet werden. Die Laute hatten eine Grundfrequenz von 3,8 kHz und konnten durch anxiolytische, nicht jedoch panikolytische Substanzen verringert werden. Mangan-verstärkte MRT-Aufnahmen deuteten auf eine erhöhte tonische Aktivität unter anderem im periaquäduktalen Höhlengrau (PAG) hin. Die Inhibition des PAG durch Muscimol hat nicht nur die hörbare Vokalisierung komplett ausgeschaltet, sondern auch das Angstverhalten reduziert. Um die ökologische Relevanz der defensiven Vokalisierung zu untersuchen, habe ich abschließend Playback-Experimente mit Artgenossen und potenziellen Fressfeinden durchgeführt. Die Quiek-Laute stellten sich als aversiv für HAB-Mäuse heraus, wurden jedoch appetitiv sowohl für Mäuse als auch Ratten, wenn sich während der Playbacks eine Stimulusmaus in der Arena befand.

Zusammengefasst liefern die Ergebnisse dieser Dissertation neue Erkenntnisse bezüglich Angst- und Furchtverhalten und geben Einblicke in deren mechanistischen Grundlagen und ökologische Relevanz.

1. INTRODUCTION

According to our understanding of natural selection, the species adapting best to changes in its environment will survive. Breaking this down to the level of individual organisms, only those individuals that survive will pass on their genes. Survival requires basic needs like access to food, water, and shelter, but also avoidance of predatory and other harmful threats. Adaptive responses to those threats are supported by the individual's emotions, especially fear.

In our everyday language, the terms fear and anxiety are used interchangeably while they actually describe different conditions. The exact definitions and distinctions are discussed since decades and up to today (for review see McNaughton and Corr, 2004; Perusini and Fanselow, 2015; Mobbs et al., 2019). Fear is elicited by an imminent threat and triggers behaviors that aim at its avoidance. These behaviors are sensitive to panicolytic drugs but insensitive to anxiolytics (Blanchard et al., 1993). Anxiety is a state defined by a potential or anticipated but absent threat and reactions like heightened vigilance aim at gathering information of potential dangers and enabling rapid responses to avoid potential hazards (McNaughton and Corr, 2004). A third category describes panic. This state is characterized by strong uncontrollable fear reactions that might occur in life-threatening situations.

1.1. Disorders of Fear, Anxiety and Panic

Anxiety, fear, and panic behaviors are essential and important for survival allowing the organism to adequately respond to threats. However, if these states persist beyond a time when threats are no longer present, they become maladaptive and possibly even pathological. The Diagnostic and Statistic Manual of Mental Disorders 5th Edition (DSM-5, American Psychiatric Association, 2013) and the International Classification of Disease 10th Edition (ICD-10, World Health Organization, 1992) define these dysfunctions under the umbrella of Anxiety Disorders. With a 12-month prevalence of 14 % in the year 2010, anxiety disorders are the most frequent mental illness within the European Union (Wittchen et al., 2011). Anxiety disorders include, among others, Specific Phobias, Panic Disorders, Agoraphobia, and Generalized Anxiety Disorder (GAD) that tend to be highly comorbid with each other and with other psychiatric disorders like depression and bipolar disorder (Merikangas and Swanson, 2010). The disorders are often accompanied by disproportionate avoidance of potentially aversive places or situations that disable

patients in their daily life. Individuals with GAD experience excessive and persistent anxiety and worry and have difficulties controlling these thoughts. In Panic Disorder, affected individuals undergo recurrent panic attacks that are followed by concerns and fear of potential future unexpected panic attacks. A panic attack itself involves sudden feelings of intense fear that may even peak in fear of dying. They are accompanied by physiological symptoms like accelerated heart rate and sweating (Nashold et al., 1969; Goetz et al., 1996; American Psychiatric Association, 2013).

Alike most psychiatric disorders, genetic predisposition and heredity play a role in anxiety disorders as association studies and twin and family studies suggested (Hettema et al., 2001; Otowa et al., 2016; Purves et al., 2020, for review see Sharma et al., 2016; Meier and Deckert, 2019). However, complex diseases are considered to be caused by a combination of inherited susceptibility and exposure to environmental factors (for review see Hunter, 2005).

The development of Posttraumatic Stress Disorder (PTSD) is triggered by such an exposure to an environmental stressor. In the DSM-5, PTSD is no longer categorized as part of anxiety disorders (American Psychiatric Association, 1994) but belongs to the class of newly included Trauma- and Stressor-Related Disorders (American Psychiatric Association, 2013). Traumatic events leading to the manifestation of PTSD may include combat exposure, threatened or physical abuse, violence, or experience of natural disasters. Individuals suffering from PTSD often experience recurrent memories in the form of dreams or flashbacks of the traumatic incident which is accompanied by avoidance behavior (e.g., of certain places or situations) to prevent the re-experience of those memories. Further, negative alterations in mood and cognition and changes in arousal come into play. Hyperarousal is a prominent symptom that can be observed in terms of exaggerated startle responses and hypervigilance (American Psychiatric Association, 2013). The lifetime prevalence of PTSD across 24 countries has been estimated at 5.6 % (Koenen et al., 2017).

1.2. The Predator Imminence Continuum

Fear, anxiety, and panic have further been defined on basis of the predator imminence continuum, a model shaped over decades by Gray, Fanselow, McNaughton, Caroline and Robert J. Blanchard and others (Fanselow and Lester, 1988; Blanchard and Blanchard, 1990; Gray and McNaughton, 1996; McNaughton and Corr, 2004). In this theory, the

defensive distance, i.e., the perceived proximity to a threat, determines the defensive reaction of an animal (Fanselow and Lester, 1988). It encompasses three stages: Pre-encounter, post-encounter, and circa-strike (Figure 1; for reviews see Perusini and Fanselow, 2015; Mobbs et al., 2020). In the pre-encounter phase, a risk of danger but no actual threat is present. An animal leaving a safe place to forage or search for mating partners would be an example for that stage. It is associated with heightened cautiousness and arousal and might be ascribed to anxiety-related behaviors. Post-encounter describes the stage once the threat is detected, e.g., the prey detects the predator. Here, fear responses come into play that aim at decreasing detection and reducing the chance of an encounter. Once the predator has detected its prey, the circa-strike phase starts and induces another switch in behavior in the prey animal. Species-specific defensive behaviors could include fight, flight, and aggression to ensure survival and could be ascribed to panic-related behaviors.

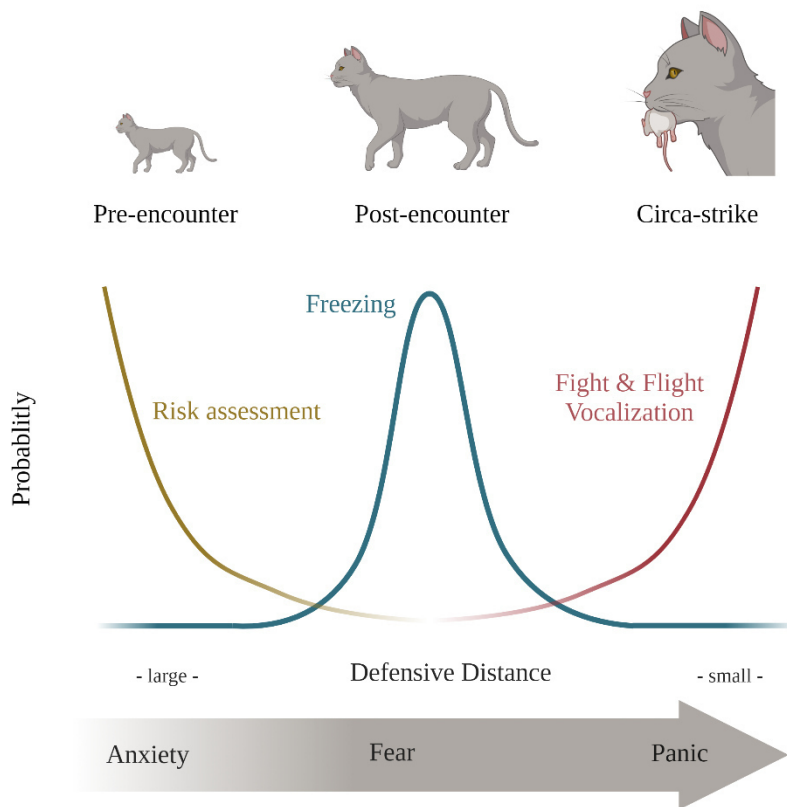


Figure 1: The Predator Imminence Continuum

Defensive behaviors switch with the change in defensive distance. Pre-encounter is defined by cautiousness and heightened vigilance. Distant threats might induce freezing behaviors which undergo an explosive switch to more active coping behaviors in case of a predatory attack. Figure created with BioRender.com.

1.3. Defensive Behaviors in Rodents

Along the stages of the predator imminence continuum, rodents display different sets of behavioral responses depending on the emotional state and the defensive distance of the threat.

Arousal

While arousal does not officially fall into the category of defensive behaviors, it is a state important to facilitate defensive reactions. It can be described as wakefulness and being highly reactive to stimuli. Arousal increases attention and alert and is priming an individual for threatening stimuli and survival. It is highly adaptive in pre-encounter stages. This is orchestrated by several physiological systems and results in increased heart rate, blood pressure and muscle tension. Arousal is classically examined via the startle response, both in humans and rodents. The startle response is a reflexive innate reaction to sudden intense stimuli like noises or air puffs and has a protective function. Responses in humans involve fast contraction of muscles in order to close the eyes, move up the shoulders, or lower the head which reduces the risk of potential damage by an attack from behind or facilitates flight (Yeomans and Frankland, 1995). The acoustic startle response (ASR) is classically used to study startle behavior and is triggered in response to a loud (>80 dB) acoustic stimulus (Pilz et al., 1987). The latency and magnitude of the reaction are measured. These measures are largely influenced by external and internal factors, e.g., the stimulus intensity, the environment, and the emotional state of the animal (Pilz et al., 1988; Vrana et al., 1988; Lang et al., 1990; Walker and Davis, 1997). Presentation of an acoustic stimulus shortly before the startle pulse leads to a decreased startle amplitude. This phenomenon is called pre-pulse inhibition (Hoffman and Ison, 1980). Also, repeated presentation of the stimulus leads to a decrease in the response and habituation (Rimpel et al., 1982). Conversely, the startle magnitude is increased if the organism is in an aversive state (e.g., in an anxiety state, Brown et al., 1951). An important neuronal hub for mediating the ASR is the caudal pontine reticular nucleus (PnC). It receives direct inputs from nuclei of the auditory pathway e.g., the cochlear root nucleus. The neurons of the PnC in turn project directly onto spinal, cranial and facial motor neurons (Davis et al., 1982). This short pathway allows for very short ASR latencies of about 10 ms (Cassella et al., 1986). Further, the PnC receives inputs from the basolateral amygdala (BLA), the PAG and the ventral tegmental nucleus, brain areas involved in the fear potentiation and sensitization of the ASR (Hitchcock and Davis, 1991; Davis et al., 1993; Fendt et al., 1994, for review see Koch, 1999).

Freezing and Escape

Once a threat has been detected, the organism needs to switch from an alert state to a set of behaviors that attempt avoidance of the threat. Two behaviors highly conserved across mammals come into play: freezing and escape. Freezing describes the absence of any movement except respiratory motions (Curti, 1935; Grossen and Kelley, 1972). In his 1872 book entitled “The Expression of the Emotions in Man and Animals”, Darwin notes the following concerning fear responses in humans: “The frightened man at first stands like a statue, motionless and breathless, or crouches down as if instinctively to escape observation.” (Darwin, 1872). The reduction in motion reduces visibility which is particularly effective for slow rodents. However, if the distance to the threat drops below a certain boundary, i.e., the defensive distance is small, escape or flight behavior is more adaptive. It aims at increasing the distance between animal and threat to ultimately avoid an encounter and enhancing the chance to escape. This is also illustrated in the Flight Initiation Distance (FID), a model that takes the economic costs of a flight reaction into account (Ydenberg and Dill, 1986). It is the distance at which the costs for remaining, e.g., at a rich food source, exceeds the cost for escaping. The behavioral switch from freezing to fleeing has been demonstrated in mice using a visual representation of a cruising and an approaching aerial predator. While a small sweeping dot on a screen above the mouse arena induced freezing, a rapidly expanding looming stimulus triggered a flight response to the shelter (De Franceschi et al., 2016). Looming stimuli have been found to be innately threatening and trigger escape behaviors across phyla, in insects, fish, birds, and mammals including humans (Schiff et al., 1962; King et al., 1992; Wu et al., 2005; Hammond and O’Shea, 2007; Yilmaz and Meister, 2013; Temizer et al., 2015; Vale et al., 2017).

Vocalization

If the above-described defensive behaviors were unsuccessful in preventing contact with the threat, circa-strike behaviors come into play. With this explosive switch in response, the prey intends to discourage the predator from further attacks. Circa-strike behaviors may include fighting, jumping, biting, and vocalizations (Blanchard et al., 1980, 1998; Fanselow and Lester, 1988).

“As fear rises to an extreme pitch, a dreadful scream of terror is heard”, Darwin observed in frightened humans (Darwin, 1872). Screams are short and intense vocal calls that are

innately emitted by a wide range of species in different contexts (Lingle et al., 2012; Frühholz et al., 2021). They seem to be quickly recognized and trigger a fast response in the receiver, such as predator-related alarm screams of monkeys or marmosets (Zuberbühler, 2000; Blumstein et al., 2008). This has been attributed to the roughness and non-linear structure of these calls (Fitch et al., 2002; Blumstein and Récapet, 2009; Arnal et al., 2015; Schwartz et al., 2020).

While mice and rats also emit scream-like calls in circa-strike situations like capture or when in pain, they mostly communicate in the ultrasonic range (for reviews see Musolf and Penn, 2012; Wöhr and Schwarting, 2013; Portfors and Perkel, 2014). Ultrasound is defined as sound wave frequencies above the human hearing limit which is at about 20 kHz. Since this frequency range is also inaudible to certain predators (e.g., birds of prey or reptiles), and ultrasonic signals are more easily attenuated and deflected by environmental objects than audible sounds, ultrasonic communication might be advantageous to rodents to evade predator detection and localization (Brudzynski, 2009; Brudzynski and Fletcher, 2010). Mouse and rat ultrasonic vocalization (USV) have been studied since decades striving to decode its meaning, function, structure, and its role in different emotional states and contexts. Mice and rats emit ultrasonic calls early on during their development. Zippelius and Schleidt showed that USVs indeed serve a communicative function. Pups that are isolated from the nest emit USVs. In response to such vocalizations which they termed “Pfeiffen des Verlassenseins” (“whistles of loneliness”) the mother leaves the nest to retrieve the pup (Zippelius and Schleidt, 1956; Sewell, 1970). Discussions emerged on whether these vocalizations reflect a negative affective state of the animal or whether they appear as a byproduct of impaired thermoregulation during isolation (Blumberg and Sokoloff, 2001). In support of a role in emotions and affect are studies showing a reduction in isolation-induced USV following treatment with anxiolytics (Fish et al., 2000; Krömer et al., 2005; Takahashi et al., 2009). Adult mice emit USVs of 30-110 kHz mostly in response to a social interaction partner. During courtship, male mice produce song-like USV in the presence of a female, and female urine alone is sufficient to trigger such calls (Whitney et al., 1974; Nyby et al., 1976; Nyby, 1983). This type of vocalization was found to have temporal and structural features and complexity similar to bird songs (Holy and Guo, 2005) and it does trigger approach behavior of female mice (Pomerantz et al., 1983; Hammerschmidt et al., 2009). While USV during adult male-male interaction is rare, females emit USVs during an encounter with another female or with males (Maggio and Whitney, 1985; Moles et al., 2007; Neunuebel et al., 2015; Heckman et al., 2017; Warren et al., 2020).

While more and more studies try to classify mouse ultrasonic calls into different subtypes (Holy and Guo, 2005; Panksepp et al., 2007; Scattoni et al., 2008; Lahvis et al., 2011) using novel machine learning tools (Van Segbroeck et al., 2017; Coffey et al., 2019; Vogel et al., 2019; Sangiamo et al., 2020), the picture appears to be simpler in rats. Besides isolation-induced pup USVs emitted at around 40 kHz (Allin and Banks, 1972; Hofer and Shair, 1978), adult rats produce USVs classified as low and high frequency USVs. Low frequency or 22-kHz USVs are long calls (300-4000 ms) at a frequency range of 18-32 kHz (Miczek and Van Der Poel, 1991; Brudzynski, 2001) that are emitted in aversive situations like predator exposure (Blanchard et al., 1991), startling sounds (Kaltwasser, 1991), fighting (Kaltwasser, 1990), foot shocks (Cuomo et al., 1988) or drug withdrawal (Vivian et al., 1994). It is debated whether 22-kHz calls function as alarm calls (Blanchard et al., 1991; Wöhr and Schwarting, 2008) but it could be shown that the presentation of such USV induces neuronal activity in brain areas implicated in fear and anxiety such as the PAG and the amygdala (Beckett et al., 1997; Sadananda et al., 2008). High frequency or so-called 50-kHz USVs are emitted at 32-96 kHz and are short in comparison to 22-kHz USV (30-50 ms, White et al., 1990). This type of vocalization has been attributed to positive affect since it is emitted during mating (Thomas and Barfield, 1985), in anticipation of food (Burgdorf et al., 2000), in juvenile play (Knutson et al., 1999), when rats are tickled (Panksepp and Burgdorf, 2000), and it induces social exploratory behaviors (Wöhr and Schwarting, 2007).

Mammalian sound production requires three essential components: The respiratory system, the larynx and supralaryngeal elements. Ultrasonic and sonic vocalizations are produced via different mechanisms. While audible sounds are created by mechanical vocal fold vibrations (for review see Fitch, 2006), the exact mechanism of USV production is still investigated. The larynx has been identified as the important anatomical structure (Roberts, 1975a, 1975b; Brudzynski and Fletcher, 2010; Johnson et al., 2010) and models of intralaryngeal planar ping-pong jets (Mahrt et al., 2016), edge-tone mechanisms involving the alar cartilage (Riede et al., 2017) and a shallow cavity model (Handley and Mithani, 1984) are discussed.

The respiratory, laryngeal and supralaryngeal muscles orchestrating vocal production are innervated by motoneurons arising from the lumbar to cervical spinal cord and the hindbrain. Since no direct reciprocal connections between the motoneurons have been found (Cunningham and Sawchenko, 2000), vocal and respiratory motor coordination and synchronization must be achieved by a higher order structure. Both the hindbrain nucleus

retroambiguus and the reticular formation have direct connections to vocal and respiratory motoneurons, and electrical stimulation of the structures triggered vocalizations in a wide range of mammals (for reviews see Jürgens and Hage, 2007; Holstege and Subramanian, 2016). Yet, indispensable for the production of vocalization is the midbrain PAG (for details on this brain structure see chapter 1.4). Lesions or traumatic injuries of the PAG lead to mutism and electrical or neurochemical stimulation trigger naturally sounding vocalizations in a wide range of species including humans (Adametz and O’Leary, 1959; Skultety, 1962; Jürgens and Pratt, 1979; Esposito et al., 1999). It is assumed that the PAG serves as a gating center for the initiation of innate vocalization rather than contributing to the patterning of vocalizations.

A recent study identified a subset of neurons in the lateral PAG projecting to the nucleus retroambiguus that are required for USV of male mice (Tschida et al., 2019). Further, it was shown that these neurons are controlled in a bidirectional manner by an inhibitory projection from the amygdala and a disinhibitory circuit from the preoptic area (Gao et al., 2019; Michael et al., 2020; Chen et al., 2021). In primates, two distinct forebrain-to-hindbrain vocal pathways are established. The so-called “primary vocal motor network” comprises projections from the anterior cingulate cortex and other forebrain structures to the PAG and initiates innate vocalizations such as crying depending on the affective state. In the “volitional articulation motor network” which is underdeveloped in non-human primates, the laryngeal motor cortex sends direct projections to vocal motoneurons, which is essential for volitional human speech (for reviews see Jürgens, 2002, 2009; Hage and Nieder, 2016; Nieder and Mooney, 2020). In rodents, it is assumed that laryngeal motor neurons receive no direct input from the motor cortex, although one study could show such a projection (Arriaga et al., 2012). A functional involvement of this pathway in vocalization rather than the control of other laryngeal tasks like swallowing remains to be shown. Transsynaptic retrograde rabies tracing from the laryngeal muscles showed cortical, amygdalar and hypothalamic labeling only several synapses upwards (Van Daele and Cassell, 2009). Also, the mouse motor cortex seems to be dispensable for the patterning of vocalization, as lesion studies could show (Arriaga et al., 2012; Hammerschmidt et al., 2015).

Patients with psychiatric and neurodevelopmental disorders often exhibit communicative impairments. Autistic individuals have been shown to have difficulties in appropriate intonation, volume, and pitch of speech which masks the emotional state to the listener (Fine et al., 1991; Shriberg et al., 2001). Likewise, individuals suffering from

schizophrenia, depression, or mania may experience communication deficiencies (Docherty, 2005). Aiming at disentangling the genetic and neuronal basis of those disorders, several rodent models have been established, some of which include the investigation of vocalization. Administration of amphetamine in rats leads to substantial increases in 50-kHz USV emission (Engelhardt et al., 2017) and locomotion (Cox et al., 1971), a phenotype used to model the elevated mood and hyperactivity in mania (for review see Wöhr, 2021). *Shank3* is a gene associated with autism and Phelan–McDermid syndrome and *Shank3* null mutant mice were found to exhibit altered USV (for review see Wöhr, 2014). Further, the inbred mouse strain BTBR T+ *tf/J*, used as a model for autism, revealed an unusual pattern of ultrasonic call types (Scattoni et al., 2008).

1.4. Neuronal Circuits of Defensive Responses

The neuronal circuits orchestrating the behavioral response to a threat entail brain regions involved in sensory threat detection, along with brain areas that integrate those environmental inputs with the internal state of the animal and convey the information to output structures that coordinate the resulting defensive behaviors (for review see Pereira and Moita, 2016; Silva et al., 2016; Branco and Redgrave, 2020).

Animals detect threats of different sensory modalities such as olfactory, visual, tactile, auditory, or multimodal cues. For rodents, olfactory inputs play a major role and are processed by the main olfactory system (volatile cues) and the associated olfactory system (non-volatile cues). The beforementioned looming and other visual stimuli are detected by the retinal ganglion cells which send projections to the superior colliculus (SC). Auditory stimuli are processed in the auditory cortex that sends projections to the inferior colliculus. Major hubs of sensory processing and integration of threatening stimuli are the amygdala and the medial hypothalamus. The amygdala is a heterogenous structure comprising several subnuclei that integrate auditory (lateral amygdala), visual (lateral amygdala), and olfactory (cortical and medial amygdala) inputs. This information is further relayed to the medial hypothalamic defensive circuit consisting of two parallel pathways (Canteras, 2002; Gross and Canteras, 2012; Silva et al., 2013). Cues concerning aggressive conspecifics are conveyed from the medial amygdala to the ventrolateral part of the ventromedial nucleus of the hypothalamus (VMH) to activate the conspecific response circuit. The parallel and independent predator response circuit comes into play in response to predator cues conveyed via the medial amygdala to the dorsomedial VMH. Projections from a wide range of sensory processing areas as well as such that provide further

contextual information (e.g., the hippocampus, Canteras, 2002) make the medial hypothalamus a candidate integration hub. This is further supported by loss-of-function and activation studies which could show that activation of the medial hypothalamus triggers defensive behaviors such as freezing or flight which are impaired by the blockage of the site (Brutus et al., 1985; Canteras et al., 1997; Silva et al., 2013; Wang et al., 2015).

Both the medial hypothalamus and the amygdala send strong projections to the midbrain PAG (Hopkins and Holstege, 1978; Marchand and Hagino, 1983; Rizvi et al., 1991). The PAG is a heterogenous structure that has been implicated in numerous tasks. It is considered an essential output site for defensive responses since stimulation of the amygdala, or the medial hypothalamus could trigger defensive reactions in cats that were abolished when the PAG was lesioned. However, defensive behaviors elicited by the stimulation of the PAG could not be blocked by amygdalar or hypothalamic lesions (Hunsperger, 1963). Further hints for a fundamental function in control of defensive behaviors come from studies that analyzed immediate early gene expression after exposure of rodents to a predator or predator odor. Beside c-Fos upregulation in the amygdala and the medial hypothalamus, immediate early gene expression was also increased in the PAG (Canteras and Goto, 1999; Dielenberg et al., 2001; Comoli et al., 2003; Martinez et al., 2008). Stimulation of the PAG induces species-specific defensive reactions or even explosive panic-like behaviors (Fardin et al., 1984; Brandão et al., 1999; Bittencourt et al., 2004; Evans et al., 2018). In search of treatment for chronic pain, deep brain stimulation of the patients' PAG elicited intense feelings of fear, panic, and of imminent death (Nashold et al., 1969; Schenberg et al., 2001). Further evidence for a role of the PAG in circa-strike behaviors came from human functional MRI studies conducted by Mobbs and colleagues. Participants were confronted with a virtual predator and the task to escape the threat in order to avoid an electric shock. While distal threats led to increased prefrontal cortex (PFC) activity, a proximal threat induced a forebrain-to-midbrain switch with increased activity in the PAG (Mobbs et al., 2007, 2009). This is in line with models suggesting a hierarchical defensive system with an involvement of the PFC and the hippocampus in gathering contextual information (McNaughton and Corr, 2004).

Classically, the elongated area around the cerebral aqueduct has been structured into anatomical longitudinal subcolumns, each serving different and partly opposing functions and integrated into distinct neuronal circuitries (Bandler et al., 1991). These include the dorsomedial (dmPAG), dorsolateral (dlPAG), lateral (lPAG) and ventrolateral (vlPAG)

subdivisions. Given their close anatomical proximity and overlapping functions, the dmPAG, dlPAG, and lPAG are sometimes referred to as dorsal PAG (dPAG). Traditionally, the dorsal and ventral parts have been ascribed to opposing roles in defensive behaviors and autonomic functions: While the ventral part is associated with passive behavioral states involving quiescence, freezing, hypotension and bradycardia, the dorsal part is linked to more active coping strategies including flight, hypertension, tachycardia, and vocalization (Zhang et al., 1990; Bandler and Shipley, 1994; Keay and Bandler, 2001). Both divisions are further involved in non-opioid and opioid-mediated analgesia (Fardin et al., 1984; Besson et al., 1991). Beside this predominant dorsoventral division, functional differences along the caudo-rostral and interior-exterior axis have been established (for review see Silva and McNaughton, 2019).

Predatory and conspecific threats are conveyed via the medial hypothalamic defensive circuit to the dPAG (dl and dm respectively, Canteras et al., 1994; Canteras, 2002; Tovote et al., 2016; Wang et al., 2021). Recent optogenetic studies provided insights into the functional involvement of hypothalamic and PAG substructural pathways. Optogenetic stimulation of a dmVMH-PAG projection has been shown to promote immobility (Wang et al., 2015) and activation of a l/vlPAG projecting γ -aminobutyric acid (GABA)-ergic pathway from the lateral hypothalamus elicited escape behavior (Li et al., 2018). Optogenetic inhibition of cholecystokinin (CCK)-expressing neurons of the premammillary nucleus to dlPAG projection decreased escape behaviors in response to threats (Wang et al., 2021). Apart from hypothalamic projections, the dPAG receives direct input from the SC, but not the IC, that trigger innate flight reactions in response to auditory threats (Xiong et al., 2015; Evans et al., 2018). From the amygdala complex, only the central nucleus of the amygdala (CeA) sends projections to the PAG, mostly terminating in the l/vlPAG. No CeA afferents reach the dlPAG (Hopkins and Holstege, 1978; Rizvi et al., 1991). Tovote and colleagues showed that glutamatergic vlPAG efferents are inhibited by local GABAergic interneurons. In an opposing manner, an inhibitory projection from the CeA disinhibits the output to allow freezing, while a local excitatory projection from the dlPAG onto the interneurons inhibits the vlPAG efferents and promotes flight reactions. These responses are mediated by vlPAG efferents to the medulla (Tovote et al., 2016). The vlPAG also sends projections to the CeA, the hypothalamus, the thalamus, the locus coeruleus, the raphe nucleus, the reticular formation and the cerebellum. The dorsal and lateral divisions project to the hypothalamus, the raphe nucleus, the medulla (for detailed review on PAG afferents and efferents see Silva and McNaughton, 2019).

1.5. Potential Regulatory Systems

The regulation of fear and anxiety involves a variety of neurotransmitter and neuromodulator systems that enable defensive behaviors in response to stressors and that might be altered in stress-related pathologies. Two well-investigated systems that are expressed throughout important brain structures regulating fear, anxiety, and stress are the endocannabinoid (eCB) and the CRF system.

The CRF System

The perception of a threat such as a predator leads to behavioral and emotional changes that are facilitated by adaptations of the autonomic nervous system (ANS) and the release of glucocorticoids. The neuropeptide CRF has been described as the central mediator of the stress response since it activates the hypothalamic-pituitary-adrenal (HPA) axis. Upon perception of a stressor, CRF is released from parvocellular neurons of the paraventricular nucleus of the hypothalamus (PVN) into the hypophyseal portal vasculature and transported to corticotrope cells of the anterior pituitary. There it triggers the release of the adrenocorticotrophic hormone (ACTH) which in turn mobilizes the release of glucocorticoids (GCs, corticosterone in rodents, cortisol in humans) in the adrenal cortex (Figure 2). GCs, next to the ANS activity, initiate physiological reactions that supports the organism's fight-or-flight response: Energy mobilization, increases in heart and respiratory rate, anti-inflammatory effects, enhanced analgesia, suppression of feeding and the reproductive system, but also increased arousal and focused attention (for review see Charmandari et al., 2005). While these effects are largely mediated via the mineralocorticoid receptor (MR), the glucocorticoid receptor (GR) is an important player in the termination of the stress response. Circulating GCs feed back to the pituitary, the PVN, the amygdala and the hippocampus to cease the release of CRF and ACTH (Gjerstad et al., 2018).

CRF is widely expressed throughout the brain, including the piriform cortex, the neocortex, the hippocampus, the PVN, the central amygdala, the BNST, the Barrington's nucleus, and the inferior olive (Alon et al., 2009; Peng et al., 2017). It is found mostly in different types of GABAergic cells depending on the brain region. In the hippocampus, it is expressed by parvalbumin (PV)-positive, CCK-negative basket cells while in the neocortex it is found in PV-negative, somatostatin-expressing and even CCK-positive cells

(Kubota et al., 2011). In the piriform cortex and the PVN, CRF-positive neurons are glutamatergic (Dabrowska et al., 2013; Kono et al., 2017).

CRF signals through two G protein-coupled receptors (GPCRs), corticotropin-releasing factor receptor (CRFR) 1 and CRFR2, exhibiting a higher affinity for the former. The peptide functions as a neuromodulator, meaning it alters the action of neurotransmitters on the membrane potential. The exact mode of action is complex and remains partly unknown. Depending on cell type and brain area, CRF affects intracellular signaling pathways, can influence ionic currents of potassium (K^+) and calcium ions (Ca^{2+}) and has been found to increase action potential firing and to decrease afterhyperpolarization in the hippocampus (Aldenhoff et al., 1983; Rainnie et al., 1992; Chen et al., 2012).

While the role of CRF in the regulation of the HPA axis is well understood, its effect on behavioral responses is more complex (for reviews see Dedic et al., 2017; Deussing and Chen, 2018). After the isolation of the CRF molecule (Vale et al., 1982), studies using intracerebroventricular administration of the peptide or CRFR1 agonists showed that such central increases in CRF led to phenotypes similar to those of stressed animals, including increased anxiety-like behavior and arousal (Britton et al., 1982; Liang et al., 1992; Momose et al., 1999; Devigny et al., 2011). Similarly, CRF-overexpression mice exhibited an anxiogenic phenotype and displayed increased active stress-coping behaviors, which could be reverted by CRFR1 antagonists (Britton et al., 1986; Stenzel-Poore et al., 1994; Lu et al., 2008; Toth et al., 2014). This effect is likely mediated via forebrain glutamatergic CRFR1, while midbrain dopaminergic CRFR1-expressing neurons display anxiolytic characteristics (Refojo et al., 2011). Several psychopathologies have been linked to dysfunctions of the CRF system. In depressive patients and suicide victims increased levels of CRF have been found in the cerebrospinal fluid (CSF) and in several brain regions (Nemeroff et al., 1984; Arató et al., 1989; Raadsheer et al., 1995; Bissette et al., 2003). Along the line, CRFR1 has been found to be downregulated in the prefrontal cortex which is attributed to a compensatory reaction to the elevated central CRF (Nemeroff et al., 1988; Merali et al., 2004). Besides, patients suffering from PTSD exhibited increased levels of CRF in the CSF (Bremner et al., 1997; Baker et al., 1999).

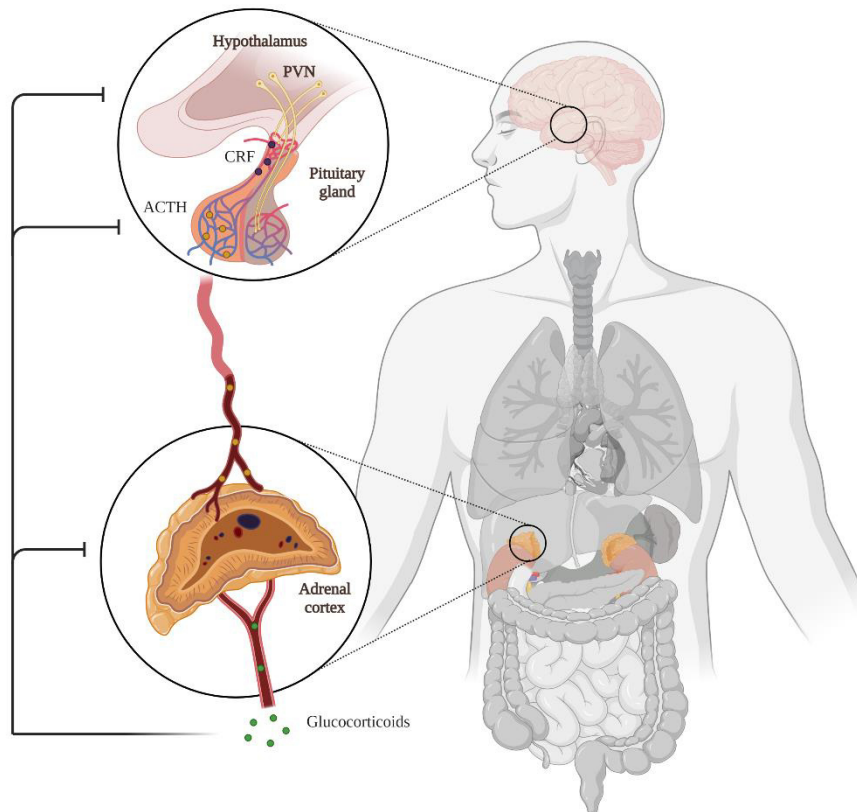


Figure 2: The Hypothalamic-Pituitary-Adrenal Axis

In response to a stressor, corticotropin-releasing factor (CRF) is released from the paraventricular nucleus of the hypothalamus (PVN) into the hypophyseal portal vasculature and reaches the anterior pituitary where it stimulates the secretion of adrenocorticotropic hormone (ACTH) into the blood. The peptide travels to the adrenal cortex and triggers the release of glucocorticoids (GCs) which contribute to physiological stress reactions. Circulating GCs bind to glucocorticoid receptors at all levels of the HPA axis and contribute to the termination of the stress response. Figure created with BioRender.com.

The Endocannabinoid System

The eCB system is a neuromodulatory system highly conserved from fish to humans (McPartland et al., 2006). Only decades after the discovery of Δ^9 -tetrahydrocannabinol (Δ^9 -THC) as the psychoactive component of *Cannabis sativa* and the elucidation of its chemical structure (Gaoni and Mechoulam, 1964), the CB1 receptor has been identified as an endogenous target (Matsuda et al., 1990). Soon after, a second cannabinoid receptor has been discovered (CB2, Munro et al., 1993), along with the endogenous cannabinoids anandamide (AEA; Devane et al., 1992) and 2-arachidonoylglycerol (2-AG; Mechoulam et al., 1995; Sugiura et al., 1995). The eCB system further consists of the main synthesizing and degrading enzymes of the endocannabinoids: N-acyl phosphatidyl ethanolamine-

phospholipase D (NAPE-PLD; Okamoto et al., 2004), diacylglycerol lipase- α (DAGL α ; Bisogno et al., 2003), fatty acid amide hydrolase (FAAH; Cravatt et al., 1996), and monoacylglycerol lipase (MAGL; Dinh et al., 2002).

The eCB system acts as a retrograde messenger system at various synapses. Its mechanism of action comprises numerous molecules, overlaps with other pathways, depends on the type of synapse and the intensity of neuronal activation. A simplified model is depicted in Figure 3. The CB1 receptor is a GPCR mostly integrated in the presynaptic plasma membrane. Ca²⁺ influx via voltage-gated calcium channels, AMPA or metabotropic glutamate receptor activation contribute to the biosynthesis of endocannabinoids in the postsynapse. Accordingly, endocannabinoids are synthesized “on demand”, unlike classical neurotransmitters. Upon release, endocannabinoids diffuse to and travel through the synaptic cleft in a retrograde manner and bind to CB1 receptors. Activated CB1 receptors, mostly via G_o, inhibit voltage-gated Ca²⁺ channels and activate inwardly rectifying K⁺ channels leading to a reduction in intracellular Ca²⁺ levels and thereby inhibiting neurotransmitter release (Shen et al., 1996; Katona et al., 1999). Thus, the eCB system acts as a transient negative feedback mechanism upon stimulation to reduce synaptic transmission. Applying electrophysiological tools, it has been found that depolarization-induced suppression of excitation (DSE, Kreitzer and Regehr, 2001; Maejima et al., 2001) or inhibition (DSI, Ohno-Shosaku et al., 2001; Wilson and Nicoll, 2001) can be mediated by endocannabinoids. It is noteworthy that AEA shows a greater affinity for the CB1 receptor than 2-AG. However, 2-AG can be found in much higher concentrations than AEA in several tissues, e.g., the brain of rodents (Buczynski and Parsons, 2010).

CB1 receptors are abundantly expressed throughout the central nervous system, and receptor autoradiography revealed high expression levels in the brain (Herkenham et al., 1990, 1991). Prominent expression can be found in the cortex, hippocampus, amygdala, dorsal raphe nucleus, PAG and the cerebellum. In cortical areas, the CB1 receptor is highly expressed on GABAergic CCK-positive interneurons but also on glutamatergic neurons (Marsicano and Lutz, 1999; Katona et al., 2006). Besides, it has been found on serotonergic, cholinergic and noradrenergic cells (Degroot et al., 2006; Häring et al., 2007; Carvalho et al., 2010).

Numerous pharmacological compounds have been developed that facilitate disentangling the mechanisms and effects of the eCB system *in vitro* and *in vivo* and that have been used as therapeutics (for reviews see Howlett et al., 2002; Di Marzo et al., 2004; Micale et al., 2013). The development of FAAH and MAGL inhibitors allowed to study the effects of

increased cannabinoid tones without the administration of exogenous CB1 agonists like Δ^9 -THC. The compounds URB597 and JZL184 block AEA and 2-AG degradation via FAAH and MAGL inhibition, respectively (Kathuria et al., 2003; Long et al., 2009). SR141716A was the first compound found to act as an inverse agonist on the CB1 receptor (Rinaldi-Carmona et al., 1994). It had received approval by the European Medicines Agency as an anti-obesity drug under the market name rimonabant but was withdrawn a year later due to severe psychiatric side effects (Traynor, 2007).

This observation highlights the sensitive role of the eCB system in regulating various behavioral and emotional responses as it modulates synaptic transmission throughout the brain. These effects become evident once the system has been triggered above threshold such as by a strong negative environmental stimulus (Kamprath et al., 2009). Under such conditions, numerous studies have shown the regulatory effects of the eCB system on anxiety-like behaviors using pharmacological and genetic tools in rodents (for reviews see Riebe et al., 2012; Ruehle et al., 2012; Lutz et al., 2015; Petrie et al., 2021). While CB1-deficient mice exhibited an anxiogenic phenotype under aversive conditions (Jacob et al., 2009), conditional knock-out mutants revealed opposing roles of glutamatergic and GABAergic CB1-expressing neurons in anxiety-related behavior (Rey et al., 2012). The loss of CB1 on glutamatergic neurons increased anxiety-like behaviors (Lafenêtre et al., 2009; Häring et al., 2011) which could be rescued by re-expression of the receptor (Ruehle et al., 2013). Conversely, deletion of CB1 from forebrain GABAergic neurons leads to decreased anxiety like behaviors (Lafenêtre et al., 2009; Häring et al., 2011). Similarly, opposing roles for these cell types have also been described for fear responses. Conditional knock-out mice lacking CB1 on cortical glutamatergic neurons showed increased behavioral inhibition (Genewsky and Wotjak, 2017) and higher levels of passive fear responses in classical fear conditioning (Metna-Laurent et al., 2012), while CB1 on GABAergic neurons was found to play a role in passive avoidance (Genewsky and Wotjak, 2017) and enhanced fear expression (Llorente-Berzal et al., 2015). The CB1 agonist Δ^9 -THC acts in dose-dependent manner, with high doses leading to passive fear responses but low doses triggering active fear coping strategies (Metna-Laurent et al., 2012). AEA was found to promote acute fear relief and to have panicolytic characteristics, while 2-AG mediated conditioned fear expression (Llorente-Berzal et al., 2015; Heinz et al., 2017).

In respect to PTSD, a deficit in eCB signaling has been suggested (for review see Hill et al., 2018). Patients with PTSD showed lower levels of circulating 2-AG (Hill et al., 2013) and AEA, and increased CB1 receptor expression in the brain (Neumeister et al., 2013).

In line with this, rodent studies report that 2-AG augmentation in the amygdala and the nucleus accumbens lead to a stress-resilient phenotype in mice (Bosch-Bouju et al., 2016; Bluett et al., 2017). Taken together, the eCB system is considered to act as a buffering system to guard against harmful effects of environmental stressors and to balance emotional responses.

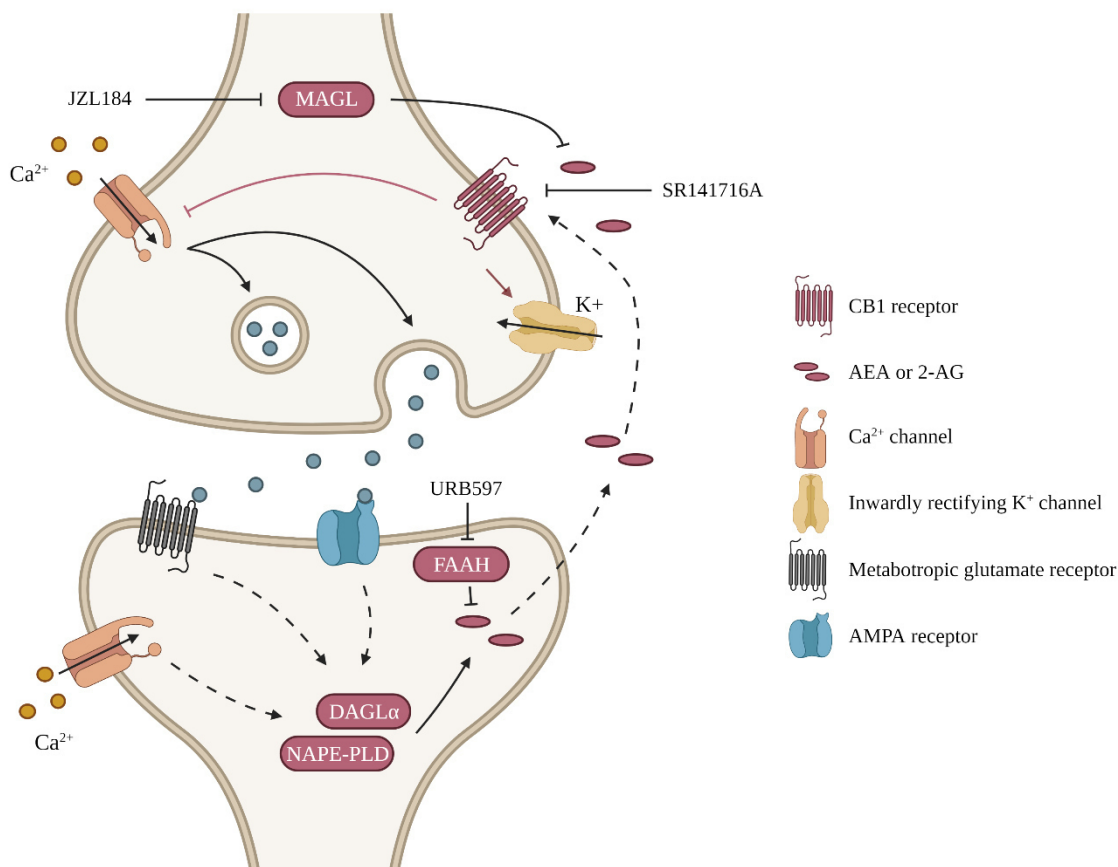


Figure 3: The Endocannabinoid System

Upon synaptic stimulation, the endocannabinoids anandamide (AEA) and 2-arachidonoylglycerol (2-AG) are synthesized by N-acyl phosphatidyl ethanolamine-phospholipase D (NAPE-PLD) and diacylglycerol lipase- α (DAGL α), respectively. After diffusion, the molecules travel through the synaptic cleft in a retrograde manner and bind at the cannabinoid receptor type 1 (CB1). CB1 acts via intracellular pathways which leads to an inhibition of neurotransmitter release from the presynapse. Endocannabinoids are degraded by the enzymes fatty acid amide hydrolase (FAAH) in case of AEA and monoacylglycerol lipase (MAGL) in case of 2-AG which in turn can be pharmacologically inhibited by the compounds URB597 and JZL184, respectively. SR141716A is a selective CB1 antagonist. Figure created with BioRender.com.

1.6. Aims of the Thesis

Defensive behaviors along the predator imminence continuum from arousal to panic-like flight responses have been described in various species. In humans, the exaggeration and persistence of related behaviors beyond the presence of a threat or other stressor have been associated with anxiety and stress-related disorders, such as PTSD. While new methodologies and technologies that arose during the last decades helped to elucidate the malfunctions of such disorders, much of the underlying mechanisms including neuronal circuits and neuromodulatory systems remain to be explained.

In this thesis, the following objectives have been addressed:

Objective 1: Assessment of the interaction of CRF and CB1 in the context of fear, anxiety, and stress.

The objective was tackled by the behavioral evaluation of a newly generated conditional knockout mouse line that selectively lacks CB1 expression in CRF-positive neurons. The results are presented in section 2.1.

Objective 2: Identify correlates of grey matter volume changes and hyperarousal severity induced by a traumatic experience.

To address this objective, we combined MRI scans before and after a traumatic incident for grey matter volume measures with behavioral assessments after trauma incubation in wild-type mice. For methodology and results, please see section 2.2.

Objective 3: Characterization of sonic mouse vocalization including the dissection of the underlying neuronal circuits and investigation of its ecological relevance.

This objective involved the description of sonic vocalization observed in mice bred for high anxiety-related behavior as well as *in vivo* imaging, pharmacological and chemogenetic manipulations to identify brain areas involved followed by playback experiments to highlight the ecological function of the calls. See section 2.3 for results.

2. RESULTS

2.1. CB1 Receptors in Corticotropin-Releasing Factor Neurons Selectively Control the Acoustic Startle Response in Male Mice

Ruat J, Hartmann A, Heinz DE, Nemcova P, Stoffel R, Deussing JM, Chen A, Wotjak CT

Originally published in *Genes, Brain and Behavior*

2021, October 21

DOI: [10.1111/gbb.12775](https://doi.org/10.1111/gbb.12775)

ORIGINAL ARTICLE

CB1 receptors in corticotropin-releasing factor neurons selectively control the acoustic startle response in male mice

Julia Ruat^{1,2,3}  | Alice Hartmann³  | Daniel E. Heinz^{3,4}  | Paulina Nemcova³  |
Rainer Stoffel¹ | Jan M. Deussing^{5,6}  | Alon Chen^{1,7}  | Carsten T. Wotjak^{3,4,8} 

¹Department Stress Neurobiology and Neurogenetics, Max Planck Institute of Psychiatry, Munich, Germany

²International Max Planck Research School for Translational Psychiatry (IMPRS-TP), Max Planck Institute of Psychiatry, Munich, Germany

³Research Group Neuronal Plasticity, Max Planck Institute of Psychiatry, Munich, Germany

⁴Max Planck School of Cognition, Max Planck Institute for Human Cognitive and Brain Sciences, Leipzig, Germany

⁵Research Group Molecular Neurogenetics, Max Planck Institute of Psychiatry, Munich, Germany

⁶Scientific Core Unit Genetically Engineered Mouse Models, Max Planck Institute of Psychiatry, Munich, Germany

⁷Department of Neurobiology, Weizmann Institute of Science, Rehovot, Israel

⁸Central Nervous System Diseases Research (CNSDR), Boehringer Ingelheim Pharma GmbH & Co KG, Biberach an der Riss, Germany

Correspondence

Alon Chen, Department Stress Neurobiology and Neurogenetics, Max Planck Institute of Psychiatry, 80804 Munich, Germany.
Email: alon.chen@weizmann.ac.il

Carsten T. Wotjak, Research Group Neuronal Plasticity, Max Planck Institute of Psychiatry, 80804 Munich, Germany.
Email: wotjak@psych.mpg.de

Funding information

Bruno and Simone Licht; Bundesministerium für Bildung und Forschung; Fundação de Amparo à Pesquisa do Estado de São Paulo, Grant/Award Number: BEPE-2018/17387-9; German-Israeli Foundation for Scientific Research and Development, Grant/Award Number: I-1442-421. 13/2017; International Max Planck Research School for Translational Psychiatry (IMPRS-TP); Max-Planck-Gesellschaft; Roberto and Renata Ruhman; Weizmann Institute of Science

Abstract

The endocannabinoid system is an important regulator of the hormonal and behavioral stress responses, which critically involve corticotropin-releasing factor (CRF) and its receptors. While it has been shown that CRF and the cannabinoid type 1 (CB1) receptor are co-localized in several brain regions, the physiological relevance of this co-expression remains unclear. Using double *in situ* hybridization, we confirmed co-localization in the piriform cortex, the lateral hypothalamic area, the paraventricular nucleus, and the Barrington's nucleus, albeit at low levels. To study the behavioral and physiological implications of this co-expression, we generated a conditional knockout mouse line that selectively lacks the expression of CB1 receptors in CRF neurons. We found no effects on fear and anxiety-related behaviors under basal conditions nor after a traumatic experience. Additionally, plasma corticosterone levels were unaffected at baseline and after restraint stress. Only acoustic startle responses were significantly enhanced in male, but not female, knockout mice. Taken together, the consequences of depleting CB1 in CRF-positive neurons caused a confined hyperarousal phenotype in a sex-dependent manner. The current results suggest that the important interplay between the central endocannabinoid and CRF systems in regulating the organism's stress response is predominantly taking place at the level of CRF receptor-expressing neurons.

Alon Chen and Carsten T. Wotjak shared senior authorship

This is an open access article under the terms of the Creative Commons Attribution-NonCommercial License, which permits use, distribution and reproduction in any medium, provided the original work is properly cited and is not used for commercial purposes.

© 2021 The Authors. Genes, Brain and Behavior published by International Behavioural and Neural Genetics Society and John Wiley & Sons Ltd.

KEYWORDS

corticotropin-releasing factor, endocannabinoid system, mouse behavior, startle response, trauma

1 | INTRODUCTION

The corticotropin-releasing factor (CRF) and the endocannabinoid (eCB) systems are important players of the negative valence system and are implicated in various stress-related psychopathologies (for reviews see Reference [1,2]). The role of the neuropeptide CRF in the regulation of the endocrine and behavioral stress response has been well described.¹ CRF secretion from neurons of the paraventricular nucleus of the hypothalamus (PVN) into the portal blood of the median eminence triggers the activation of the hypothalamic–pituitary–adrenal (HPA) axis. Within the brain, release of CRF modifies anxiety-related behavior via CRF receptor type 1 (CRFR1) in a cell type-specific manner.^{3,4} Intracerebroventricular (ICV) injections and central overexpression of CRF promote anxiogenic effects in rodents that are mediated by CRFR1, likely expressed by forebrain glutamatergic neurons.^{4–10} Likewise, reducing CRF activity, and CRFR1 signaling via midbrain dopaminergic neurons leads to anxiolytic behavioral phenotypes.^{3,4,11,12} Human studies have also showed a role for CRF in anxiety disorders as CRF levels are elevated in individuals suffering from post-traumatic stress disorder (PTSD).^{13,14} Besides its involvement in promoting anxiety, CRF also plays a role in arousal. In rodents, increased central CRF led to increased acoustic startle responses (ASR) and decreased startle habituation.^{15–18}

The eCB system is a retrograde messenger system modulating synaptic transmission, whereby the stimulation of the presynaptically located cannabinoid type 1 (CB1) receptor by endocannabinoids suppresses neurotransmitter release. Studies using CB1-deficient mice and pharmacological manipulations confirmed a role of the eCB system in regulating anxiety-related behaviors in rodents, again in a cell type-dependent manner. Confronted with strongly aversive stimuli, CB1 knockout mice exhibited an increased anxiety-like behavior.¹⁹ Hereby, the cellular identity of CB1-expressing neurons plays an opposing role with GABAergic neurons mediating anxiogenic and glutamatergic neurons anxiolytic effects (for review see Reference [2]). In respect to PTSD, affected individuals have been found to have reduced levels of the eCB anandamide (AEA) and upregulated CB1 receptor expression.^{20,21}

Interestingly, CRF and the eCB system seem to regulate fear, anxiety, behavioral and hormonal stress responses in an antagonistic manner. A considerably large body of literature describes the functional interaction of the systems with a focus on HPA axis regulation (for reviews see Reference [22,23]). For instance, Di and colleagues described a model that suggests a glucocorticoid receptor-triggered activation of eCB synthesis on parvocellular neurons leading to a CB1-mediated inhibition of glutamate release from presynaptic neurons as a mechanism for the fast feedback inhibition of CRF by corticosterone (CORT;²⁴ for review see Reference [25]). As another

example of this interaction, CRF acts via CRFR1 to trigger fatty acid amide hydrolase (FAAH) activity within the basolateral amygdala. Activation of FAAH, the main degrading enzyme of AEA, attenuates retrograde AEA signaling thus disinhibiting glutamatergic inputs to the basolateral amygdala. The resulting activation of the pyramidal projection neurons facilitates HPA axis activation.^{26–33} Furthermore, the medial prefrontal cortex has been identified as a critical hub for the negative feedback inhibition of the HPA axis with a CB1-mediated cessation of the stress response.³⁴

CRF and CB1 are co-localized in several brain regions, for example, in the piriform and prefrontal cortex, the bed nucleus of the stria terminalis (BNST), the PVN, the amygdala and the locus coeruleus.^{35–37} In spite of the intriguing involvement of both the CRF and eCB system in anxiety-related behaviors, nothing is known about the physiological relevance of this co-expression. Therefore, here we crossbred previously generated and validated mouse lines, the CRF-IRES-Cre³⁸ and the CB1-floxed³⁹ mice to generate a conditional knockout mouse line lacking CB1 specifically in CRF-positive neurons (CB1^{CKO-CRF}). CB1^{CKO-CRF} and wildtype littermates were assessed for anxiety and fear-related behavior, arousal, and HPA axis function. We additionally characterized the mutant mice after a traumatic experience, given the potential involvement of both CRF^{40,41} and endocannabinoids in PTSD-like phenotypes (for reviews see Reference [42,43]).

2 | MATERIALS AND METHODS

2.1 | Animals

Male and female CB1^{CKO-CRF} and CB1^{Ctrl} (male: 2–7 months age, female: 2–6 months age) and male C57BL/6NRjMpi (originating from Janvier, 3 months age) mice were bred in the vivarium of the Max Planck Institute of Biochemistry, Martinsried, Germany. After the transfer to the animal facility at the Max Planck Institute of Psychiatry, mice were permitted a recovery period of at least 10 days before starting experiments. The animals were group-housed under standard housing conditions in Green Line IVC Sealsafe mouse cages (Tecniplast, Hohenpeißenberg, Germany) equipped with bedding and nesting material and a wooden rodent tunnel (ABEDD, Vienna, Austria). Animals had access to food and water ad libitum and were maintained in a 12/12-hours normal light/dark cycle (lights on at 6 am). Behavioral testing was performed during the light phase. All experimental procedures were approved by the Government of Upper Bavaria (Regierung von Oberbayern, 55.2-2532.Vet_02-17-206) and performed according to the European Community Council Directive 2010/63/EEC. All efforts were made to reduce the number of experimental subjects and to minimize, if not exclude, any suffering.

2.2 | Generation of CB1^{CKO-CRF} mice and genotyping

CB1^{CKO-CRF} mice originated from crossing of female CRF-IRES-Cre mice³⁸ (Jackson Laboratory stock no: 012704) with male CB1-floxed mice³⁹ (CB1 coding region is flanked by two loxP sites). Experimental animals were generated by breeding female heterozygous CB1^{CKO-CRF} with male heterozygous CB1-floxed mice. Cre-positive (CB1^{CKO-CRF}) and Cre-negative (CB1^{Ctrl}) littermates were used for experiments. Genotyping was performed by PCR using the following primers: G50 (5'-GCTGTCTCTGGTCTCTTAAA-3'), G51 (5'-GGTGTCACCTCTGAAACAGA-3'), G53 (5'-CTCCTGTATGCCATAGCTCTT-3'), G100 (5'-CGGCATGGTGCAAGTTGAATA-3'), and G101 (5'-GCGATCGCTATTTCCATGAG-3'). All animals were re-genotyped after completion of the experiment.

2.3 | Single and double *in situ* hybridization

Expression analysis was performed on 20 μ m thick coronal brain slices thaw mounted onto SuperFrost Plus slides (Thermo Fisher Scientific, Waltham, MA, USA). Single and double *in situ* hybridization was performed as described previously.⁴ The following riboprobes were used: *Crf* (nucleotides 70–469 of GenBank accession number NM_205769.2) and *Cnr1* (nucleotides 597–2129 of NM_007726.4). For double *in situ* hybridization, CRF riboprobes were labeled with radioactive sulfur while CB1 riboprobes were digoxigenin (DIG)-labeled. Image analysis was performed blind of genotype using open-source Fiji image processing software.⁴⁴ Gray values were measured in defined areas of the piriform cortex which are outlined in Figure 1F, G. To facilitate the reading flow, we use capitalized abbreviations for gene, mRNA and protein names throughout the manuscript.

2.4 | Stress and behavioral procedures

Male and female mice were tested as different groups (i.e., on different times of the day or different days) to avoid unspecific carry-over effects by sex pheromones. We therefore do not draw conclusions on sex differences, only genotype differences.

2.4.1 | Open field test

The open field test (OFT) was used to assess locomotor activity and anxiety measures. Mice were placed into a dimly lit (100 lx) square arena (W50 \times L50 \times H40 cm) with opaque walls facing the wall. The animals could freely explore the arena for 15 min. The movement of the mouse was video recorded using ANY-maze software (Stoelting Co., Dublin, Ireland) and the time spent in the center zone (W35 \times L35 cm, 1225 cm²) versus the outer zone (W7.5 cm, 1275 cm²) and the total distance moved were analyzed. The arena was cleaned with soap and water after each trial.

2.4.2 | Elevated plus maze

In the elevated plus maze (EPM) test, mice were exposed to an elevated (32 cm above ground) plus-shaped maze consisting of two opposing arms enclosed by opaque Plexiglas walls (L27 \times W5 \times H14 cm) and two opposing arms (L27 \times W5 cm) without walls (except for a small rim), connected by a central zone (L5 \times W5 cm). After being placed in the end of one of the closed arms facing the wall, mice could freely explore the maze for 15 min. The experiment was video-recorded using ANY-maze tracking software and the time spent in the open arms and the latency to enter an open arm were determined. The setup was cleaned with soap and water after each trial.

2.4.3 | Light dark box

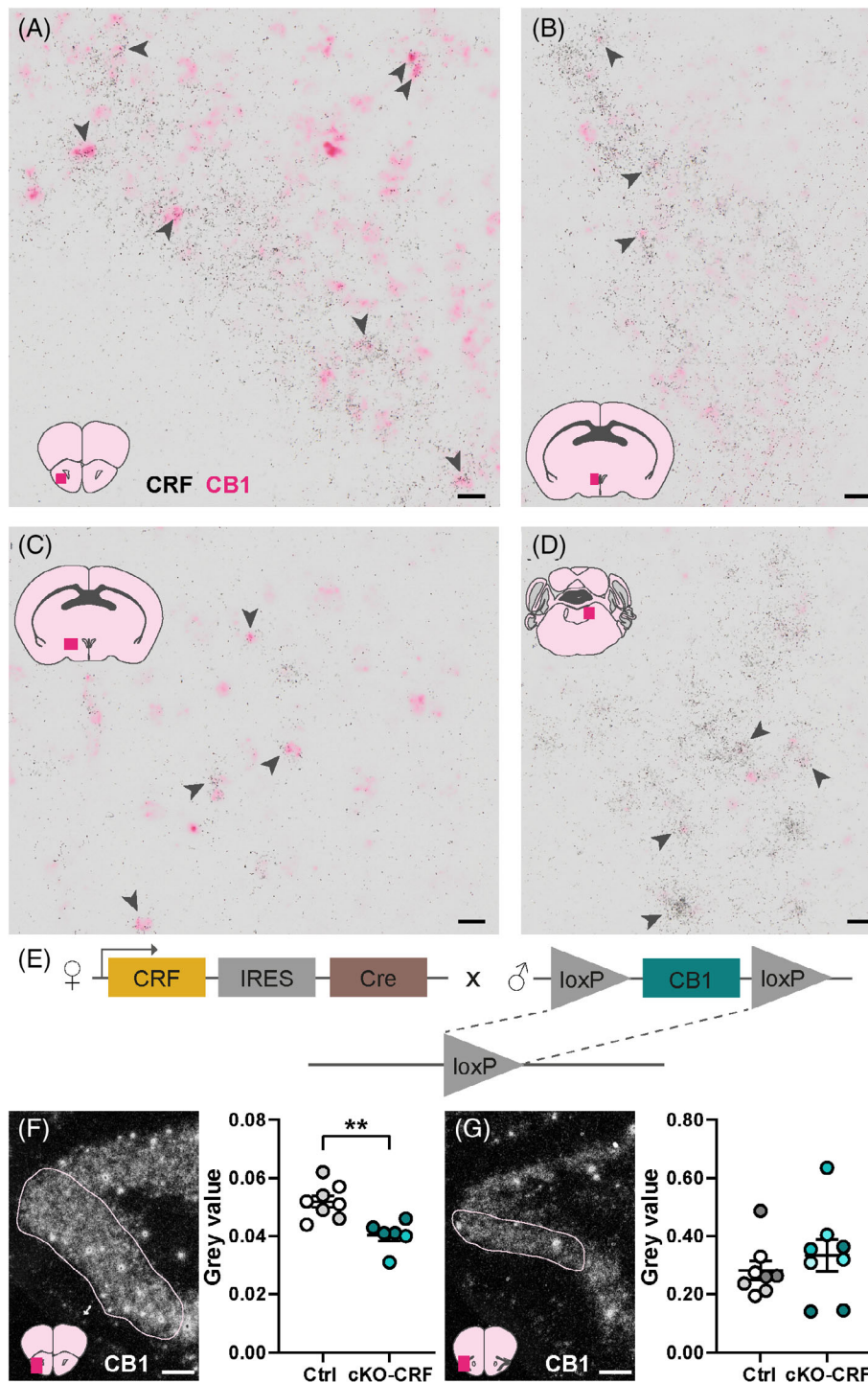
The light dark box (LDB) apparatus consisted of two compartments. One compartment (W20 \times L29 \times H25 cm) was made of white plexiglass walls and brightly lit (200 lx) while the other one was a black dark box (W20 \times L15 \times H25 cm). Both compartments were connected via a door (W6 \times H10 cm). The animal was placed in the brightly lit compartment and was allowed to freely move between to two areas for 15 min. The experiment was videotaped by ANY-maze tracking software and the time spent in the light zone was analyzed. The number of fecal boli were counted. The arena was cleaned with soap and water after each trial.

2.4.4 | Beetle Mania Task

The Beetle Mania task (BMT) was performed essentially as described previously.⁴⁵ In brief, mice were placed into the end of a gray polyethylene arena (L100 \times W15 \times H37 cm; 80–120 lx) and the number of rearings was scored during the first 5 min (habituation phase). Subsequently, a robo-beetle (Hexbug Nano, Innovation First Labs Inc., Greenville, TX, USA) was inserted most distantly from the mouse. For another 5 min, the number of contacts and avoidance behavior (mouse withdrew from the beetle upon contact) were scored by an experienced observer blind to genotype and experimental condition. The arena was cleaned with soap and water after each trial.

2.4.5 | Acoustic startle response

In the acoustic startle response (ASR) test, startle reflexes to acoustic stimuli were measured using the Startle Response System (TSE Systems GmbH, Bad Homburg, Germany). Animals were placed into the metal grid cage (L9.5 \times W4 \times H4.5 cm) sitting on the measuring platform. For the measurement of the intensity-response curve, the following protocol was applied: After a 5-min habituation period without sound presentation, white noise pulses of 70 dB(A), 90 dB(A), and 105 dB(A) (duration: 20 ms) were presented in a pseudo-randomized



order 30 times each, interspersed with 18 control trials (no sound presentation). Inter-trial intervals were of 13–25 s length. The startle amplitude was defined as the peak amplitude in grams within the first 100 ms after stimulus onset. The prepulse inhibition (PPI) protocol consisted of 5 initial white noise pulses of 105 dB(A) followed by pulses of 105 dB(A) with prepulses of 75 dB(A). Prepulses were presented 50, 150 and 500 ms prior to the startle pulse. Each prepulse combination was presented 27 times in a pseudo-randomized order interspersed with 27 white noise pulses of 105 dB(A). Inter-trial

intervals were of 13–25 s length. PPI was calculated as a percentage $\text{PPI} = 100 \times (1 - [\text{startle response for prepulse} + \text{startle trial}] / [\text{startle response for startle stimulus alone trial}])$.

2.4.6 | Trauma protocol

Foot shock delivery and trauma memory assessment were performed as described previously.⁴⁶ In brief, animals were placed into a cubic-

shaped conditioning chamber (MED Associates, Fairfax, VT, USA) with a metal grid floor through which two electric foot shocks of 1.5 mA and 2 s duration were delivered. The chamber had been cleaned with 70 % ethanol. Animals of the control group underwent the same procedure without receiving a foot shock. Thirty days later, all animals were placed into a neutral context (a cylindrical chamber with bedding instead of metal grid and cleaned with 1 % acetic acid) for 3 min. On the subsequent day, the mice were re-exposed to the conditioning chamber that had been cleaned with ethanol to test for conditioned fear. The trials were videotaped and freezing time and number of rearings were analyzed by an experienced observer.

2.4.7 | Acute stress and plasma CORT measurements

Mice were single-housed for 10 days. On testing day, the animals were restrained in a 50 ml Falcon tube (equipped with holes for tail movement and oxygen supply) for 15 min in their home cage during morning hours of the light phase. At the end of the restraint (t15), a tail cut was made at the middle part of the tail. Blood was collected in EDTA-coated tubes (Sarstedt, Nümbrecht, Germany). Blood collection was repeated 30 min (t30) and 90 min (t90) after the onset of the restraint. Trunk blood was collected 2 weeks after the restraint stress (basal) during morning hours of the light phase. All blood samples were centrifuged at 8g for 15 min at 4°C. Plasma was retrieved from the supernatant and CORT concentrations were measured using a commercially available radioimmunoassay kit (MP Biomedicals, Eschwege, Germany).

2.5 | Statistical analysis

Data are presented as means \pm SEM. For normally distributed data, unpaired t-tests, one-way analysis of variance (ANOVA) followed by Tukey's post-hoc test or two-way analysis of variance (ANOVA) for repeated measures followed by Bonferroni post-hoc analysis were performed. Kruskal-Wallis followed by Dunn's multiple comparison tests was employed for non-parametric distribution. Statistical significance was accepted if $p < 0.05$. All statistical analyses were performed using GraphPad Prism 9.0.

3 | RESULTS

3.1 | Co-localization of CRF and CB1 in the mouse brain

To assess the level of CRF and CB1 co-expressing cells in the mouse brain, we performed a double *in situ* hybridization on brain slices of male C57BL/6 mice. We found a moderate level of co-localization in the piriform cortex (mostly in the anterior part, Figure 1A), and the Barrington's nucleus (Figure 1D). A low level of co-localization was

observed in the PVN (Figure 1B) and the lateral hypothalamic area (Figure 1C). We found no co-localization in the central and basolateral amygdala and the BNST (data not shown).

3.2 | Conditional knockout of CB1 in CRF-positive neurons

To study the effect of a potential unrestrained CRF release from CB1-positive neurons, we bred female CRF-IRES-Cre mice with male CB1-floxed mice (Figure 1E). The resulting conditional knockout mice (CB1^{CKO-CRF}) were expected to express a reduced level of CB1 in the aforementioned brain areas compared with the wildtype littermates (CB1^{Ctrl}). To confirm this assumption, we performed a single CB1 *in situ* hybridization on brain slices of male CB1^{CKO-CRF} and CB1^{Ctrl} mice. We measured the gray values of a defined area of the lateral anterior and posterior piriform cortex (Figure 1F, G), a region shown to harbor CRF-CB1 double-positive cells. We found a reduction of gray value in CB1^{CKO-CRF} compared with wildtype mice in the anterior piriform cortex ($t_{12} = 3.9$, $p < 0.01$; Figure 1F) but not in the more posterior part of this area ($t_{14} = 0.8$, $p = 0.44$; Figure 1G).

3.3 | Baseline behavioral characterization of CB1^{CKO-CRF}

To assess behavioral consequences of the conditional knockout, we exposed male and female CB1^{CKO-CRF} and CB1^{Ctrl} mice to a battery of behavioral tests (Figure 2A). We found no significant differences between knockout and wildtype animals in a 15-min OFT, measuring the total distance traveled (males: $t_{20} = 0.14$, $p = 0.89$; females: $t_{22} = 0.46$, $p = 0.65$; Figure 2B) nor in the time spent in the inner and outer zone of the arena (males: $F_{(1,40)} = 2.25$, $p = 0.14$; females: $F_{(1,44)} = 0.56$, $p = 0.46$; Figure 2C). The mice were next tested in the EPM for anxiety-like behavior. No differences in the time spent in the open arms (males: $U = 46$, $p = 0.23$; females: $t_{22} = 1.60$, $p = 0.12$; Figure 2D) nor in the latency to enter the open arms (males: $U = 41$, $p = 0.13$; females: $U = 63$, $p = 0.62$; Figure 2E) were observed between the genotypes. Similarly, there were no differences in the time spent in the light compartment during a 15-min LDB test (males: $t_{21} = 0.28$, $p = 0.78$; females: $t_{22} = 1.06$, $p = 0.30$; Figure 2F) nor in defecation (males: $t_{21} = 0.25$, $p = 0.81$; females: $t_{22} = 0.17$, $p = 0.86$; Figure 2G).

To assess active versus passive fear responses to a potentially threatening stimulus, the animals were subjected to the BMT. We could not show any differences in the number of rearing events during the baseline period (males: $t_{21} = 0.12$, $p = 0.90$; females: $t_{22} = 0.00$, $p > 0.99$; Figure 2H). Also, upon confrontation with the robo-beetle, there was no significant difference in the avoidance behavior between the two genotypes (males: $t_{21} = 1.57$, $p = 0.13$; females: $t_{22} = 1.28$, $p = 0.21$; Figure 2I).

A new cohort of male and female CB1^{CKO-CRF} and CB1^{Ctrl} mice was tested for the ASR and for circulating CORT levels (Figure 3A).

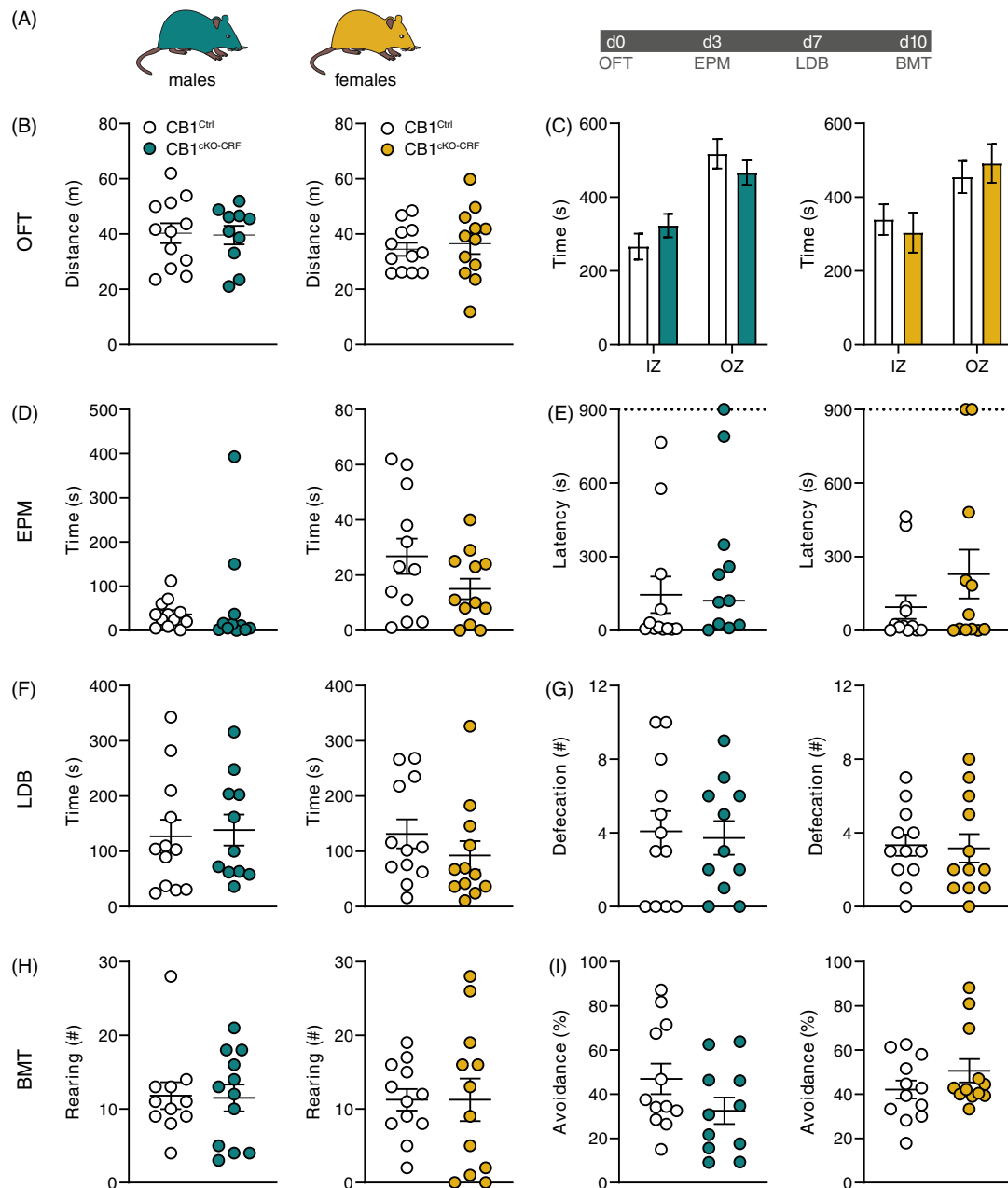


FIGURE 2 Baseline behavioral characterization. (A) CB1^{CKO-CRF} and CB1^{Ctrl} male ($n = 11/12$) and female ($n = 12/12$) mice were exposed to a behavioral test battery for baseline characterization. d, day. Distance moved (B) and time in the inner (IZ) and outer zone (OZ, C) in the open field test (OFT). Time spent in the open arms (D) and latency to the first open arm entry (E) in the elevated plus maze test (EPM). Time spent in the light zone (F) and defecation (G) during the light-dark box test (LDB). Number of rearing events (H) and avoidance behavior as a fraction of total contacts with the robo-beetle (I) during the Beetle Mania Task (BMT).⁴⁵

We exposed mice to white noise pulses of different intensity and measured the startle amplitude. As showed by 2-way ANOVA, there was a significant interaction between genotype and startle pulse intensity in male mice ($F_{3,69} = 4.47$, $p < 0.01$; Figure 3B) with post-hoc analysis confirming a higher startle amplitude of CB1^{CKO-CRF} at the highest white noise intensity (105 dB(A)) compared with wildtype controls. This effect could not be observed in female mice ($F_{3,66} = 0.16$, $p = 0.92$; Figure 3B). Next, mice were tested in a PPI task. No significant difference in the startle response could be shown

between CB1^{CKO-CRF} and wildtype mice (males: $F_{2,46} = 2.07$, $p = 0.14$; females: $F_{2,44} = 0.59$, $p = 0.56$; Figure 3C). After sufficient time for recovery, we measured basal and post-stress blood plasma CORT concentrations. Mice were restrained for 15 min and blood was sampled via a tail cut at the end of the restraint period (t15), as well as 30 (t30) and 90 (t90) min after the beginning of the stressor. Mice showed an increase in plasma CORT after the restraint, but there was no significant difference between the genotypes (males: $F_{3,69} = 0.75$, $p = 0.53$; females: $F_{3,63} = 0.48$, $p = 0.70$; Figure 3D).

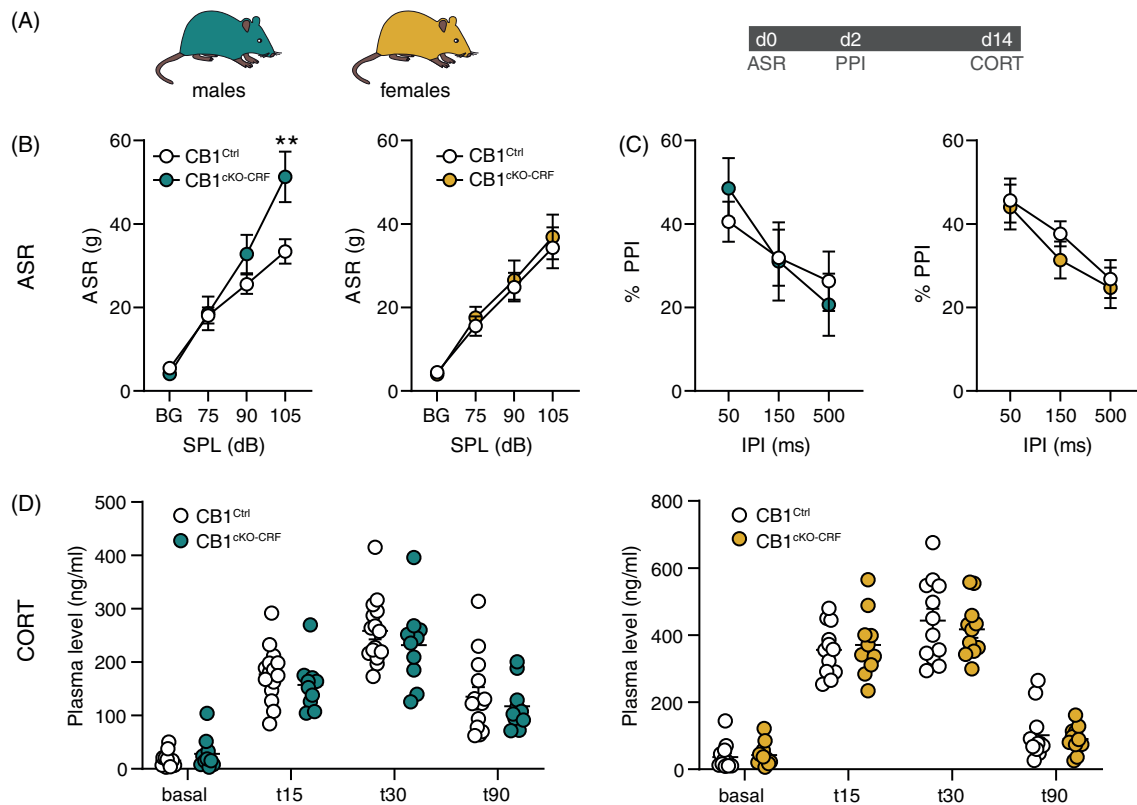


FIGURE 3 Startle response and CORT measurements. A new cohort of male and female CB1^{cKO-CRF} and CB1^{Ctrl} mice was tested for acoustic startle responses (ASR; $n_{\text{male}} = 13/12$, $n_{\text{female}} = 12/12$) and plasma corticosterone (CORT; $n_{\text{male}} = 11/15$, $n_{\text{female}} = 11/12$) levels. d: day (A). Intensity-response relationship between sound-pressure levels (SPL) of the white noise pulses and ASR (B). Prepulse inhibition (PPI) with different inter-pulse intervals (IPI, C). CORT blood plasma concentrations at basal and 15, 30, and 90 min after restraint stress (D). ** $p < 0.01$ (two-way rm-ANOVA followed by Bonferroni's post-hoc test)

3.4 | Behavioral characterization of CB1^{cKO-CRF} after trauma incubation

Both the CRF and CB1 systems are known to be involved in trauma-related behavioral changes. Therefore, we exposed experimentally naïve male and female CB1^{cKO-CRF} and wildtype controls to a trauma protocol. Mice were assigned to four experimental groups per sex, following a 2×2 design (genotype \times trauma). All groups were placed into a shock chamber, with two groups receiving two electric foot shocks of 1.5 mA (cKO-S+ and Ctrl-S+), while the other two groups remained non-shocked (cKO-S- and Ctrl-S-). Four weeks later, we assessed generalized trauma-associated fear followed by measurement of active and passive fear responses (Figure 4A). Mice that had received a foot shock froze significantly more (Kruskal-Wallis test; males: $p < 0.0001$; females: $p < 0.0001$; Figure 4B) and exhibited significantly fewer rearing events than non-shocked controls upon exposure to a neutral test context (Kruskal-Wallis test; males: $p < 0.0001$; females: $p < 0.0001$; Figure 4C). These observations were independent of genotype or sex. The same findings for freezing and rearing were shown when the mice were re-exposed to the shock context on the next day (Kruskal-Wallis test; males: $p < 0.0001$; females: $p < 0.0001$; Figure 4D,E).

Next, we tested the mice in the BMT to measure the consequences of trauma on active versus passive fear responses. During

the baseline period without robo-beetle, cKO-S+ mice showed significantly reduced vertical exploration behavior (rearing events) compared with cKO-S- (Kruskal-Wallis test; males: $p < 0.01$; females: $p < 0.001$) but there was no significant difference between CB1^{cKO-CRF} and CB1^{Ctrl} (Figure 4F). Avoidance behavior in response to the robo-beetle was unchanged between genotypes and trauma experience (males: $F_{3,39} = 0.88$, $p = 0.46$; females: $F_{3,40} = 2.09$, $p = 0.12$; Figure 4G).

4 | DISCUSSION

The current study investigated consequences of the selective deletion of CB1 receptors from CRF neurons by means of a newly generated conditional knockout mouse line (CB1^{cKO-CRF}). The cell-type specific lack of CB1 expression caused an increase in the ASR in male but not female mice with no consequences on locomotion, anxiety- and fear-related behavior and HPA axis activity. Likewise, no behavioral differences were found following trauma exposure.

In wildtype mice, we could show the co-localization of CB1 and CRF mRNA in the piriform cortex, the PVN, the lateral hypothalamic area, and the Barrington's nucleus. This is in agreement with previous studies, which additionally report co-expression in the prefrontal

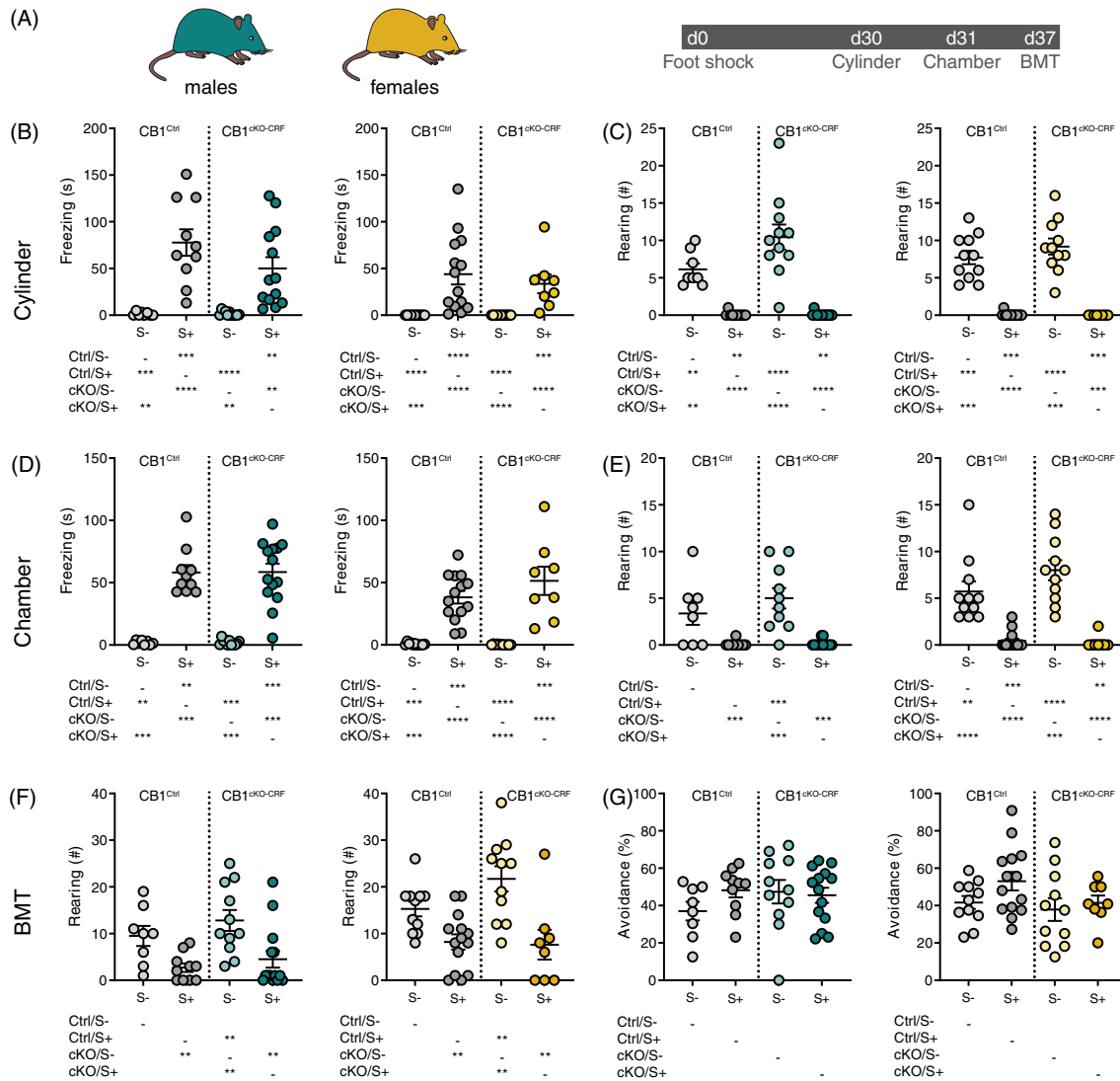


FIGURE 4 Behavioral characterization after trauma exposure. (A) Male ($n = 8-14$ per group) and female ($n = 8-14$ per group) CB1^{CKO-CRF} and CB1^{Ctrl} mice received two electric foot shocks of 1.5 mA (cKO-S+ and Ctrl-S+) or were assigned to the non-shocked control group (cKO-S- and Ctrl-S-). After an incubation time of 30 days, generalized and contextual fear were assessed in a novel (cylinder) and in the shock context (chamber), respectively. One week later, mice were exposed to the Beetle Mania Task (BMT). Time spent freezing (B) and number of rearing events (C) during exposure to the novel environment. Time spent freezing (D) and number of rearing events (E) during re-exposure to the shock environment. Number of rearing events (F) and avoidance behavior as a fraction of total contacts with the robo-beetle (G) during the BMT. ** $p < 0.01$, *** $p < 0.001$, **** $p < 0.0001$ (1-way ANOVA for B-E, G; Kruskal-Wallis test for F)

cortex, the BNST, and the amygdala.^{35,36} An immunohistochemical approach showed CB1 and CRF protein co-localization in the locus coeruleus in axon terminals of neurons projecting from the central amygdala (CeA).³⁷ Our failure to show co-localization in the amygdala might be ascribed to differences in the sensitivity of the methods and/or generally low levels of expression of both CB1 and CRF under basal conditions.

To study the consequences of CB1 loss on CRF-expressing neurons, we crossed CRF-IRES-Cre³⁸ and CB1-floxed³⁹ mouse lines. Both mutant mouse lines have been well investigated and successfully used for knockout and mapping studies.^{3,47-50} Using *in situ* hybridization, we could confirm a reduction of CB1 for the piriform cortex of CB1^{CKO-CRF}. Even though we did not perform co-expression analyses

in mutant mice due to the low abundant expression of both CRF and CB1, it is highly likely that this reduction results from the selective deletion of CB1 expression in CRF-positive neurons.

In order to study behavioral consequences of the knockout on the negative valence system, we exposed male and female mutants and their respective wildtype littermate controls to a variety of behavioral paradigms. We found no difference in locomotor activity or fear and anxiety-related behaviors between CB1^{CKO-CRF} and controls of both sexes. If we assume that the lack of CB1 receptors may result in unrestrained release of CRF, we would have expected increased locomotion and anxiety.^{6,9,10,51-54}

Male CB1^{CKO-CRF} showed an increased startle amplitude compared with male littermate controls. This is in line with previous

studies reporting increased ASR and decreased startle habituation following ICV administration of CRF or overexpression of CRF.^{15–17,55,56} The lack of an arousal effect in female CB1^{CKO-CRF} could be attributed to sex dimorphisms of the CRF system, as has been shown in terms of behavior, HPA axis function, and gene expression¹⁷ (for reviews see Reference [57,58]). We can only speculate about the pathway involved in the hyperarousal shown by male mutants. There is the likelihood of an involvement of projections from the CeA to the BNST.¹⁸ A contribution of CRF signaling within the CeA for the generation of active versus passive fear⁵⁹ however, appears to be less likely, given the lack of effects in the BMT, a test designed to measure unconditioned active versus passive fear.^{45,60,61} Besides, we could not reproduce the previously described co-localization of CRF and CB1 within the CeA.

Under basal conditions, our experiments showed no effects from the knockout on fear and anxiety. This might be due to a lack of activation of the CRF system under the experimental conditions. Exposure to a stressor has been found to increase CRF expression in various brain regions,⁶² and it has been suggested that endogenous CRF release must be triggered by a stressor prior to a paradigm in order to observe behavioral effects.⁶³ To challenge the CRF system, we exposed the mice to both an acute restraint followed by measurement of HPA axis activity and assessed behavior after incubation of a traumatic event.⁴⁶ Despite the well-described regulation of CB1 on the HPA axis, we failed to detect differences in plasma CORT levels between the genotypes, both at basal and post-stress time points. Likewise, no behavioral changes were observed after trauma exposure.

The very distinct behavioral phenotype of male CB1^{CKO-CRF} might be explained in several ways. We observed an overall low level of co-localization of CRF and CB1 throughout the brain, that is, only a low number of cells is affected by the knockout. Next, it is unclear whether these cells are activated at all during the tasks employed and whether enough CRF is released under basal conditions. Another important question is whether CRF release is even under control of CB1. Depolarization-induced suppression of excitation and inhibition are well-established concepts of CB1-controlled release of the neurotransmitters glutamate and GABA, respectively.^{64,65} Less is known about CB1 inhibiting the release of neuropeptides. A functional interaction of CB1 and the cholecystokinin (CCK) system in regulating fear memory has been shown.^{66,67} But while CCK and CB1 are very highly co-expressed for example in hippocampal basket cells, we observed an overall low abundant co-expression of CRF and CB1. Moreover, the possibility of neurotransmitter co-transmission must be borne in mind. CRF is mostly expressed in GABAergic neurons in the brain,^{68,69} with the exception of the piriform cortex and the PVN where it is expressed in glutamatergic neurons.^{70,71} Thus, whether the observed hyperarousal of male CB1^{CKO-CRF} can be attributed to disinhibited release of CRF or neurotransmitters remains to be confirmed using CRFR1 or CRFR2 antagonists or new genetic models.

In conclusion, we show a selective increase in the ASR of male mice lacking CB1 receptor expression in CRF neurons with no alterations in the negative valence system and HPA axis activity.

ACKNOWLEDGMENTS

We thank Andrea Ressler and the Scientific Core Unit for Genetically Engineered Mouse Models for performing the genotyping of the mouse line. We would like to thank Dr. Jessica Keverne for proofreading of the manuscript.

Julia Ruat was supported by the International Max Planck Research School for Translational Psychiatry (IMPRS-TP). Alice Hartmann received a fellowship from Fundação de Amparo à Pesquisa do Estado de São Paulo (FAPESP; BEPE-2018/17387-9). Daniel E. Heinz was supported by the Federal Ministry of Education and Research (BMBF) and the Max Planck Society. Alon Chen is the incumbent of the Vera and John Schwartz Professorial Chair in Neurobiology at the Weizmann Institute of Science; the Head of the Max Planck Society–Weizmann Institute of Science Laboratory for Experimental Neuropsychiatry and Behavioral Neurogenetics gratefully funded by the Max Planck Foundation; and the Head of Ruhman Family Laboratory for Research in the Neurobiology of Stress at the Weizmann Institute of Science. This work is supported by Bruno and Simone Licht (AC) and Roberto and Renata Ruhman. This study was further supported by the German-Israeli Foundation for Scientific Research and Development (GIF; I-1442-421. 13/2017) to Carsten T. Wotjak.

CONFLICT OF INTEREST

The authors declare no conflict of interest.

DATA AVAILABILITY STATEMENT

The data that support the findings of this study are available from the corresponding author upon reasonable request.

ORCID


Julia Ruat  <https://orcid.org/0000-0002-0751-080X>

Alice Hartmann  <https://orcid.org/0000-0002-8355-8100>

Daniel E. Heinz  <https://orcid.org/0000-0001-7103-9621>

Paulina Nemcova  <https://orcid.org/0000-0002-0323-8079>

Jan M. Deussing  <https://orcid.org/0000-0002-9329-5252>

Alon Chen  <https://orcid.org/0000-0003-3625-8233>

Carsten T. Wotjak  <https://orcid.org/0000-0002-2159-5379>

REFERENCES

1. Deussing JM, Chen A. The corticotropin-releasing factor family: physiology of the stress response. *Physiol Rev.* 2018;98:2225–2286.
2. Lutz B, Marsicano G, Maldonado R, Hillard CJ. The endocannabinoid system in guarding against fear, anxiety and stress. *Nat Rev Neurosci.* 2015;16:705–718.
3. Dedic N, Kühne C, Jakovcevski M, et al. Chronic CRH depletion from GABAergic, long-range projection neurons in the extended amygdala reduces dopamine release and increases anxiety. *Nat Neurosci.* 2018; 21:803–807.
4. Refojo D, Schweizer M, Kuehne C, et al. Glutamatergic and dopaminergic neurons mediate anxiogenic and anxiolytic effects of CRHR1. *Science.* 2011;333:1903–1907.
5. Britton DR, Koob GF, Rivier J, Vale M. Intraventricular corticotropin-releasing factor enhances behavioral effects of novelty. *Life Sci.* 1982; 31:363–367.

6. Dedic N, Touma C, Romanowski CP, et al. Assessing behavioural effects of chronic HPA axis activation using conditional CRH-overexpressing mice. *Cell Mol Neurobiol*. 2012;32:815-828.
7. Müller MB, Zimmermann S, Sillaber I, et al. Limbic corticotropin-releasing hormone receptor 1 mediates anxiety-related behavior and hormonal adaptation to stress. *Nat Neurosci*. 2003;6:1100-1107.
8. Regev L, Neufeld-Cohen A, Tsoory M, et al. Prolonged and site-specific over-expression of corticotropin-releasing factor reveals differential roles for extended amygdala nuclei in emotional regulation. *Mol Psychiatry*. 2011a;16:714-728.
9. Spina M, Merlo-Pich E, Akwa Y, et al. Time-dependent induction of anxiogenic-like effects after central infusion of urocortin or corticotropin-releasing factor in the rat. *Psychopharmacology (Berl)*. 2002;160:113-121.
10. Stenzel-Poore MP, Heinrichs SC, Rivest S, Koob GF, Vale WW. Overproduction of corticotropin-releasing factor in transgenic mice: a genetic model of anxiogenic behavior. *J Neurosci*. 1994;14:2579-2584.
11. Skutella T, Criswell H, Moy S, et al. Corticotropin-releasing hormone (crh) antisense oligodeoxynucleotide induces anxiolytic effects in rat. *Neuroreport*. 1994a;5:2181-2185.
12. Skutella T, Montkowski A, Stöhr T, et al. Corticotropin-releasing hormone (CRH) antisense oligodeoxynucleotide treatment attenuates social defeat-induced anxiety in rats. *Cell Mol Neurobiol*. 1994b;14:579-588.
13. Baker DG, West SA, Nicholson WE, et al. Serial CSF corticotropin-releasing hormone levels and adrenocortical activity in combat veterans with posttraumatic stress disorder. *Am J Psychiatry*. 1999;156:585-588.
14. Bremner JD, Licinio J, Darnell A, et al. Elevated CSF corticotropin-releasing factor concentrations in posttraumatic stress disorder. *Am J Psychiatry*. 1997;154:624-629.
15. Flandreau E, Risbrough V, Lu A, et al. Cell type-specific modifications of corticotropin-releasing factor (CRF) and its type 1 receptor (CRF1) on startle behavior and sensorimotor gating. *Psychoneuroendocrinology*. 2015;53:16-28.
16. Swerdlow NR, Geyer MA, Vale WW, Koob GF. Corticotropin-releasing factor potentiates acoustic startle in rats: blockade by chloridiazepoxide. *Psychopharmacology (Berl)*. 1986;88:147-152.
17. Toth M, Gresack JE, Bangasser DA, et al. Forebrain-specific CRF overproduction during development is sufficient to induce enduring anxiety and startle abnormalities in adult mice. *Neuropsychopharmacology*. 2014;39:1409-1419.
18. Walker D, Yang Y, Ratti E, Corsi M, Trist D, Davis M. Differential effects of the CRF-R1 antagonist GSK876008 on fear-potentiated, light- and CRF-enhanced startle suggest preferential involvement in sustained vs phasic threat responses. *Neuropsychopharmacology*. 2009;34:1533-1542.
19. Jacob W, Yassouridis A, Marsicano G, Monory K, Lutz B, Wotjak CT. Endocannabinoids render exploratory behaviour largely independent of the test aversiveness: role of glutamatergic transmission. *Genes Brain Behav*. 2009;8:685-698.
20. Hill MN, Bierer LM, Makotkine I, et al. Reductions in circulating endocannabinoid levels in individuals with post-traumatic stress disorder following exposure to the world trade center attacks. *Psychoneuroendocrinology*. 2013;38:2952-2961.
21. Neumeister A, Normandin MD, Pietrzak RH, et al. Elevated brain cannabinoid CB 1 receptor availability in post-traumatic stress disorder: a positron emission tomography study. *Mol Psychiatry*. 2013;18:1034-1040.
22. Balsevich G, Petrie GN, Hill MN. Endocannabinoids: effectors of glucocorticoid signaling. *Front Neuroendocrinol*. 2017;47:86-108.
23. Steiner MA, Wotjak CT. Role of the endocannabinoid system in regulation of the hypothalamic-pituitary-adrenocortical axis. *In Progress in Brain Research*. 2008;170:397-432.
24. Di S, Malcher-Lopes R, Halmos KC, Tasker JG. Nongenomic glucocorticoid inhibition via endocannabinoid release in the hypothalamus: a fast feedback mechanism. *J Neurosci*. 2003;23:4850-4857.
25. Tasker JG, Herman JP. Mechanisms of rapid glucocorticoid feedback inhibition of the hypothalamic-pituitary-adrenal axis. *Stress*. 2011;14:398-406.
26. Ganon-Elazar E, Akirav I. Cannabinoid receptor activation in the basolateral amygdala blocks the effects of stress on the conditioning and extinction of inhibitory avoidance. *J Neurosci*. 2009;29:11078-11088.
27. Gray JM, Vecchiarelli HA, Morena M, et al. Corticotropin-releasing hormone drives anandamide hydrolysis in the amygdala to promote anxiety. *J Neurosci*. 2015;35:3879-3892.
28. Gray JM, Wilson CD, Lee TTY, et al. Sustained glucocorticoid exposure recruits cortico-limbic CRH signaling to modulate endocannabinoid function. *Psychoneuroendocrinology*. 2016;66:151-158.
29. Hill MN, McLaughlin RJ, Bingham B, et al. Endogenous cannabinoid signaling is essential for stress adaptation. *Proc Natl Acad Sci U S A*. 2010;107:9406-9411.
30. Hill MN, McLaughlin RJ, Morrish AC, et al. Suppression of amygdalar endocannabinoid signaling by stress contributes to activation of the hypothalamic-pituitary-adrenal axis. *Neuropsychopharmacology*. 2009;34:2733-2745.
31. Natividad LA, Buczynski MW, Herman MA, et al. Constitutive increases in Amygdalar Corticotropin-releasing factor and fatty acid amide hydrolase drive an anxious phenotype. *Biol Psychiatry*. 2017;82:500-510.
32. Patel S, Roelke CT, Rademacher DJ, Hillard CJ. Inhibition of restraint stress-induced neural and behavioural activation by endogenous cannabinoid signalling. *Eur J Neurosci*. 2005;21:1057-1069.
33. Rademacher DJ, Meier SE, Shi L, Vanessa Ho WS, Jarrahan A, Hillard CJ. Effects of acute and repeated restraint stress on endocannabinoid content in the amygdala, ventral striatum, and medial prefrontal cortex in mice. *Neuropharmacology*. 2008;54:108-116.
34. Hill MN, McLaughlin RJ, Pan B, et al. Recruitment of prefrontal cortical endocannabinoid signaling by glucocorticoids contributes to termination of the stress response. *J Neurosci*. 2011;31:10506-10515.
35. Cota D, Marsicano G, Tschöp M, et al. The endogenous cannabinoid system affects energy balance via central orexigenic drive and peripheral lipogenesis. *J Clin Invest*. 2003;112:423-431.
36. Cota D, Steiner MA, Marsicano G, et al. Requirement of cannabinoid receptor type 1 for the basal modulation of hypothalamic-pituitary-adrenal axis function. *Endocrinology*. 2007;148:1574-1581.
37. Wyrofsky RR, Reyes BAS, Van Bockstaele EJ. Co-localization of the cannabinoid type 1 receptor with corticotropin-releasing factor-containing afferents in the noradrenergic nucleus locus coeruleus: implications for the cognitive limb of the stress response. *Brain Struct Funct*. 2017;222:3007-3023.
38. Taniguchi H, He M, Wu P, et al. A resource of Cre driver lines for genetic targeting of GABAergic neurons in cerebral cortex. *Neuron*. 2011;71:995-1013.
39. Marsicano G, Goodenough S, Monory K, et al. CB1 cannabinoid receptors and on-demand defense against excitotoxicity. *Science*. 2003;302:84-88.
40. Lebow M, Neufeld-Cohen A, Kuperman Y, Tsoory M, Gil S, Chen A. Susceptibility to PTSD-like behavior is mediated by corticotropin-releasing factor receptor type 2 levels in the bed nucleus of the stria terminalis. *J Neurosci*. 2012;32:6906-6916.
41. Thoeniger CK, Henes K, Eder M, et al. Consolidation of remote fear memories involves corticotropin-releasing hormone (CRH) receptor type 1-mediated enhancement of AMPA receptor GluR1 signaling in the dentate gyrus. *Neuropsychopharmacology*. 2012;37:787-796.
42. Hill MN, Campolongo P, Yehuda R, Patel S. Integrating Endocannabinoid signaling and cannabinoids into the biology and treatment of posttraumatic stress disorder. *Neuropsychopharmacology*. 2018;43:80-102.

43. Sbarski B, Akirav I. Cannabinoids as therapeutics for PTSD. *Pharmacol Ther.* 2020;211:107551.
44. Schindelin J, Arganda-Carreras I, Frise E, et al. Fiji: an open-source platform for biological-image analysis. *Nat Methods.* 2012;9:676-682.
45. Heinz DE, Genewsky A, Wotjak CT. Enhanced anandamide signaling reduces flight behavior elicited by an approaching robo-beetle. *Neuropharmacology.* 2017;126:233-241.
46. Siegmund A, Wotjak CT. A mouse model of posttraumatic stress disorder that distinguishes between conditioned and sensitised fear. *J Psychiatr Res.* 2007;41:848-860.
47. Ezra-Nevo G, Volk N, Ramot A, et al. Inferior olive CRF plays a role in motor performance under challenging conditions. *Transl Psychiatry.* 2018;8:107.
48. Monory K, Polack M, Remus A, Lutz B, Korte M. Cannabinoid CB1 receptor calibrates excitatory synaptic balance in the mouse hippocampus. *J Neurosci.* 2015;35:3842-3850.
49. Soria-Gómez E, Bellocchio L, Reguero L, et al. The endocannabinoid system controls food intake via olfactory processes. *Nat Neurosci.* 2014;17:407-415.
50. Wamsteeker Cusulin JI, Füzesi T, Watts AG, Bains JS. Characterization of Corticotropin-releasing hormone neurons in the Paraventricular nucleus of the hypothalamus of Crh-IRES-Cre mutant mice. *PLoS One.* 2013;8:1-10.
51. Britton KT, Lee G, Dana R, Risch SC, Koob GF. Activating and “anxiogenic” effects of corticotropin releasing factor are not inhibited by blockade of the pituitary-adrenal system with dexamethasone. *Life Sci.* 1986;39:1281-1286.
52. Butler PD, Weiss JM, Stout JC, Nemeroff CB. Corticotropin-releasing factor produces fear-enhancing and behavioral activating effects following infusion into the locus coeruleus. *J Neurosci.* 1990;10:176-183.
53. Flandreau EI, Ressler KJ, Owens MJ, Nemeroff CB. Chronic overexpression of corticotropin-releasing factor from the central amygdala produces HPA axis hyperactivity and behavioral anxiety associated with gene-expression changes in the hippocampus and paraventricular nucleus of the hypothalamus. *Psychoneuroendocrinology.* 2012;37:27-38.
54. Regev L, Neufeld-Cohen A, Tsoory M, et al. Prolonged and site-specific over-expression of corticotropin-releasing factor reveals differential roles for extended amygdala nuclei in emotional regulation. *Mol Psychiatry.* 2011b;16:714-728.
55. Dirks A, Groenink L, Schipholt MI, et al. Reduced startle reactivity and plasticity in transgenic mice overexpressing corticotropin-releasing hormone. *Biol Psychiatry.* 2002;51:583-590.
56. Liang KC, Melia KR, Miserendino MJD, Falls WA, Campeau S, Davis M. Corticotropin-releasing factor: long-lasting facilitation of the acoustic startle reflex. *J Neurosci.* 1992;12:2303-2312.
57. Bangasser DA, Valentino RJ. Sex differences in stress-related psychiatric disorders: neurobiological perspectives. *Front Neuroendocrinol.* 2014;35:303-319.
58. Brivio E, Lopez JP, Chen A. Sex differences: transcriptional signatures of stress exposure in male and female brains. *Genes Brain Behav.* 2020;19:1-22.
59. Fadok JP, Krabbe S, Markovic M, et al. A competitive inhibitory circuit for selection of active and passive fear responses. *Nature.* 2017;542:96-99.
60. Almada RC, Genewsky AJ, Heinz DE, Kaplick PM, Coimbra NC, Wotjak CT. Stimulation of the nigroreticular pathway at the level of the superior colliculus reduces threat recognition and causes a shift from avoidance to approach behavior. *Front Neural Circuits.* 2018;12:1-9.
61. Heinz DE, Schöttle VA, Nemcova P, et al. Exploratory drive, fear, and anxiety are dissociable and independent components in foraging mice. *Transl Psychiatry.* 2021;11:318.
62. Hill MN, Hellemans KGC, Verma P, Gorzalka BB, Weinberg J. Neurobiology of chronic mild stress: parallels to major depression. *Neurosci Biobehav Rev.* 2012;36:2085-2117.
63. Lu A, Steiner MA, Whittle N, et al. Conditional mouse mutants highlight mechanisms of corticotropin-releasing hormone effects on stress-coping behavior. *Mol Psychiatry.* 2008;13:1028-1042.
64. Kreitzer AC, Regehr WG. Cerebellar depolarization-induced suppression of inhibition is mediated by endogenous cannabinoids. *J Neurosci.* 2001;21:1-5.
65. Wilson RI, Nicoll RA. Endogenous cannabinoids mediate retrograde signalling at hippocampal synapses. *Nature.* 2001;410:588-592.
66. Bowers ME, Ressler KJ. Interaction between the cholecystokinin and endogenous cannabinoid systems in cued fear expression and extinction retention. *Neuropsychopharmacology.* 2015;40:688-700.
67. Chhatwal JP, Gutman AR, Maguschak KA, et al. Functional interactions between endocannabinoid and CCK neurotransmitter systems may be critical for extinction learning. *Neuropsychopharmacology.* 2009;34:509-521.
68. Chen Y, Brunson KL, Adelman G, Bender RA, Frotscher M, Baram TZ. Hippocampal corticotropin releasing hormone: pre- and postsynaptic location and release by stress. *Neuroscience.* 2004;126:533-540.
69. Kubota Y, Shigematsu N, Karube F, et al. Selective coexpression of multiple chemical markers defines discrete populations of neocortical gabaergic neurons. *Cereb Cortex.* 2011;21:1803-1817.
70. Dabrowska J, Hazra R, Guo J-D, DeWitt S, Rainnie DG. Central CRF neurons are not created equal: phenotypic differences in CRF-containing neurons of the rat paraventricular hypothalamus and the bed nucleus of the stria terminalis. *Front Neurosci.* 2013;7:156.
71. Kono J, Konno K, Talukder AH, et al. Distribution of corticotropin-releasing factor neurons in the mouse brain: a study using corticotropin-releasing factor-modified yellow fluorescent protein knock-in mouse. *Brain Struct Funct.* 2017;222:1705-1732.

How to cite this article: Ruat J, Hartmann A, Heinz DE, et al. CB1 receptors in corticotropin-releasing factor neurons selectively control the acoustic startle response in male mice. *Genes, Brain and Behavior.* 2021;e12775. doi: 10.1111/gbb.12775

2.2. Structural Correlates of Trauma-Induced Hyperarousal in Mice

Ruat J, Heinz DE, Binder FP, Stark T, Neuner R, Hartmann A, Kaplick PM, Chen A, Czisch M, Wotjak CT

Originally published in *Progress in Neuro-Psychopharmacology & Biological Psychiatry*.

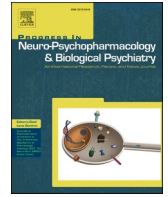
2021, July 22 (available online)

DOI: [10.1016/j.pnpbp.2021.110404](https://doi.org/10.1016/j.pnpbp.2021.110404)



Contents lists available at ScienceDirect

Progress in Neuropsychopharmacology & Biological Psychiatry

journal homepage: www.elsevier.com/locate/pnp

Structural correlates of trauma-induced hyperarousal in mice

Julia Ruat^{a,b}, Daniel E. Heinz^{c,d}, Florian P. Binder^{b,e}, Tibor Stark^{f,g}, Robert Neuner^{c,1}, Alice Hartmann^c, Paul M. Kaplick^c, Alon Chen^{a,h}, Michael Czisch^f, Carsten T. Wotjak^{c,d,i,*}

^a Department Stress Neurobiology and Neurogenetics, Max Planck Institute of Psychiatry, 80804 Munich, Germany

^b International Max Planck Research School for Translational Psychiatry (IMPRS-TP), 80804 Munich, Germany

^c Research Group Neuronal Plasticity, Max Planck Institute of Psychiatry, 80804 Munich, Germany

^d Max Planck School of Cognition, 04103 Leipzig, Germany

^e Department Translational Research in Psychiatry, Max Planck Institute of Psychiatry, 80804 Munich, Germany

^f Scientific Core Unit Neuroimaging, Max Planck Institute of Psychiatry, 80804 Munich, Germany

^g Department of Pharmacology, Faculty of Medicine, Masaryk University, 62500 Brno, Czechia

^h Department of Neurobiology, Weizmann Institute of Science, 76100 Rehovot, Israel

ⁱ Central Nervous System Diseases Research (CNSDR), Boehringer Ingelheim Pharma GmbH & Co KG, 88397, Biberach an der Riss, Germany

ARTICLE INFO

Keywords:

Post-traumatic stress disorder

Hyperarousal

Magnetic resonance imaging

Grey matter volume

Animal model

ABSTRACT

Post-traumatic stress disorder (PTSD) is a chronic disease caused by traumatic incidents. Numerous studies have revealed grey matter volume differences in affected individuals. The nature of the disease renders it difficult to distinguish between *a priori* versus *a posteriori* changes. To overcome this difficulty, we studied the consequences of a traumatic event on brain morphology in mice before and 4 weeks after exposure to brief foot shocks (or sham treatment), and correlated morphology with symptoms of hyperarousal. In the latter context, we assessed hyperarousal upon confrontation with acoustic, visual, or composite (acoustic/visual/tactile) threats and integrated the individual readouts into a single Hyperarousal Score using logistic regression analysis. MRI scans with subsequent whole-brain deformation-based morphometry (DBM) analysis revealed a volume decrease of the dorsal hippocampus and an increase of the reticular nucleus in shocked mice when compared to non-shocked controls. Using the Hyperarousal Score as regressor for the post-exposure MRI measurement, we observed negative correlations with several brain structures including the dorsal hippocampus. If the development of changes with respect to the basal MRI was considered, reduction in globus pallidus volume reflected hyperarousal severity. Our findings demonstrate that a brief traumatic incident can cause volume changes in defined brain structures and suggest the globus pallidus as an important hub for the control of fear responses to threatening stimuli of different sensory modalities.

1. Introduction

Post-traumatic stress disorder (PTSD) is a severe psychiatric disease that may develop after an exposure to a traumatic event such as combat experience, natural disasters or sexual abuse. It is characterized by intrusive symptoms, avoidance behavior, negative changes in thought, and hyperarousal, with these symptoms persisting for longer than a month (Del Barrio, 2016). During the last decades, numerous studies aimed at examining molecular and brain morphological changes occurring in the aftermath of the traumatic incident. Key brain areas of interest became the hippocampus, the prefrontal cortex, and the amygdala (Armony et al., 2005; Gilbertson et al., 2002; O'Doherty et al.,

2015; Shin et al., 2004; Wignall et al., 2004; Woodward et al., 2006; Yamasue et al., 2003). Neuroimaging methods, such as magnetic resonance imaging (MRI), allow to assess brain volumetric changes of patients diagnosed with PTSD. However, human studies come with the limitations of heterogenous samples (e.g., severity of the trauma or medical treatment) and methodology, often leading to controversial results. While a number of studies found no volumetric changes in the hippocampus of patients with PTSD (Bonne et al., 2001; Carrion et al., 2001; De Bellis et al., 2001; Fennema-Notestine et al., 2002), others reported reduced hippocampal volume compared to controls (Gilbertson et al., 2002; Logue et al., 2018; Wignall et al., 2004). Noteworthy, such studies rarely involved longitudinal designs with measurements before

* Corresponding author at: Research Group Neuronal Plasticity, Max Planck Institute of Psychiatry, Kraepelinstrasse 2-10, 80804 Munich, Germany.

E-mail address: wotjak@psych.mpg.de (C.T. Wotjak).

¹ deceased.

<https://doi.org/10.1016/j.pnpbp.2021.110404>

Received 4 May 2021; Received in revised form 23 June 2021; Accepted 17 July 2021

Available online 22 July 2021

0278-5846/© 2021 Published by Elsevier Inc.

and after the trauma. This gains particular importance if one considers that a priori differences in brain volume may serve as susceptibility/resilience factors for the development of PTSD (Gilbertson et al., 2002) and not necessarily consequences of the trauma. Therefore, the monitoring of intraindividual trajectories of brain volume appears to be the most sensitive measure of PTSD-related changes in grey matter volume. To overcome these limitations, several rodent models of PTSD have been established (for reviews see Deslauriers et al., 2018; Verbitsky et al., 2020). We have previously studied consequences of a traumatic experience (*i.e.*, exposure to an electric foot shock (Siegmond and Wotjak, 2007)) on hippocampal volume of inbred mice using *in vivo* and *ex vivo* approaches after long-term incubation of the trauma (Golub et al., 2011). We observed a reduced hippocampal volume (Golub et al., 2011), which coincided with a reduction in synaptic markers at late time points after the trauma (Herrmann et al., 2012). The present study should extend those observations to within-subject measurements before and after the trauma. Moreover, we employed voxel-based whole brain analyses rather than region of interest measurements. In a two-step process, we initially assessed the behavioral consequences of exposure to an inescapable electric foot shock after trauma incubation, with particular focus on the hyperarousal domain. Classically, hyperarousal is measured as a startle response to a sudden loud noise. It is unclear to which extent hyperarousal can be seen in response to stimuli of different sensory modality, such as visual or tactile threats. Based on the various behavioral data, we performed a logistic regression analysis to obtain individual "Hyperarousal Scores" that allowed us to distinguish trauma-exposed animals and controls. In a second step, we conducted longitudinal measurements of brain morphometry using whole-brain MRI scans in new cohorts of mice. Animals were subjected to a basal MRI prior to the foot shock. After trauma incubation, the animals underwent a second MRI scan and subsequent behavioral screening. This experimental design permitted both cross-sectional and longitudinal within-subject analyses. In addition, we could use the individual Hyperarousal Scores as regressors to identify brain structures which reflect changes in hyperarousal in a parametric rather than categorical manner.

2. Materials & methods

2.1. Animals

Adult male C57BL/6NRjMpi mice (B6NR, originating from Janvier; $n = 67$, 2–5 months age) were bred in the vivarium of the Max Planck Institute of Biochemistry (Martinsried, Germany). Due to changes in the animal facility of the Max Planck Institute of Psychiatry, the two cohorts of mice had to be housed under different conditions. Animals of the first cohort were group-housed under standard housing conditions in Makrolon type II cages with food and water *ad libitum* and maintained in a 12/12-h inverse light/dark cycle (lights off at 6 am). Behavioral testing took place during the active phase of the mice (between 7 am and 5 pm), except for the trauma protocol which was performed during the light phase. The second cohort of mice was group-housed in Green Line IVC mouse cages with food and water *ad libitum* and maintained in a 12/12-h normal light/dark cycle (lights on at 6 am). Behavioral testing took place during the light phase (between 7 am and 5 pm). After admission at the Max Planck Institute of Psychiatry, mice were permitted a recovery period of at least 10 days before starting with the experiments. Experimental procedures were approved by the Government of Upper Bavaria (Regierung von Oberbayern, 55.2-2532.Vet_02-17-206) and performed according to the European Community Council Directive 2010/63/EEC. All efforts were made to reduce the number of experimental subjects and to minimize, if not exclude, any suffering.

2.2. Behavioral procedures

2.2.1. Trauma protocol

Foot shock delivery and assessment of sensitized and conditioned fear has been performed as previously described (Siegmond and Wotjak,

2007). In brief: On day 0, mice were placed onto a metal grid in a conditioning chamber (cubic shaped) that had been cleaned with alcohol-based disinfectant (Pursept A, Schülke & Mayr GmbH, Norderstedt, Germany). After 198 s, they received two electric foot shocks of 1.5 mA (duration: 2 s), interspaced by 60 s. They were returned to their home cage another 60 s later. Animals of the control group underwent the same procedure without receiving a foot shock. To assess trauma-related sensitized fear, all animals were placed into a neutral test context (cylindrical Plexiglas wall, no metal grid but bedding, supplemented with 1% acetic acid) for 3 min 23–35 days after foot shock delivery. On the following day, conditioned fear was tested by re-exposing the mice for 3 min to the conditioning context (chamber, cleaned with Pursept A). The sessions were video-recorded, and the following behavioral measures were scored by an experienced observer unaware of the group affiliations: Freezing time, number of rearings and stretch-attend postures (SAPs).

2.3. Acoustic Startle Response (ASR)

Stimulus-response curves were performed using the SR-LAB Startle Response System (San Diego Instruments, San Diego, USA) with a custom-built animal enclosure. The enclosure consisted of black plastic walls (H17 cm) sitting on the upward bended edges of a plastic floor (L5 x W9 cm). During testing, the enclosure was covered with a lid to prevent the mice from escaping. Movement was detected by a piezo element mounted under the floor of the enclosure and connected to the control unit of the SR-LAB system. The enclosure was placed into a cabinet with the fan turned on. The intensity-response curve protocol consisted of a 5-min habituation period followed by 20 ms white noise pulses of 70 dB (A), 90 dB(A), and 105 dB(A). The pulses were each presented 30 times in a pseudo-randomized order, interspersed with 18 control trials (background noise only, 55 dB(A)). Inter-trial intervals were 13–25 s in length. The startle amplitude was defined as the peak voltage output within the first 100 ms after stimulus onset. The enclosure was cleaned with soap and water after each trial.

2.3.1. Beetle Mania Task (BMT)

The Beetle Mania Task (BMT) was used to study defensive reactions to a combined visual, acoustic, and tactile threat as previously described (Heinz et al., 2017). In brief: Experiments were performed in an arena (L150 × W15 × H37 cm for Experiment 1 and L100 × W15 × H37 cm for Experiment 2) made of grey polyethylene under low light conditions (<50 lx). During the initial habituation phase of 5 min, mice were inserted to one end of the arena, and the latency to reach the opposite end segment as well as the number of rearings were scored. In the end of the habituation phase, we inserted an erratically moving robo-beetle (Hexbug Nano, Innovation First Labs Inc., Greenville, TX, USA) far most distant from the mouse and scored the following behavioral measures over the course of 10 min: (1) contacts (number of physical contacts between the beetle and the mouse), (2) passive behavior (tolerance of the approaching or by-passing beetle), (3) avoidance behavior (whereby the mouse withdrew from the robo-beetle with accelerated speed), (4) approach behavior (events during which the mouse followed the by-passing robo-beetle in close vicinity), and (5) jumps. The behavioral measures (2)–(5) were expressed as the percentage of the number of contacts.

2.3.2. Visual Threat Task (VTT)

This task exposed the animals to two visual threats: a sweeping dot (SD) (De Franceschi et al., 2016), followed by a looming disk (LD) (Yilmaz and Meister, 2013). The visual stimuli were presented in a white Plexiglas arena (L34 x W47 x H30 cm; 70 lx in the center) equipped with an opaque triangular shelter (W19 x H11.5 cm; 10 lx) in the corner (De Franceschi et al., 2016). A monitor (L30 x W47.5 cm, Samsung SyncMaster T220, 60 Hz) was placed on top of the arena, leaving a gap for the camera (DMK 23UV024, The Imaging Source) to capture the mouse

movements. The SD stimulus was a black dot of 3 cm diameter presented in one corner of the display. The dot moved diagonally over the screen four times with a speed of 0.1 m/s. The LD stimulus was a black dot of 3 cm diameter presented in the center of the screen, that expanded in size to 21 cm diameter within 250 ms. The stimulus was repeated 20 times. Both stimuli had a total duration of 20 s and were presented on a grey background. The VTT was performed on two consecutive days. On the first day, the animals were habituated to the arena for 15 min without behavioral analysis. During this time, the arena was covered with the monitor presenting the grey screen without any stimulus. On the next day, animals were habituated to the arena for another 5 min (baseline), with presentation of the grey screen. Thereafter, the sweeping stimulus was triggered, and the behavior was recorded for 5 min after stimulus onset. In the third phase, the looming disk stimulus was presented, and the behavior was monitored for another 5 min. The stimuli were only triggered once the animals were located in the center of the arena. The test was stopped, and the behavior not further analyzed, if an animal failed to leave the shelter for 30 min. Therefore, the total test time could differ significantly between the animals. We considered the following behavioral measures: Number of rearings, freezing duration, the time spent in the shelter, and the latency to enter the shelter after the onset of the stimulus (if a mouse did not enter the shelter within the 20 s after stimulus onset, we assigned an escape latency of 21 s).

2.3.3. *In vivo magnetic resonance imaging (MRI) and deformation-based morphometry (DBM) analysis*

Anesthesia was initiated and maintained using isoflurane (cp-pharma, Burgdorf, Germany). Mice were then stereotactically fixed on an MR compatible animal bed in prone position. Eye ointment (Bepanthen, BAYER AG, Leverkusen, Germany) was applied to protect the eyes from dehydration. Respiration and body temperature were constantly monitored. Body temperature was kept between 36.5 °C and 37.5 °C, using a water flow heating pad (Haake S 5P, Thermo Fisher Scientific, Waltham, United States).

MRI experiments were run on a BioSpec 94/20 animal MRI system operating on Paravision 6.0.1 (Bruker BioSpin GmbH Rheinstetten, Germany) equipped with a 9.4 T horizontal bore magnet of 20 cm diameter and a two-channel cryogenic transmit-receive radio frequency coil. Structural images were recorded using a 3D gradient echo sequence with a repetition time of 34.1 ms, echo time = 6.25 ms, excitation pulse angle = 10°, number of averages = 3, matrix dimension = 256 × 166 × 205, pixel resolution 77 μm. After visual inspection of the data and exclusion of certain mice due to motion artefacts, a total of 20 animals were included in the final analysis.

Images were converted to NIFTI format, with the voxel size of mice image data artificially multiplied by ten (in order to fully exploit analysis pipelines optimized for the human sized brain).

In a two-step procedure, brain extraction was performed: In a first preprocessing step, mouse data was segmented and bias corrected using Statistical Parametric Mapping software (SPM12, Wellcome Department of Cognitive Neurology, London, UK) and the Hikishima C57Bl6 template (Hikishima et al., 2017) comprised of 5 different compartments. The resulting bias-corrected images were filtered using a spatial adaptive non-local means denoising filter (Manjón et al., 2010) as implemented in the cat12 toolbox of SPM (www.neuro.uni-jena.de/cat). The initial grey matter (GM), white matter (WM) and cerebrospinal fluid (CSF) probability maps were summed, and binarized for image intensities larger 0.3, to create a first brain mask. Holes in this mask were filled using MATLAB's (MathWorks, Natick, Massachusetts, USA) `imfill` function, the mask was dilated by five voxels, and applied to the bias-corrected spatially filtered images. In a second step, the resulting images were again segmented, this time using a modified version of the Hikishima template for which the original CSF template was divided into two sub-templates: ventricular inner CSF and surface cortical CSF. After this second segmentation step, GM, WM and ventricular inner CSF compartments were again summed, binarized using an intensity threshold >0.1,

and remaining holes inside the brain mask filled and slightly dilated. Finally, the resulting mask was applied to the spatially filtered and bias corrected images of the first step. These brain-extracted 3D images were then segmented using the SPM12 old segment function, now using only three compartments of the modified version of the Hikishima template, namely GM, WM and inner ventricular CSF.

For cross-sectional DBM analyses focusing on the second experimental time point, DARTEL normalization first imported the brain extracted images of two segments (GM, WM), and a study-specific template based on GM and WM was generated in seven iterations, along with flow-fields which parameterize the deformations. The flow-fields were then converted to Jacobian determinant fields, which were spatially smoothed with a Gaussian kernel of about 6 times the voxel size.

Longitudinal analysis used the rodent longitudinal toolbox (RLT, Version 1; dbm.neuro.uni-jena.de) for SPM12. Bias corrected images (no brain extraction) entered the RLT analysis. Again, C57Bl6 Hikishima templates were used, with a maturation rate of 45 (adult mice). The Jacobian determinant fields for each set of measurements were calculated with respect to the subject's temporal average image, and then subtracted from each other to generate a deformation image from MRI 1 to 2 (Jacobian difference images). The average images per subject were used to create a DARTEL study specific template. Finally, the Jacobian difference images were normalized to the template space and smoothed with a Gaussian kernel of about 6 times the voxel size.

Total intracranial volume (TIV) was approximated as the sum of all modulated tissue probabilities (for the longitudinal analysis, these were derived from the temporal average images), excluding the olfactory bulb and the cerebellum, as well as brain regions inferior to the anterior commissure, due to lower signal-to-noise in these regions because of the surface coil characteristics.

2.4. Experiments

In a first step, we assessed behavioral changes of mice in response to a traumatic event and described these in a Hyperarousal Score (Experiment 1). Subsequently, we applied the same mathematical approach to a new batch of mice, which were repeatedly scanned in the MRI before behavioral screening (Experiment 2) in order to relate volumetric changes of the brain to individual behavioral consequence of the trauma.

2.4.1. Experiment 1: long-term consequences of a traumatic experience

To examine long-term effects of a traumatic event on defensive responses to threatening stimuli of different sensory modality, we randomly assigned B6NR mice to two groups which either received two electric foot shocks (S+, $n = 24$) or not (S-, $n = 20$). Three weeks later, we measured generalized fear upon exposure to the neutral context (cylinder), followed by measurement of conditioned fear upon re-exposure to the shock context (chamber) 24 h later. Subsequently, all mice underwent the ASR, the VTT and the BMT, with one week of recovery in between two tests.

2.4.2. Experiment 2: structural correlates of defensive reactions

Experimentally naïve B6NR mice underwent a first MRI scan (MRI1). After a recovery phase of at least 3 days, we randomly assigned the animals to two groups which either received a foot shock (S+, $n = 11$) or not (S-, $n = 12$), followed by a second MRI scan for both groups (MRI2; 28–30 days later). Thereafter, we assessed generalized and conditioned fear (35 days after foot shock), defensive responses to the robo-beetle (BMT; 41 days after foot shock), acoustic threats (ASR; 47 days after foot shock), and visual threats (VTT; 53 days after foot shock) similarly to Experiment 1.

2.5. Statistics

Behavioral data is presented as means ± standard error (SEM), if appropriate. In case of normal distribution, groups were compared by

paired and unpaired *t*-tests, one-way analysis of variance (ANOVA) followed by Tukey’s post-hoc test or 2-way analysis of variance (ANOVA) for repeated measures followed by Bonferroni post-hoc analysis. In case of non-parametric distribution, we employed Mann-Whitney *U* tests, and for contingency analyses Chi square tests. Statistically significant differences were accepted if $p < 0.05$. All statistical analyses were performed using GraphPad Prism 8.2.

2.5.1. Logistic regression analysis

We performed a logistic regression analysis in MATLAB R2020a on the z-scores of all readouts of the ASR, BMT, and VTT to predict whether an animal has undergone the preceding PTSD procedure. The analysis was based on the data of Experiment 1. The resulting coefficients were used to calculate the behavior-based Hyperarousal Scores for all animals of both experiments. Therefore, the data of Experiment 2 served as a hold-out validation sample.

2.5.2. MRI

To test the volumetric difference between the shocked and the non-shocked group (MRI2), analysis was run as a two-sample *t*-test, applying proportional scaling on the TIV to consider unspecific global effects. To test if local brain volumes at MRI2 correlated with the results of the logistic regression on the behavioral readouts, a multiple regression design was used in SPM12, with the TIV entered as a nuisance variable (global normalization using ANCOVA). Volumetric changes between MRI 1 and 2 were analyzed using the Jacobian difference images. Again, TIV was included as nuisance regressor. T-maps were thresholded at an uncorrected $p < 0.005$ or $p < 0.001$ with a minimum cluster extent of 20 voxels. Clusters surviving family-wise error correction as a whole are shown at $p_{FWE,cluster} < 0.05$.

3. Results

3.1. Trauma-related changes in threat responding (Experiment 1)

Experimentally naïve B6NR mice were randomly assigned to two experimental groups. Both groups were placed into a shock chamber, with one group receiving two electric foot shocks (S+), while the other remained non-shocked (S-). Starting 3 weeks later, we assessed generalized trauma-associated fear followed by measurements of hyperarousal upon confrontation with threatening stimuli of different sensory modality.

3.1.1. Generalization of trauma-associated fear memories

S+ mice froze significantly more than S- controls ($U = 7, p < 0.0001$, Fig. 1A) upon exposure to a neutral test context 3 weeks after foot shock (S+) or control exposure to the chamber (S-). Moreover, S+ mice reared less ($U = 0, p < 0.0001$, Fig. 1B), which also became evident if we considered the number of mice which failed to rear at all (S+: 42%, S-: 0%; $\chi^2 = 10.8, p < 0.01$; Fig. 1B). The behavior of S+ mice cannot be explained by a general decrease in locomotor activity due to a trauma-related reduction in exploratory drive, since S+ showed significantly more risk assessment than S- controls ($U = 51, p < 0.0001$; Fig. 1C). This was reflected by the number of mice which displayed SAPs at all (S+: 96%, S-: 40%; $\chi^2 = 16.3, p < 0.0001$; Fig. 1C). Re-exposure to the original shock context another day later revealed essentially the same findings with significantly higher freezing levels ($U = 2, p < 0.0001$, Fig. 1D), reduced rearing ($U = 13, p < 0.0001$, Fig. 1E; with 61% S+, but 0% S- showing no rearing at all, $\chi^2 = 18.1, p < 0.0001$; Fig. 1E) and increased risk assessment ($U = 118, p < 0.001$; with 52% S+, but only 5% S- showing risk assessment, $\chi^2 = 11.3, p < 0.001$, Fig. 1F).

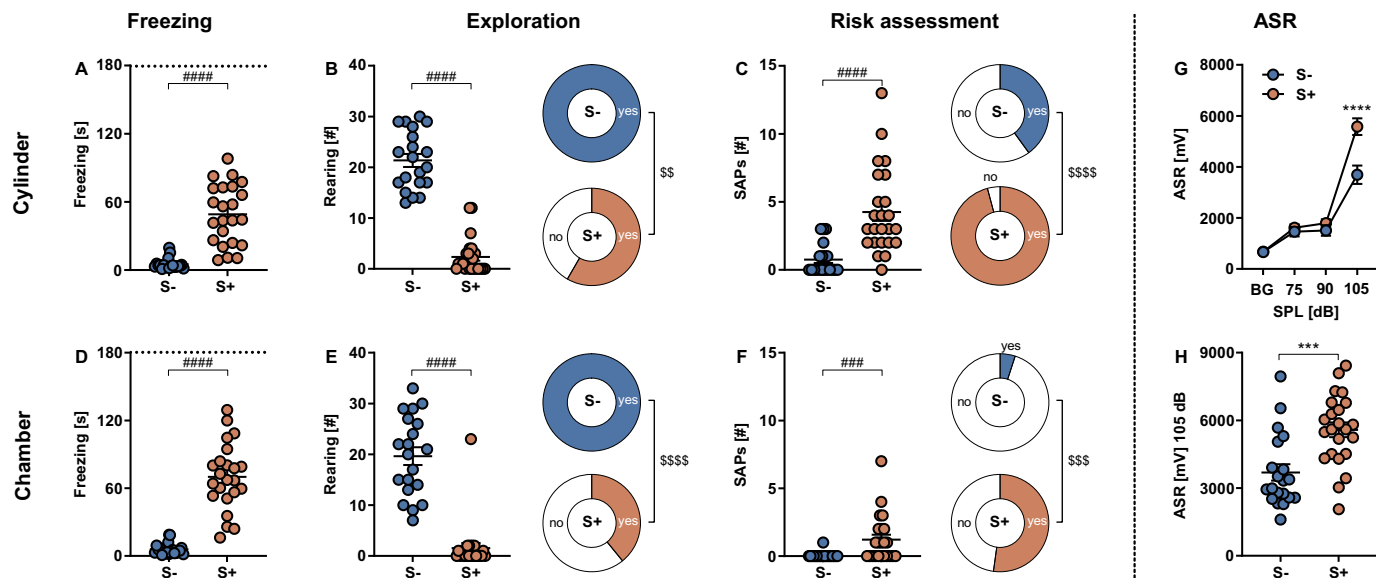


Fig. 1. Generalized trauma-associated fear memory and acoustic startle responses (ASR) after trauma incubation. Mice were (re-)exposed to (A–C) a neutral test context (cylinder) and (D–F) the shock context (chamber) 23 and 24 days after they had received electric foot shocks in the shock chamber (S+) or not (S-). We assessed (A, D) freezing behavior, (B, E) the number of rearings per mouse, as well as the proportion of mice per group which reared at all, and (C, F) risk assessment on basis of the number of stretch-attend postures (SAPs) per mouse and as the proportion of mice which showed SAPs at all. (G) Intensity-response relationship between sound-pressure levels (SPL) of the white noise pulses and the ASR for S+ and S- mice 6 weeks after foot shock or control exposure. (H) Startle responses elicited by white noise pulses of 105 dB(A). ### $p < 0.001$, #### $p < 0.0001$ (Mann-Whitney test for (A–F)) and \$\$\$ $p < 0.001$, \$\$\$\$ $p < 0.0001$ (Chi square test). **** $p < 0.0001$ (2-Way ANOVA followed by Bonferroni post-hoc test) and *** $p < 0.001$ (unpaired *t*-test).

3.1.2. Acoustic startle response after trauma incubation

Four weeks after foot shock application, we exposed the S+ and S- mice to white noise pulses of different intensity and measured their acoustic startle responses. As revealed by 2-way ANOVA, there was a

significant interaction between shock and startle pulse intensity ($F_{3,123} = 11.1, p < 0.0001$). Post-hoc analyses confirmed that S+ mice showed a higher startle response at the highest startle pulse intensity (105 dB(A)) compared to S- controls ($t_{41} = 3.9, p < 0.001$; Fig. 1G-H).

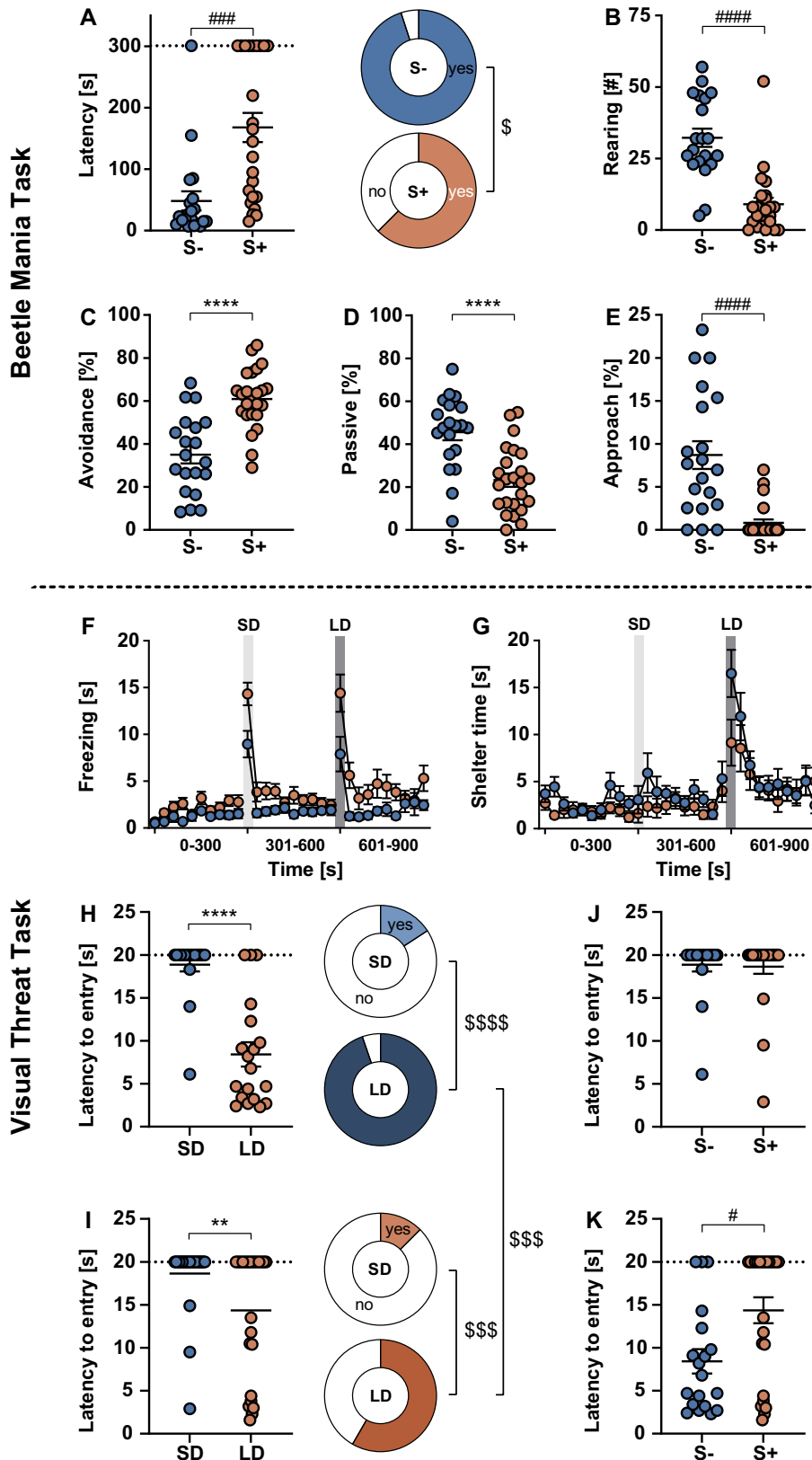


Fig. 2. Beetle Mania Task (A-E) and Visual Threat Task (F-K). In absence of the robo-beetle during the baseline period (0-5 min), we measured (A) horizontal (i.e., latency to end exploration, including information of the proportion of mice which failed to explore the end of the arena at all) and (B) vertical (i.e., number of rearings) exploration in mice with (S+) or without (S-) foot shock administration. (C) Active and (D) passive responses, and (E) approach behavior upon contact with the robo-beetle (expressed as the percentage of the number of contacts) during the subsequent confrontation with a robo-beetle (5-15 min). The time course of freezing responses (F) and the time spent in the shelter (G) during the VTT is presented in 30-s time bins. The time bin of stimulus presentation is highlighted by a grey bar (SD Sweeping Disk, LD Looming Disk). The latency to entering the shelter after stimulus onset (individual data) and the proportions of animals entering the shelter within the 20-s stimulus are presented for S- (H) and the S+ (I) and are directly compared during the SD (J) and LD stimulus (K). # $p < 0.05$, ### $p < 0.001$, #### $p < 0.0001$ (Mann-Whitney test for (A-B), (F-G) and (K)); **** $p < 0.0001$ (unpaired t-test for (D-E)); ** $p < 0.01$, **** $p < 0.0001$ (paired t-test for (H-I)); \$ $p < 0.05$, \$\$ $p < 0.01$, \$\$\$ $p < 0.001$, \$\$\$ $p < 0.0001$ (Chi-square test for (A) and (H-I)).

3.1.3. Beetle mania task after trauma incubation

To assess consequences of trauma on active *versus* passive fear responses to a potentially threatening stimulus, we submitted S+ and S- mice to the BMT four weeks after foot shock. During the baseline exploration without robo-beetle (0–5 min), S+ showed significantly reduced horizontal (assessed by the latency to reach the end of the arena; $U = 74, p < 0.0001$, Fig. 2A; whereby only 63% compared to 95% of S- reached the opposite end of the arena at all, $\chi^2 = 6.6, p < 0.05$; Fig. 2A) and vertical exploration (assessed by the number of rearings; $U = 44.5, p < 0.0001$, Fig. 2B).

Subsequent confrontation with the erratically moving robo-beetle (5–15 min) resulted in the same number of contacts (mean S+ = 42.2 ± 1.2 *versus* mean S- = 41.9 ± 1.0 , $t_{42} = 0.2$). However, S+ responded differently from S- to the contacts: S+ mice showed an increase in avoidance behavior ($t_{42} = 5.4, p < 0.0001$, Fig. 2C) which was mirrored by a corresponding decrease in passive behavior ($t_{42} = 4.6, p < 0.0001$, Fig. 2D). Besides, S+ mice reacted with more jumps (range S+ = 0–54, median = 1.5 *versus* range S- = 0–72, median = 8.0, $U = 149.5, p < 0.05$) and a lower level of proactive approaching of the bypassing robo-beetle compared to S- controls ($U = 59, p < 0.0001$, Fig. 2E).

3.1.4. Visual threat task after trauma incubation

Eight weeks after foot shock, we tested the reaction of S+ and S- mice to two different visual overhead stimuli, following habituation to the setup the day before, and a 5-min basal exposure to the arena on the test day. There were no group differences in freezing (2-way ANOVA RM; $p = 0.51$) and shelter time (2-way ANOVA RM; $p = 0.261$) during baseline (0–300 s). 2-way ANOVA (group, time bin) for repeated measures revealed no differences when comparing the time spent freezing (Fig. 2F) and the time spent in the shelter (Fig. 2G) during the 30-s time bin containing the 20-s SD stimulus presentation (301–330 s) and the following 30-s time bin (331–360 s; statistics not shown). Considering the latency to enter the shelter after the onset of the visual stimulus, both the S- controls ($t_{18} = 7.5, p < 0.0001$, Fig. 2H) and the S+ animals ($t_{23} = 3.0, p < 0.01$, Fig. 2I) showed a decreased latency in response to the LD stimulus compared to the SD stimulus. While both groups showed an increase in the number of animals entering the shelter at all in response to the LD compared to the SD stimulus ($\chi^2 = 24.0, p < 0.0001$ for S-; $\chi^2 = 11.0, p < 0.001$ for S+, Fig. 2H–I), a smaller fraction of S+ animals escaped to the shelter during the LD stimulus compared to S- ($\chi^2 = 13.2, p < 0.001$). There was no difference between the groups in the latency to shelter entry during the SD phase ($U = 222, p = 0.94$; Fig. 2J), but S+ animals had a higher latency to enter the shelter in response to the LD stimulus ($U = 132.5, p < 0.05$, Fig. 2K). In summary, shocked animals tended to express more passive behavior in comparison to non-shocked control animals, irrespective of the nature of the overhead visual stimulus.

3.2. Structural changes in brain morphometry after trauma (Experiment 2).

To assess structural correlates of trauma exposure, an experimentally naïve cohort of B6NR mice underwent a first volumetric MRI scan. Subsequently, the cohort was split into two groups, one receiving two electric foot shocks (S+), while the other remained non-shocked (S-). One month later, both groups were subjected to a second MRI scan. DBM was used to detect morphological differences between the two groups. Whole-brain analysis after the shock (MRI2) revealed a reduced volume of the right dorsal hippocampus, affecting areas CA1 and CA2 (Fig. 3A) and an increased volume of the caudal linear raphe nucleus and the right reticular nucleus (Fig. 3B) in S+ compared to S- mice ($p < 0.005$).

To relate the interindividual variability in PTSD-related symptoms to morphometric measures while reducing the dimensions of the data and, thus, the fallacies associated with multiple comparisons, we decided to condense the different behavioral readouts from ASR, BMT and VVT into a single Hyperarousal Score. We performed a logistic regression analysis based on the z-scores of the individual readouts to predict the condition (S- and S+) of the mice of Experiment 1. The resulting coefficients were used to calculate the Hyperarousal Score for all mice from both experiments (Fig. 4A). In this way, the sample from Experiment 2 served as a hold-out validation sample (data of the individual behavioral tests not shown). The high accuracy of 83% to predict the condition in the hold-out sample supports the stability of the score despite the relatively small sample size in Experiment 2.

The highest positive loadings were dominated by avoidance behavior and latency to explore the arena in the BMT, and the time spent in the shelter during the LD stimulus in the VTT. The strongest negative loadings resulted from rearing behavior in the BMT, time spent in the shelter and latency to enter the shelter during the SD stimulus in the VTT (Table 1).

The inter-individual differences in the individual Hyperarousal Scores of S+ and S- mice from Experiment 2 allowed us to use the behavior-based score as a regressor for volumetric changes. When applied to MRI2, we found that higher Hyperarousal Score values correlated with smaller volumes of the left ventrolateral and lateral orbital cortex, the dorsal and ventral agranular insular cortex, the gustatory cortex (Fig. 4B), the primary somatosensory cortex (Fig. 4B–C), the right ventral part of the caudate putamen (Fig. 4C), the right dorsal hippocampus (specifically the dorsal CA1/CA2/CA3 regions; Fig. 4D) and the right subiculum (Fig. 4E). On the other end, higher Hyperarousal Scores correlated with larger volumes in the right nucleus of the diagonal band (Fig. 4C), the pontine reticular nucleus and the right pontine grey (Fig. 4F; $p < 0.005$; cluster extent >30).

Next, we related the individual Hyperarousal Scores to longitudinal within-subject changes in brain volume from baseline to post-shock conditions (MRI2–MRI1). We obtained a negative correlation between the Hyperarousal Score and the volume change of the right internal and external segment of the globus pallidus (Fig. 4G and H), the secondary motor area, the medial amygdala (Fig. 4H), the dorsal raphe nucleus and

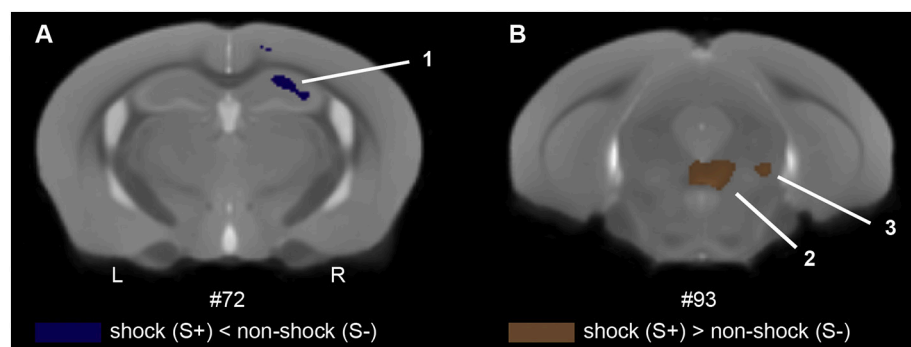
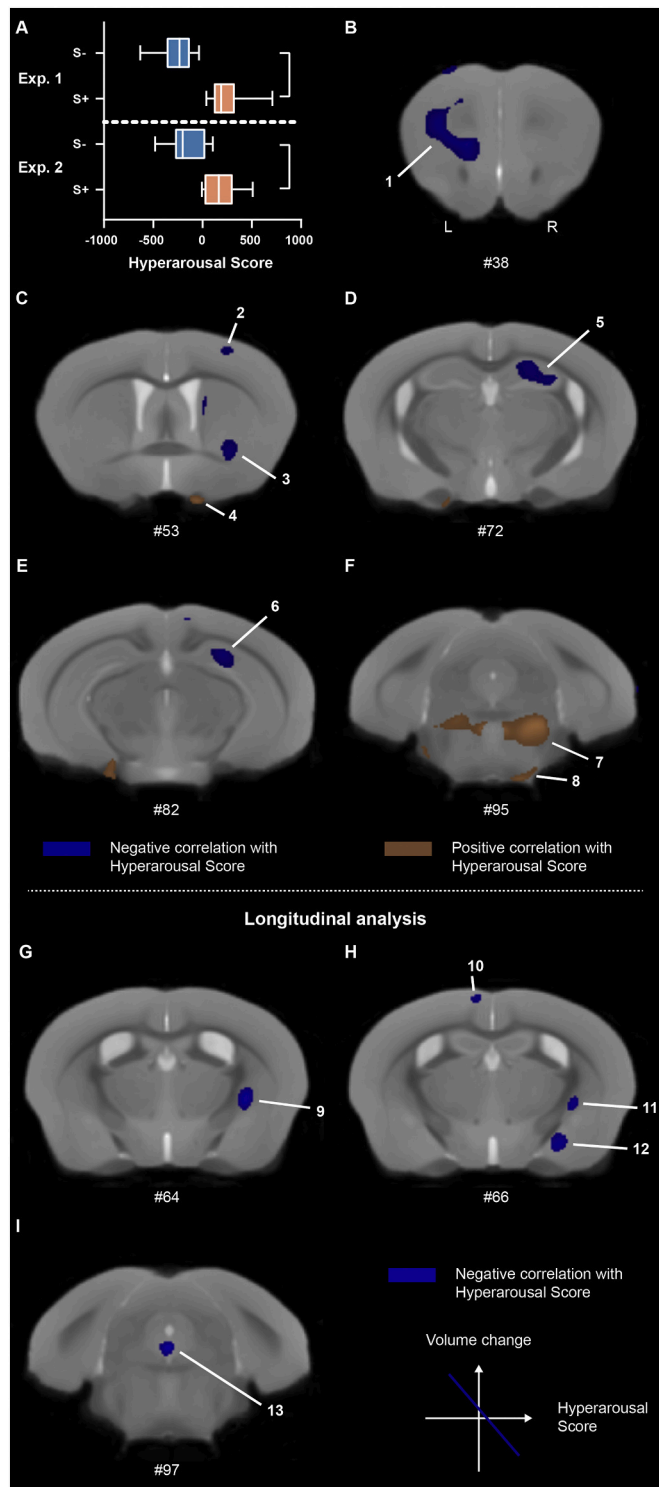


Fig. 3. DBM on brains of trauma-exposed and control mice. Coronal brain slice indicating smaller right dorsal hippocampal volume (A) and an increased volume in the caudal linear raphe nucleus and the right reticular nucleus (B) in S+ mice four weeks after foot shock (MRI2). Brain structures indicated: 1 dorsal hippocampus, 2 caudal linear raphe nucleus, 3 pontine reticular nucleus. Numbers (#) under the slides indicate image numbers of corresponding reference images in the Allen Brain Atlas. Statistical threshold is set at $p < 0.005$, with cluster extent >30 .



(caption on next column)

the ventromedial periaqueductal grey (Fig. 4I; $p_{FWE, cluster} < 0.05$, with a collection threshold of $p < 0.001$) with higher Hyperarousal Scores correlating with a decrease in volume after trauma incubation.

4. Discussion

We employed a well-established mouse model of PTSD (Siegmund and Wotjak, 2007) to study the association between trauma-related hyperarousal and volumetric changes in the mouse brain. Trauma-

Fig. 4. Logistic regression analysis and correlation with brain morphology. Hyperarousal Scores for Experiment 1 and 2 (A). Coronal brain slices indicating brain areas correlating with the Hyperarousal Score at scan time point 2 (B-F; $p < 0.005$, cluster extent > 30) and in the longitudinal within-subject analysis (G-I; $p_{FWE, cluster} < 0.05$, with a collection threshold of $p < 0.001$). Blue color indicates a negative correlation, brown color indicates a positive correlation with the Hyperarousal Score for (B–I). Brain structures indicated in figures: 1 ventrolateral and lateral orbital cortex, dorsal and ventral agranular insular cortex, gustatory cortex, primary somatosensory cortex; 2 primary somatosensory cortex; 3 ventral caudate putamen; 4 nucleus of the diagonal band; 5 dorsal hippocampus; 6 subiculum; 7 pontine reticular nucleus; 8 pontine grey; 9 + 11 internal and external segment of the globus pallidus; 10 secondary motor area; 12 medial amygdala; 13 dorsal raphe nucleus and the ventromedial periaqueductal grey. Numbers (#) under slides indicate image numbers of corresponding reference images in the Allen Brain Atlas. (For interpretation of the references to color in this figure legend, the reader is referred to the web version of this article.)

exposed mice exhibited increased generalized and conditioned fear reactions, accompanied by increased acoustic startle responses and increased active fear in response to a robo-beetle. The group differences were confirmed by the logistic regression analysis and the resulting Hyperarousal Score. Whole-brain MRI with scans prior to and after trauma exposure allowed for cross-sectional and longitudinal analyses. Shocked animals showed a decreased volume of the dorsal hippocampus and an increase of the reticular nucleus compared to non-shocked controls after trauma. Applying the Hyperarousal Scores as regressor for the cross-sectional analysis after trauma revealed, among others, a negative correlation with the dorsal hippocampus. Further, we found a negative correlation between the regressor and the globus pallidus in the longitudinal within-subject analysis.

PTSD is a disorder defined by symptoms lasting for at least one month. During the last decades, numerous animal models have been established to mimic the disorder in rodents (Verbitsky et al., 2020). Our model (Siegmund and Wotjak, 2007) could show that behavioral changes persist weeks after mice had received electric foot shocks. Besides the classic immobility measures in the conditioning and neutral context, we observed reduced exploratory behavior (rearings) and increased risk assessment (number of SAPs), indicative of increased anxiety-like behavior (Grewal et al., 1997).

Studies showed that combat-exposed PTSD patients exhibit an exaggerated startle response (Orr et al., 1995; Shalev and Rogel-Fuchs, 1992), and hyperarousal is one of the diagnostic criteria for PTSD (Del Barrio, 2016). In our study, we can show that trauma-exposed animals displayed an exaggerated acoustic startle response. Earlier rodent studies, some of them differing in the type of stressor and trauma incubation time, have come to similar results (Bourke and Neigh, 2012; Cohen et al., 2004; Golub et al., 2011; Golub et al., 2009; Pulliam et al., 2010). Aside from classic behavioral tests, we also exposed the mice to more ethobehavioral tasks to test for innate fear responses. Exposure to an erratically moving robo-beetle (Heinz et al., 2017) indicated increased active (i.e., avoidance, jumping) and decreased passive fear responses after trauma incubation. The situation appeared to be different upon confrontation with visual threats, whereby shocked mice showed a trend towards increased freezing not only to the SD (reminiscent of a cruising bird of prey (De Franceschi et al., 2016)) but also in response to a LD (reminiscent of an approaching predator (Yilmaz and Meister, 2013)), when escape would be the appropriate reaction. The lack of statistically significant group differences might be ascribed to the rather long incubation time of more than 8 weeks after foot shock or habituation due to handling associated with the exposure to previous behavioral tasks.

In order to assess the PTSD-like symptoms not only in a parametric manner but on a continuous scale for symptom intensity, we calculated a Hyperarousal Score based on the individual behavior after trauma incubation. The score does not include measures for generalized fear

Table 1

Behavioral readouts with corresponding loadings of the logistic regression analysis based on Experiment 1 (significant loadings in bold).

Variable	Loading
BMT: Avoidance in response to RB contact	102.51
BMT: Latency to end exploration during baseline	90.02
VTT: Total shelter time during LD	56.51
BMT: Jumps in response to RB contact	30.35
VTT: Total freezing time during SD	26.34
VTT: Freezing time during SD stimulus	25.19
ASR: Startle response at 105 dB(A)	22.78
VTT: Freezing time during first 20 s of baseline	8.94
Intercept	7.54
VTT: Latency to shelter entry in response to LD stimulus	6.15
VTT: Total freezing time during LD	5.98
VTT: Total shelter time during SD	5.40
VTT: Shelter time during first 20 s of baseline	3.43
VTT: Total freezing time during baseline	-12.95
VTT: SAP during SD	-28.96
VTT: Total shelter time during baseline	-31.83
VTT: Shelter time during LD stimulus	-49.75
VTT: Freezing time during LD stimulus	-71.57
VTT: Latency to shelter entry in response to SD stimulus	-75.56
VTT: Shelter time during SD stimulus	-95.88
BMT: Rearing during baseline	-126.11

because of the limited variability of the data and is therefore biased towards the hyperarousal domain. The logistic regression revealed a general increase in hyperarousal and reactivity irrespective of the sensory modalities of the threatening stimuli. This supports a scenario, whereby perception and incubation of the foot shock leads to long-term changes in brain structures generally involved in threat responding, rather than in individual stimulus-response pathways.

To narrow down those brain structures, we combined behavioral assessment with *in vivo* brain volume measurements. We based this attempt on the premise that changes in neuronal activity may result in changes in grey matter volume. Numerous structural MRI studies have been performed comparing PTSD patients and non-traumatized controls or trauma-exposed healthy individuals. Many of them applied region-of-interest-driven approaches and a cross-sectional design. Recent meta-analyses have reported reduced volume of the hippocampus, the amygdala, the anterior cingulate and the occipital cortex in PTSD patients compared to healthy controls without trauma exposure (Bromis et al., 2018; Li et al., 2014; Meng et al., 2014; O'Doherty et al., 2015). The same studies revealed a reduction in the hippocampus, the left temporal gyrus, and the right superior frontal gyrus as well as the left anterior cingulate cortex, and the left insula in PTSD patients compared to trauma-exposed individuals that did not develop PTSD (Li et al., 2014; Logue et al., 2018; Meng et al., 2014; O'Doherty et al., 2015; Woon et al., 2010). In our mouse model we applied a whole brain voxel-wise analysis and could demonstrate a reduction of the right dorsal hippocampus of shocked mice compared to the non-shocked control group. This confirms earlier work from Golub and colleagues applying ultra-microscopy and manganese-enhanced MRI (Golub et al., 2011). Further, we saw a volume increase in the reticular nucleus and the raphe nucleus of trauma-exposed mice, both brain structures being part of the so-called reticular activating system. The reticular nuclei are known to serve a fundamental role in the promotion and maintenance of an arousal state and defensive reactions in rodents and humans (Davis et al., 1982; Steriade, 1996). A recent study found enhanced pedunculo-pontine nuclei resting state functional connectivity to brain areas involved in threat responding such as the amygdala or the medial prefrontal cortex in individuals with the dissociative subtype PTSD compared to healthy controls (Thome et al., 2019).

Applying the Hyperarousal Score as a regressor for cross-sectional volumetric measures revealed a correlation with two brain structures already identified in the shock/non-shock comparison. We found a negative correlation with the right dorsal hippocampus and a positive

correlation with the reticular nucleus. Additionally, the subiculum as part of the hippocampal formation showed a negative correlation with the Hyperarousal Score, indicating a smaller grey matter volume in animals with a high score. Several studies have analyzed volumetric differences in hippocampal subfields in individuals affected with PTSD and controls. Some of these found a reduced volume of the subiculum in PTSD patients (Luo et al., 2017; Teicher et al., 2012) while others failed to reveal differences (Bonne et al., 2008; Chen et al., 2018; Wang et al., 2010). We wish to emphasize that our analysis does not explore categorical differences between trauma-exposed individuals and controls but include the inter-individual differences in the severity of trauma-related hyperarousal regarding brain volume changes (i.e., parametric differences).

Studying PTSD in a mouse model comes with the advantage of standardized trauma intensity and incubation time. But more importantly, it allows us to measure grey matter volume before and after the traumatic event, an experimental design which is difficult to employ in humans. Our longitudinal regression analysis revealed a negative correlation between the Hyperarousal Score and the globus pallidus, the medial amygdala, and the dorsal raphe nucleus/ventral periaqueductal grey area. Animals with a higher severity of symptoms therefore show a volume decrease in these areas. Smaller volumes of the globus pallidus have been linked to higher symptomatic scores in active police soldiers that had been exposed to work-related traumatic events (Shucard et al., 2012). Another study found the globus pallidus as a cluster of decreased neuronal activity in PTSD-affected individuals compared to controls (Disner et al., 2018). However, no volumetric difference in globus pallidus volume was found by Sussmann and colleagues when comparing soldiers with PTSD and combat-exposed controls in a cross-sectional analysis (Sussman et al., 2016).

Several of the volumetric differences were only detected unilaterally in our study. This might be attributed to brain lateralization, a feature conserved across species, including mice (Ehret, 1987; Kawakami et al., 2003). On the other hand, we cannot exclude the possibility that the lack of bilateral evidence is due to the small sample size.

Our study confirms trauma-induced changes in brain morphology as opposed to *a priori* differences which would define individual susceptibility to traumatic events. We can only speculate about the mechanisms underlying the volume changes in response to such events. Previous work has shown that grey matter volume loss can be explained by decreased neurogenesis in dentate gyrus (Gould et al., 1997), loss of dendritic length and branching and reduction in the number of synapses (Kassem et al., 2013; Radley et al., 2006) and decrease in the number of oligodendrocytes (Banar et al., 2007) in response to stress in rodents. It is conceivable that those structural changes may resemble compensatory mechanisms in neuronal circuits aimed at protecting against devastating consequences of hyperexcitation. Also elevated cortisol levels have been linked to decreases in brain volume, e.g., in the hippocampus (Echouffo-Tcheugui et al., 2018; Fowler et al., 2021; Geerlings et al., 2015; Lupien et al., 1998; Pruessner et al., 2005). In our model, we do not have evidence for sustained changes in corticosterone (Kao et al., 2015), which is different from a subset of patients which even show reduced plasma cortisol levels and increased negative feedback of the HPA axis (Mason et al., 1986; Yehuda et al., 1996). Nevertheless, we cannot rule out that the rise in corticosterone in the early aftermath of the traumatic incident has contributed to the volumetric changes observed several weeks later. It remains to be demonstrated in future studies, to which extent those scenarios account for the trauma-related changes in brain volume observed in the present study.

Our study comes with several limitations, first of which is the relatively small sample size for longitudinal volumetric measures. Due to this power issue, we were only able to characterize the strongest changes. Increasing animal numbers might allow for detecting more subtle structural changes and bilateral effects. This study only includes male mice and the results provided might not be valid when it comes to behavioral and morphological trauma-related changes in females.

Further, our behavioral readouts have a bias towards the hyperarousal domain of PTSD symptoms and do not cover other important symptom criteria such as avoidance of trauma-related cues. The current study provides a correlational analysis which generates hypotheses. It is up to future studies to deliver proofs of functional involvement of the brain areas discussed in the neuronal circuits of PTSD.

5. Conclusion

Our findings demonstrate that a brief traumatic event is sufficient to trigger changes in grey matter volume and that, among others, the globus pallidus plays an important role in the control of fear responses to threats of different sensory modalities.

Ethical statement

Experimental procedures were approved by the Government of Upper Bavaria (Regierung von Oberbayern, 55.2-2532.Vet_02-17-206) and performed according to the European Community Council Directive 2010/63/EEC. All efforts were made to reduce the number of experimental subjects and to minimize, if not exclude, any suffering.

Declaration of Competing Interest

The authors declare no competing interests.

Acknowledgments

This work was supported by the German-Israeli Foundation for Scientific Research and Development (I-1442-421. 13/2017) and by Vienna Science and Technology Fund (CS18-019) to C.T.W.. D.E.H. was supported by the Federal Ministry for Education and Research and the Max Planck Society. A.H. received a fellowship from the Fundação de Amparo à Pesquisa do Estado de São Paulo (BEPE-2018/17387-9). T.S. was supported by the Specific University Research (MUNI/A/1249/2020) provided by MŠMT.

References

- Armony, J.L., Corbo, V., Clément, M.H., Brunet, A., 2005. Amygdala response in patients with acute PTSD to masked and unmasked emotional facial expressions. *Am. J. Psychiatry* 162, 1961–1963. <https://doi.org/10.1176/appi.ajp.162.10.1961>.
- Banasr, M., Valentine, G.W., Li, X.Y., Gourley, S.L., Taylor, J.R., Duman, R.S., 2007. Chronic unpredictable stress decreases cell proliferation in the cerebral cortex of the adult rat. *Biol. Psychiatry* 62, 496–504. <https://doi.org/10.1016/j.biopsych.2007.02.006>.
- Bonne, O., Brandes, D., Gilboa, A., Gomori, J.M., Shenton, M.E., Pitman, R.K., Shalev, A. Y., 2001. Longitudinal MRI study of hippocampal volume in trauma survivors with PTSD. *Am. J. Psychiatry* 158, 1248–1251. <https://doi.org/10.1176/appi.ajp.158.8.1248>.
- Bonne, O., Vythilingam, M., Inagaki, M., Wood, S., Neumeister, A., Nugent, A.C., Snow, J., Luckenbaugh, D.A., Bain, E.E., Drevets, W.C., Charney, D.S., 2008. Reduced posterior hippocampal volume in posttraumatic stress disorder. *J. Clin. Psychiatry* 69, 1087–1091. <https://doi.org/10.4088/JCP.v69n0707>.
- Bourke, C.H., Neigh, G.N., 2012. Exposure to repeated maternal aggression induces depressive-like behavior and increases startle in adult female rats. *Behav. Brain Res.* 227, 270–275. <https://doi.org/10.1016/j.bbr.2011.11.001>.
- Bromis, K., Calem, M., Reinders, A.A.T.S., Williams, S.C.R., Kempton, M.J., 2018. Meta-analysis of 89 structural MRI studies in posttraumatic stress disorder and comparison with major depressive disorder. *Am. J. Psychiatry* 175, 989–998. <https://doi.org/10.1176/appi.ajp.2018.17111199>.
- Carrion, V.G., Weems, C.F., Eliez, S., Patwardhan, A., Brown, W., Ray, R.D., Reiss, A.L., 2001. Attenuation of frontal asymmetry in pediatric posttraumatic stress disorder. *Biol. Psychiatry* 50, 943–951. [https://doi.org/10.1016/S0006-3223\(01\)01218-5](https://doi.org/10.1016/S0006-3223(01)01218-5).
- Chen, L.W., Sun, D., Davis, S.L., Haswell, C.C., Dennis, E.L., Swanson, C.A., Whelan, C.D., Gutman, B., Jahanshad, N., Iglesias, J.E., Thompson, P., Wagner, H.R., Saemann, P., LaBar, K.S., Morey, R.A., 2018. Smaller hippocampal CA1 subfield volume in posttraumatic stress disorder. *Depress. Anxiety* 35, 1018–1029. <https://doi.org/10.1002/da.22833>.
- Cohen, H., Zohar, J., Matar, M.A., Zeev, K., Loewenthal, U., Richter-Levin, G., 2004. Setting apart the affected: the use of behavioral criteria in animal models of post traumatic stress disorder. *Neuropsychopharmacology* 29, 1962–1970. <https://doi.org/10.1038/sj.npp.1300523>.

- Davis, M., Parisi, T., Gendelman, D.S., Tischler, M., Kehne, J.H., 1982. Habituation and sensitization of startle reflexes elicited electrically from the brainstem. *Science* 218, 688–690. <https://doi.org/10.1126/science.7134967>.
- De Bellis, M.D., Hall, J., Boring, A.M., Frustaci, K., Moritz, G., 2001. A pilot longitudinal study of hippocampal volumes in pediatric maltreatment-related posttraumatic stress disorder. *Biol. Psychiatry* 50, 305–309. [https://doi.org/10.1016/S0006-3223\(01\)01105-2](https://doi.org/10.1016/S0006-3223(01)01105-2).
- De Franceschi, G., Vivattanasarn, T., Saleem, A.B., Solomon, S.G., 2016. Vision guides selection of freeze or flight defense strategies in mice. *Curr. Biol.* 26, 2150–2154. <https://doi.org/10.1016/j.cub.2016.06.006>.
- Del Barrio, V., 2016. Diagnostic and Statistical Manual of Mental Disorders, 5th Revise. Ed, The Curated Reference Collection in Neuroscience and Biobehavioral Psychology. American Psychiatric Association Publishing, Arlington, USA. <https://doi.org/10.1016/B978-0-12-809324-5.05530-9>.
- Deslauriers, J., Toth, M., Der-Avakian, A., Risbrough, V.B., 2018. Current status of animal models of posttraumatic stress disorder: behavioral and biological phenotypes, and future challenges in improving translation. *Biol. Psychiatry* 83, 895–907. <https://doi.org/10.1016/j.biopsych.2017.11.019>.
- Disner, S.G., Marquardt, C.A., Mueller, B.A., Burton, P.C., Sponheim, S.R., 2018. Spontaneous neural activity differences in posttraumatic stress disorder: a quantitative resting-state meta-analysis and fMRI validation. *Hum. Brain Mapp.* 39, 837–850. <https://doi.org/10.1002/hbm.23886>.
- Echouffo-Tcheugui, J.B., Conner, S.C., Himali, J.J., Maillard, P., Decarli, C.S., Beiser, A. S., Vasan, R.S., Seshadri, S., 2018. Circulating cortisol and cognitive and structural brain measures. *Neurology* 91, E1961–E1970. <https://doi.org/10.1212/WNL.0000000000006549>.
- Ehret, G., 1987. Left hemisphere advantage in the mouse brain for recognizing ultrasonic communication calls. *Nature* 325, 249–251. <https://doi.org/10.1038/325249a0>.
- Fennema-Notestine, C., Stein, M.B., Kennedy, C.M., Archibald, S.L., Jernigan, T.L., 2002. Brain morphometry in female victims of intimate partner violence with and without posttraumatic stress disorder. *Biol. Psychiatry* 52, 1089–1101. [https://doi.org/10.1016/S0006-3223\(02\)01413-0](https://doi.org/10.1016/S0006-3223(02)01413-0).
- Fowler, C.H., Bogdan, R., Gaffrey, M.S., 2021. Stress-induced cortisol response is associated with right amygdala volume in early childhood. *Neurobiol. Stress* 14, 100329. <https://doi.org/10.1016/j.ynstr.2021.100329>.
- Geerlings, M.I., Sigurdsson, S., Eiriksdottir, G., Garcia, M.E., Harris, T.B., Gudnason, V., Launer, L.J., 2015. Salivary cortisol, brain volumes, and cognition in community-dwelling elderly without dementia. *Neurology* 85, 976–983. <https://doi.org/10.1212/WNL.0000000000001931>.
- Gilbertson, M.W., Shenton, M.E., Ciszewski, A., Kasai, K., Lasko, N.B., Orr, S.P., Pitman, R.K., 2002. Smaller hippocampal volume predicts pathologic vulnerability to psychological trauma. *Nat. Neurosci.* 5, 1242–1247. <https://doi.org/10.1038/nn958>.
- Golub, Y., Mauch, C.P., Dahlhoff, M., Wotjak, C.T., 2009. Consequences of extinction training on associative and non-associative fear in a mouse model of posttraumatic stress disorder (PTSD). *Behav. Brain Res.* 205, 544–549. <https://doi.org/10.1016/j.bbr.2009.08.019>.
- Golub, Y., Kaltwasser, S.F., Mauch, C.P., Herrmann, L., Schmidt, U., Holsboer, F., Czisch, M., Wotjak, C.T., 2011. Reduced hippocampus volume in the mouse model of posttraumatic stress disorder. *J. Psychiatr. Res.* 45, 650–659. <https://doi.org/10.1016/j.jpsychires.2010.10.014>.
- Gould, E., McEwen, B.S., Tanapat, P., Galea, L.A.M., Fuchs, E., 1997. Neurogenesis in the dentate gyrus of the adult tree shrew is regulated by psychosocial stress and NMDA receptor activation. *J. Neurosci.* 17, 2492–2498. <https://doi.org/10.1523/jneurosci.17-07-02492.1997>.
- Grewal, S.S., Shepherd, J.K., Bill, D.J., Fletcher, A., Dourish, C.T., 1997. Behavioural and pharmacological characterisation of the canopy stretched anted posture test as a model of anxiety in mice and rats. *Psychopharmacology* 133, 29–38. <https://doi.org/10.1007/s002130050367>.
- Heinz, D.E., Genewsky, A., Wotjak, C.T., 2017. Enhanced anandamide signaling reduces flight behavior elicited by an approaching robo-beetle. *Neuropharmacology* 126, 233–241. <https://doi.org/10.1016/j.neuropharm.2017.09.010>.
- Herrmann, L., Ionescu, I.A., Henes, K., Golub, Y., Wang, N.X.R., Buell, D.R., Holsboer, F., Wotjak, C.T., Schmidt, U., 2012. Long-lasting hippocampal synaptic protein loss in a mouse model of posttraumatic stress disorder. *PLoS One* 7. <https://doi.org/10.1371/journal.pone.0042603>.
- Hikishima, K., Komaki, Y., Seki, F., Ohnishi, Y., Okano, H.J., Okano, H., 2017. In vivo microscopic voxel-based morphometry with a brain template to characterize strain-specific structures in the mouse brain. *Sci. Rep.* 7, 1–9. <https://doi.org/10.1038/s41598-017-00148-1>.
- Kao, C.Y., Stalla, G., Stalla, J., Wotjak, C.T., Anderzhanova, E., 2015. Norepinephrine and corticosterone in the medial prefrontal cortex and hippocampus predict PTSD-like symptoms in mice. *Eur. J. Neurosci.* 41, 1139–1148. <https://doi.org/10.1111/ejn.12860>.
- Kassem, M.S., Lagopoulos, J., Stait-Gardner, T., Price, W.S., Chohan, T.W., Arnold, J.C., Hatton, S.N., Bennett, M.R., 2013. Stress-induced grey matter loss determined by MRI is primarily due to loss of dendrites and their synapses. *Mol. Neurobiol.* 47, 645–661. <https://doi.org/10.1007/s12035-012-8365-7>.
- Kawakami, R., Shinohara, Y., Kato, Y., Sugiyama, H., Shigemoto, R., Ito, I., 2003. Asymmetrical allocation of NMDA receptor $\epsilon 2$ subunits in hippocampal circuitry. *Science* 300, 990–994. <https://doi.org/10.1126/science.1082609>.
- Li, L., Wu, M., Liao, Y., Ouyang, L., Du, M., Lei, D., Chen, L., Yao, L., Huang, X., Gong, Q., 2014. Grey matter reduction associated with posttraumatic stress disorder and traumatic stress. *Neurosci. Biobehav. Rev.* 43, 163–172. <https://doi.org/10.1016/j.neubiorev.2014.04.003>.

- Logue, M.W., van Rooij, S.J.H., Dennis, E.L., Davis, S.L., Hayes, J.P., Stevens, J.S., Densmore, M., Haswell, C.C., Ipser, J., Koch, S.B.J., Korgaonkar, M., Lebois, L.A.M., Peever, M., Baker, J.T., Boedhoe, P.S.W., Frijling, J.L., Gruber, S.A., Harpaz-Rotem, I., Jahanshad, N., Koopowitz, S., Levy, I., Nawijn, L., O'Connor, L., Olf, M., Salat, D.H., Sheridan, M.A., Spielberg, J.M., van Zuiden, M., Winternitz, S.R., Wolff, J.D., Wolf, E.J., Wang, X., Wrocklage, K., Abdallah, C.G., Bryant, R.A., Geuze, E., Jovanovic, T., Kaufman, M.L., King, A.P., Krystal, J.H., Lagopoulos, J., Bennett, M., Lanius, R., Liberzon, I., McGlinchey, R.E., McLaughlin, K.A., Milberg, W.P., Miller, M.W., Ressler, K.J., Veltman, D.J., Stein, D.J., Thomas, K., Thompson, P.M., Morey, R.A., 2018. Smaller hippocampal volume in posttraumatic stress disorder: a multisite ENIGMA-PGC study: subcortical volumetry results from posttraumatic stress disorder consortia. *Biol. Psychiatry* 83, 244–253. <https://doi.org/10.1016/j.biopsych.2017.09.006>.
- Luo, Y., Liu, Y., Qin, Y., Zhang, X., Ma, T., Wu, W., Yang, Y., Jiang, D., Shan, H., Cao, Z., 2017. The atrophy and laterality of the hippocampal subfields in parents with or without posttraumatic stress disorder who lost their only child in China. *Neurosci. Lett.* 38, 1241–1247. <https://doi.org/10.1007/s10072-017-2952-3>.
- Lupien, S.J., De Leon, M., De Santi, S., Convit, A., Tarshish, C., Nair, N.P.V., Thakur, M., McEwen, B.S., Hauger, R.L., Meaney, M.J., 1998. Cortisol levels during human aging predict hippocampal atrophy and memory deficits. *Nat. Neurosci.* 1, 69–73. <https://doi.org/10.1038/271>.
- Manjón, J.V., Coupé, P., Martí-Bonmati, L., Collins, D.L., Robles, M., 2010. Adaptive non-local means denoising of MR images with spatially varying noise levels. *J. Magn. Reson. Imaging* 31, 192–203. <https://doi.org/10.1002/jmri.22003>.
- Mason, J.W., Giller, E.L., Kosten, T.R., Ostroff, R.B., Podd, L., 1986. Urinary free-cortisol levels in posttraumatic stress disorder patients. *J. Nerv. Ment. Dis.* <https://doi.org/10.1097/00005053-198603000-00003>.
- Meng, Y., Qiu, C., Zhu, H., Lama, S., Lui, S., Gong, Q., Zhang, W., 2014. Anatomical deficits in adult posttraumatic stress disorder: a meta-analysis of voxel-based morphometry studies. *Behav. Brain Res.* 270, 307–315. <https://doi.org/10.1016/j.bbr.2014.05.021>.
- O'Doherty, D.C.M., Chitty, K.M., Saddiqui, S., Bennett, M.R., Lagopoulos, J., 2015. A systematic review and meta-analysis of magnetic resonance imaging measurement of structural volumes in posttraumatic stress disorder. *Psychiatry Res. Neuroimaging* 232, 1–33. <https://doi.org/10.1016/j.psychres.2015.01.002>.
- Orr, S.P., Lasko, N.B., Shalev, A.Y., Pitman, R.K., 1995. Physiological responses to loud tones in Vietnam Veterans with posttraumatic stress disorder. *J. Abnorm. Psychol.* 104, 75–82. <https://doi.org/10.1037/0021-843X.104.1.75>.
- Pruessner, J.C., Baldwin, M.W., Dedovic, K., Renwick, R., Mahani, N.K., Lord, C., Meaney, M., Lupien, S., 2005. Self-esteem, locus of control, hippocampal volume, and cortisol regulation in young and old adulthood. *Neuroimage* 28, 815–826. <https://doi.org/10.1016/j.neuroimage.2005.06.014>.
- Pulliam, J.V.K., Dawagreh, A.M., Alema-Mensah, E., Plotsky, P.M., 2010. Social defeat stress produces prolonged alterations in acoustic startle and body weight gain in male long Evans rats. *J. Psychiatr. Res.* 44, 106–111. <https://doi.org/10.1016/j.jpsychires.2009.05.005>.
- Radley, J.J., Rocher, A.B., Miller, M., Janssen, W.G.M., Liston, C., Hof, P.R., McEwen, B.S., Morrison, J.H., 2006. Repeated stress induces dendritic spine loss in the rat medial prefrontal cortex. *Cereb. Cortex* 16, 313–320. <https://doi.org/10.1093/cercor/bhi104>.
- Shalev, A.Y., Rogel-Fuchs, Y., 1992. Auditory startle reflex in post-traumatic stress disorder patients treated with clonazepam. *Isr. J. Psychiatry Relat. Sci.* 29, 1–6.
- Shin, L.M., Orr, S.P., Carson, M.A., Rauch, S.L., Macklin, M.L., Lasko, N.B., Peters, P.M., Metzger, L.J., Dougherty, D.D., Cannistraro, P.A., Alpert, N.M., Fischman, A.J., Pitman, R.K., 2004. Regional cerebral blood flow in the amygdala and medial prefrontal cortex during traumatic imagery in male and female Vietnam veterans with PTSD. *Arch. Gen. Psychiatry* 61, 168–176. <https://doi.org/10.1001/archpsyc.61.2.168>.
- Shucard, J.L., Cox, J., Shucard, D.W., Fetter, H., Chung, C., Ramasamy, D., Violanti, J., 2012. Symptoms of posttraumatic stress disorder and exposure to traumatic stressors are related to brain structural volumes and behavioral measures of affective stimulus processing in police officers. *Psychiatry Res.* 204, 25–31. <https://doi.org/10.1016/j.psychres.2012.04.006>.
- Siegmund, A., Wotjak, C.T., 2007. A mouse model of posttraumatic stress disorder that distinguishes between conditioned and sensitized fear. *J. Psychiatr. Res.* 41, 848–860. <https://doi.org/10.1016/j.jpsychires.2006.07.017>.
- Steriade, M., 1996. Arousal: revisiting the reticular activating system. *Science* 272, 225–226. <https://doi.org/10.1126/science.272.5259.225>.
- Sussman, D., Pang, E.W., Jetly, R., Dunkley, B.T., Taylor, M.J., 2016. Neuroanatomical features in soldiers with post-traumatic stress disorder. *BMC Neurosci.* 17, 1–11. <https://doi.org/10.1186/s12868-016-0247-x>.
- Teicher, M.H., Anderson, C.M., Polcari, A., 2012. Childhood maltreatment is associated with reduced volume in the hippocampal subfields CA3, dentate gyrus, and subiculum. *Proc. Natl. Acad. Sci. U. S. A.* 109 <https://doi.org/10.1073/pnas.1115396109>.
- Thome, J., Densmore, M., Koppe, G., Terpou, B., Théberge, J., McKinnon, M.C., Lanius, R.A., 2019. Back to the basics: resting state functional connectivity of the reticular activation system in PTSD and its dissociative subtype. *Chronic Stress* 3. <https://doi.org/10.1177/2470547019873663>, 2470547019873663.
- Verbitsky, A., Dopfel, D., Zhang, N., 2020. Rodent models of post-traumatic stress disorder: behavioral assessment. *Transl. Psychiatry* 10. <https://doi.org/10.1038/s41398-020-0806-x>.
- Wang, Z., Neylan, T.C., Mueller, S.G., Lenoci, M., Truran, D., Marmar, C.R., Weiner, M.W., Schuff, N., 2010. Magnetic resonance imaging of hippocampal subfields in posttraumatic stress disorder. *Arch. Gen. Psychiatry* 67, 296–303. <https://doi.org/10.1001/archgenpsychiatry.2009.205>.
- Wignall, E.L., Dickson, J.M., Vaughan, P., Farrow, T.F.D., Wilkinson, I.D., Hunter, M.D., Woodruff, P.W.R., 2004. Smaller hippocampal volume in patients with recent-onset posttraumatic stress disorder. *Biol. Psychiatry* 56, 832–836. <https://doi.org/10.1016/j.biopsych.2004.09.015>.
- Woodward, S.H., Kaloupek, D.G., Streeter, C.C., Martinez, C., Schaer, M., Eliez, S., 2006. Decreased anterior cingulate volume in combat-related PTSD. *Biol. Psychiatry* 59, 582–587. <https://doi.org/10.1016/j.biopsych.2005.07.033>.
- Woon, F.L., Sood, S., Hedges, D.W., 2010. Hippocampal volume deficits associated with exposure to psychological trauma and posttraumatic stress disorder in adults: a meta-analysis. *Prog. Neuro-Psychopharmacol. Biol. Psychiatry* 34, 1181–1188. <https://doi.org/10.1016/j.pnpbp.2010.06.016>.
- Yamasue, H., Kasai, K., Iwanami, A., Ohtani, T., Yamada, H., Abe, O., Kuroki, N., Fukuda, R., Tochigi, M., Furukawa, S., Sadamatsu, M., Sasaki, T., Aoki, S., Ohtomo, K., Asukai, N., Kato, N., 2003. Voxel-based analysis of MRI reveals anterior cingulate gray-matter volume reduction in posttraumatic stress disorder due to terrorism. *Proc. Natl. Acad. Sci. U. S. A.* 100, 9039–9043. <https://doi.org/10.1073/pnas.1530467100>.
- Yehuda, R., Teicher, M.H., Trestman, R.L., Levengood, R.A., Siever, L.J., 1996. Cortisol regulation in posttraumatic stress disorder and major depression: a chronobiological analysis. *Biol. Psychiatry* 40, 79–88. [https://doi.org/10.1016/0006-3223\(95\)00451-3](https://doi.org/10.1016/0006-3223(95)00451-3).
- Yilmaz, M., Meister, M., 2013. Rapid innate defensive responses of mice to looming visual stimuli. *Curr. Biol.* 23, 2011–2015. <https://doi.org/10.1016/j.cub.2013.08.015>.

2.3. Why Do Mice Squeak?

Ruat J, Genewsky AJ, Heinz DE, Kaltwasser SF, Canteras NS, Czisch M, Chen A, Wotjak CT

Manuscript under revision

Why do mice squeak?

Julia Ruat^{1,2,3}, Andreas J. Genewsky², Daniel E. Heinz², Sebastian F. Kaltwasser², Newton S. Canteras⁴, Michael Czisch⁵, Alon Chen^{1,6}, Carsten T. Wotjak^{2,7,*}

¹Department Stress Neurobiology and Neurogenetics, Max Planck Institute of Psychiatry, 80804 Munich, Germany.

²Research Group Neuronal Plasticity, Max Planck Institute of Psychiatry, 80804 Munich, Germany.

³International Max Planck Research School for Translational Psychiatry (IMPRS-TP), 80804 Munich, Germany.

⁴Department of Anatomy, Institute of Biomedical Sciences, University of São Paulo, São Paulo 05508-000, Brazil.

⁵Scientific Core Unit Neuroimaging, Max Planck Institute of Psychiatry, 80804 Munich, Germany.

⁶Department of Neurobiology, Weizmann Institute of Science, Rehovot 76100, Israel.

⁷Central Nervous System Diseases Research (CNSDR), Boehringer Ingelheim Pharma GmbH & Co KG, 88397 Biberach an der Riss, Germany.

***Correspondence:** wotjak@psych.mpg.de

Summary

While mice mostly communicate in the ultrasonic range, they also emit audible calls upon painful or threatening encounters. Here we demonstrate that mice selectively bred for high anxiety-related behavior (HAB) show a high disposition for emitting sonic calls when caught by the tail. The vocalization was unrelated to pain but sensitive to anxiolytics. As revealed by manganese-enhanced MRI, the increased anxiety and sonic vocalization shown by HAB mice coincided with increased tonic activity – among others – of the periaqueductal grey (PAG). Selective inhibition of its dorsolateral part not only reduced anxiety-like behavior but also completely abolished sonic calls, thus further supporting a causal link between high levels of anxiety and squeaking. Calls were emitted at a fundamental frequency of 3.8 kHz, which falls into the sensitive hearing range of numerous predators. Indeed, playback of sonic vocalization attracted rats if associated with a stimulus mouse. If played back to HAB mice, squeaks were repellent in absence but attractive in presence of a conspecific. Our data demonstrate that sonic vocalization attracts both predators and conspecifics depending on the social context. This may increase the likelihood of escaping from circa-strike situations.

Keywords

Vocalization, sonic, anxiety, periaqueductal grey, manganese-enhanced MRI, escape behavior, fear, predator, playback

Introduction

Vocalization is an essential mean of communication that conveys information to conspecifics and across species. It is produced in a diverse range of contexts and emotional states, such as during social interactions like courtship, play and maternal care, but also in threatening situations in the shape of alarm calls and cries, and in response to painful encounters. Vocalization requires an interplay of respiratory, laryngeal, and supralaryngeal components which are coordinated via hindbrain nuclei¹⁻⁵. From decades of work, the midbrain PAG has been established as a crucial gating center for vocalization from fish to humans^{3,6-9}. For instance, bilateral lesions or traumatic injury lead to mutism while electrical or neurochemical stimulation of the PAG could trigger natural vocalization sounds¹⁰⁻¹⁷. In mice, recent work has discovered a specific subpopulation of PAG neurons and their hypothalamic inputs that mediate vocalization^{9,18-20}. Research on mouse vocalization has mainly focused on ultrasonic vocalization (USV). However, beside these sounds that are inaudible for humans, mice also emit squeaks and squeals that are well within the human hearing range. Compared to our growing understanding of mouse USV neuronal circuits, its functions²¹⁻²⁵ and implications in mouse models of psychiatric disorders like autism, schizophrenia, and mania²⁶⁻³⁰, sonic vocalization has received by far less attention. Early reports refer to observations of singing house mice^{31,32} and describe sonic squeaks in the context of pain cries^{33,34} and defensive behaviors³⁵⁻³⁸. Yet, the characteristics of sonic mouse vocalization and the underlying neuronal circuits and ecological relevance are largely unexplored.

In the current study, we used a mouse line that had been selectively bred for high anxiety-related behavior³⁹ in which we had observed a high disposition of sonic calls during handling. We studied (i) the characteristics of the sonic calls in comparison to other mouse lines, (ii) assessed the consequences of anxiolytic versus panicolytic compounds, (iii) dissected the neuronal circuits for sonic vocalization by means of manganese-enhanced magnetic resonance imaging (MEMRI)^{40,41}, tracing, pharmacological and chemogenetic methods and (iv) investigated the ecological function of sonic calls in relation to conspecifics and predators.

Results

Mice bred for high anxiety-related behavior show a high disposition for sonic vocalization

Based on our observation that HAB mice emit sonic calls when lifted by their tail, we used the classic tail suspension test (TST) to trigger and record sonic vocalization (Figure 1A). To investigate whether this vocalization behavior is specific to HAB mice, we tail suspended HAB, normal anxiety-related behavior (NAB, originating from the same CD-1 strain by selective breeding), CD-1, BALB/c, DBA and C57BL/6 (B6N) mice and measured vocalization. During a 5-min TST, 75 % of HAB mice emitted sonic calls while no NAB, CD-1, nor B6N and only one out of 30 BALB/c mice produced sonic vocalization ($\chi^2 = 86.3$, $p < 0.0001$; Figure 1B). Also female HAB mice produced sonic vocalization when suspended by the tail, even though at a lower percentage than males (26 %; $\chi^2 = 9.2$, $p < 0.01$, data not shown). NAB mice weighed significantly more than HAB mice ($t_{44} = 7.9$, $p < 0.0001$; Figure 1C), and the struggling behavior did not differ between the two strains ($t_{38} = 0.8$, $p = 0.41$; Figure 1D). In the hot-plate test, HAB mice showed even a lower pain sensitivity than NAB mice ($U = 3$, $p < 0.0001$; Figure 1E). These findings preclude increased levels of physical stress and pain as the driving force behind the elevated susceptibility of HAB mice for sonic vocalization.

HAB mice were not generally more talkative, since fewer animals emitted ultrasonic calls compared to male NAB mice in the presence of a female conspecific ($\chi^2 = 4.1$, $p < 0.05$; Figure 2A), which was also reflected by a lower number of female-induced USVs ($U = 14$, $p < 0.01$; Figure 2B). The reduced ultrasonic vocalization was unrelated to the social investigation behavior, which were even more pronounced in HAB mice ($t_{18} = 6.4$, $p < 0.0001$; Figure 2C). Thus, the lower prevalence of ultrasonic vocalization shown by HAB mice is unrelated to deficits in social interaction.

Sonic vocalization is sensitive to anxiolytics

To gain insight into potential systems involved in the regulation of sonic vocalization, we treated mice systemically with anxiolytic and panicolytic compounds before tail suspension. The group of diazepam-treated HAB mice showed a trend to a reduction in the number of vocalizing animals compared to vehicle-treated HAB mice ($\chi^2 = 3.55$, $p = 0.06$; Figure 3A), with the number of sonic calls emitted significantly decreased after

diazepam administration ($U = 31.5$, $p < 0.05$; Figure 3B). Mobility during the TST, in contrast, was unchanged ($U = 57$, $p = 0.57$; Figure 3C). Diazepam treatment of male mice before a social interaction with a female did not alter the number of USV emitted compared to vehicle-treated controls ($U = 59.5$, $p = 0.69$; data not shown). This demonstrates the sensitivity of sonic, but not ultrasonic vocalization to anxiolytic drugs.

Given the panicolytic consequences of activated anandamide signaling⁴², we blocked the main degrading enzyme of this endocannabinoid, fatty acid amide hydrolase (FAAH), before the TST. Neither of the doses of URB597 (0.3 and 1 mg/kg) had an effect on the number of vocalizing animals ($\chi^2 = 0.72$, $p = 0.70$; Figure 3D), the number of calls emitted ($F_{2,36} = 0.06$, $p = 0.94$; Figure 3E), nor the mobility ($F_{2,35} = 1.24$, $p = 0.30$; Figure 3F). To rule out that anandamide signaling had already been sufficiently activated by the test procedure, which would have occluded any further changes by URB597 treatment, we administered the cannabinoid receptor type 1 (CB1) antagonist/inverse agonist SR141716A to a new cohort of mice prior to the TST. Again, we did not observe changes in the proportion of vocalizing animals ($\chi^2 = 0.02$, $p = 0.88$; Figure 3G), the number of calls ($t_{17} = 0.66$, $p = 0.52$; Figure 3H), or the struggling behavior during the TST ($U = 36$, $p = 0.44$; Figure 3I). Taken together, we could show that sonic vocalization is sensitive to anxiolytics but is most likely not controlled by the endocannabinoid system.

The dorsolateral periaqueductal grey controls sonic vocalization

In a next step, we aimed at dissecting the central pathways controlling the high levels of anxiety and sonic vocalization in HAB mice. To this end we assessed the accumulation of manganese as a measure for tonic neuronal activity using MEMRI. We identified several brain regions with differences in manganese accumulation when comparing male HAB and NAB mice (Figure 4A). Among others, HAB mice seem to have a decreased tonic neuronal activity of the superior colliculus and the reticular nucleus. Conversely, manganese accumulation was increased in the lateral septum, the hippocampus, the interpedunculo-pontine nucleus, and the rostral and caudal periaqueductal grey (Figure 4B-C, Supplementary Figure 1). Local infusions of muscimol (MUSC) into the dorsolateral PAG (dlPAG) prior to the TST (Figure 4D,E) resulted in complete abolishment of sonic vocalization ($\chi^2 = 20.1$, $p < 0.0001$, Figure 4F; $U = 14$, $p < 0.0001$, Figure 4G). In contrast, mobility was significantly increased ($U = 39$, $p < 0.05$; Figure 4H). Importantly, the same intervention caused the animals to spend significantly less time in the closed ($t_9 = 3.7$, p

< 0.01; data not shown) and significantly more time in the open arms of an Elevated Plus Maze (EPM) compared to vehicle-treated controls ($U = 1$, $p < 0.01$, Figure 4I). This finding further supports the close link between increased anxiety and high levels of sonic vocalization and suggest an essential role for the PAG in this interaction.

Since the intraneuronal accumulation of manganese is biased towards axon terminals⁴⁰, we aimed at identifying brain areas projecting to the PAG. We injected the retrograde tracer Fluoro-Gold (FG) unilaterally into the dlPAG of HAB mice (Supplementary Figure 2A) and found FG-labeled cells in the medial prefrontal cortex (mPFC), more specifically the infralimbic, prelimbic and cingulate cortex and the secondary motor area (Supplementary Figure 2B,C). Less dense labeling was observed in the lateral septum (Supplementary Figure 2D). FG-positive cells could also be seen in the medial and lateral preoptic area and the bed nucleus of stria terminalis (Supplementary Figure 2E). Strong labeling was shown in the ventromedial hypothalamus and the zona incerta, and a few FG-positive cells could be observed in the dorsomedial hypothalamus (Supplementary Figure 2F). Given the evidence for a strong projection from mPFC to the dlPAG and earlier reports on the role of the mPFC in controlling vocalization in rats, monkeys, and humans^{43–45}, we employed a double-viral approach to chemogenetically inhibit the pathway (Supplementary Figure 2G,H). The intervention did neither affect the number of vocalizing animals ($\chi^2 = 0.1$, $p = 0.75$; Supplementary Figure 2I) and the number of calls emitted ($U = 65$, $p = 0.49$; Supplementary Figure 2J), nor the struggling behavior ($U = 56.5$, $p = 0.38$; Supplementary Figure 2K) during the TST. Conversely, the inhibition of the mPFC-dlPAG pathway led to a decrease in avoidance behavior upon confrontation with an erratically moving robo-beetle ($t_{23} = 2.4$, $p < 0.05$; Supplementary Figure 2L), thus demonstrating the sufficiency of the approach to interfere with innate fear. Consequently, other projections to the PAG but from the mPFC seem to mediate sonic vocalizations in HAB mice.

Sonic mouse calls are appetitive to rats and mice in the presence of a social stimulus

Since vocalization aims at transmitting information to other individuals, we wanted to elucidate the ecological function of sonic HAB calls. In a first step, we analyzed the characteristics of the calls. A representative spectrogram of sonic calls of HAB mice is depicted in Figure 5A. The recorded calls follow a harmonic structure with a flat pattern

showing very little modulation in frequency. Besides, nonlinear features such as subharmonics and deterministic chaos can be detected in the spectrogram of the calls (Figure 5A). Most calls were emitted during the first minute of the TST and vocalization declined over time (Figure 5B). Analysis of the characteristics of the calls emitted by male HAB mice revealed a mean fundamental frequency of 3802 ± 87.6 Hz (Figure 5C) with a mean duration of 56.4 ± 4.2 ms length (Figure 5D). During a 5-min TST, male HAB mice emitted a variable number of calls, with a median call number of 7 calls (Figure 5E). To compare the measured fundamental frequency of TST-triggered calls with those emitted in other behavioral test situations and by other strains, we subjected male HAB and B6N mice to a social defeat paradigm. Sonic calls emitted by defeated HAB mice were comparable to those emitted during a TST (fundamental frequency of 3872 ± 116 Hz) and those of defeated B6N mice (3870 ± 192 Hz (data not shown)).

The fundamental frequency of the recorded calls falls within the best hearing frequencies for numerous predators^{46–50}. Since rats are muricide in the wild, we set up a playback experiment where TST-triggered sonic calls of HAB mice or a white noise control sound (Figure 6A) were presented to male Long Evans rats (Figure 6B), whereby the animals could control the presentation of the acoustic stimuli by their own behavior, thus turning it into a kind of real-time place-preference/place-avoidance paradigm. During baseline (BL; no sound presentation, no stimulus mouse; Figure 6D), rats showed no preference for one of the prospective stimulus zones ($t_{12} = 0.27$, $p = 0.80$; Figure 6G). Similarly, no preference was observed during the playback (PB) stage during which squeaks and white noise sounds were presented ($t_{12} = 1.62$, $p = 0.13$; Figure 6E,H). In the third stage of the test, male B6N stimulus mice were constrained to each playback zone in order to make the sound presentation more relevant with the presence of a social stimulus (PB+S, Figure 6F). In presence of stimulus mice, rats showed a preference for the squeak zone ($t_{12} = 2.51$, $p < 0.05$; Figure 6I). To illustrate these results more clearly, we calculated the Squeak Zone Score that indicates the preference for the squeak zone with values above 50. Rats showed a significantly higher Squeak Zone Scores in the PB+S compared to the PB stage ($F_{2,24} = 6.61$, $p < 0.01$; Figure 6J). Hence, potential predators are attracted to the squeaks if presented together with a real-life prey/mouse.

Even though the fundamental frequency of the squeaks falls below the best hearing frequencies of mice^{46,50}, the harmonics at higher frequencies render it likely that sonic calls may serve as alarm signals for conspecifics. Therefore, we repeated the playback experiments with HAB and NAB mice, analogously to the playback experiment with rats

(Figure 6C). During the BL period, both HAB ($t_8 = 0.12$, $p = 0.92$; Figure 6K) and NAB ($t_7 = 0.26$, $p = 0.80$; Figure 6O) mice spent equal amounts of time in the prospective playback arms of the test apparatus. Upon presentation of the sounds in the PB stage, HAB mice spent less time in the squeak zone compared to the white noise zone ($t_8 = 3.20$, $p < 0.05$; Figure 6L). This effect was not observed in NAB mice ($t_7 = 0.66$, $p = 0.53$; Figure 6P). Despite avoiding the squeak zone during the PB stage, HAB mice spent more time in the squeak zone compared to the white noise zone in presence of a stimulus animal during the PB+S stage ($t_8 = 2.70$, $p < 0.05$; Figure 6M). Likewise, NAB mice preferred the squeak zone over the white noise zone during the PB+S stage ($t_7 = 3.07$, $p < 0.05$; Figure 6P). Considering the Squeak Zone Score, HAB mice showed an aversion for the squeak zone when the sound was presented alone ($t_8 = 2.64$, $p < 0.05$) but revealed a preference once a stimulus animal was present ($t_8 = 2.85$, $p < 0.05$ and $F_{2,16} = 11.47$, $p < 0.001$; Figure 6N). For NAB mice the preference is only significant in the presence of a stimulus mouse during PB+S ($t_7 = 3.19$, $p < 0.05$ and $F_{2,14} = 4.76$, $p < 0.05$; Figure 6R). Together, these data indicate the aversive nature of squeaks per se to the highly anxious HAB mice. In combination with a social stimulus, however, avoidance turned into approach behavior not only in HAB but also in NAB mice.

Discussion

Mice bred for high anxiety-related behavior³⁹ showed a high disposition to vocalize when suspended by the tail compared to other mouse lines which could not be explained by different stress coping strategies or higher pain sensitivity. Sonic vocalization was sensitive to anxiolytic but not panicolytic treatment and depended on the dorsolateral PAG. Playback of sonic calls to rats and mice revealed that the squeaks trigger approach behavior, however only in the presence of a stimulus mouse.

When suspended by the tail, only HAB mice reliably vocalized. This was not related to a higher body weight, increased struggling during the test or increased pain sensitivity. Conversely, HAB mice emitted less USVs during interaction with females despite an increase in exploration time. This dissociation stands in contrast to mouse models of autism, whereby the impairment in female-induced USV emission shown by BTBR T+tf/J mice coincided with reduced investigation times²⁹.

Audible vocalizations have been reported in the context of predatory defense. Along the predator imminence continuum⁵¹, anxiety-like and fear behaviors such as risk assessment and freezing decrease with increasing proximity to the predator and switch to explosive panic-like behaviors such as fighting, biting, jumping, and vocalizations in response to an attack (for review see Perusini & Fanselow, 2015). Increasing anandamide signaling via CB1 receptors may reduce panic-like behaviors in HAB mice upon confrontation with an erratic moving robo-beetle⁴². Therefore, we treated HAB mice with URB597 to inhibit FAAH activity. However, the treatment did not show any effect on sonic vocalizations, similarly to treatment with a CB1 receptor antagonist. Together these findings speak against an involvement of endocannabinoid signaling in sonic vocalization. In contrast, treatment with the anxiolytic diazepam significantly reduced the number of sonic calls without affecting female-induced USV. Taken together the results of pharmacological treatment, sonic vocalization seems to be more closely connected to anxiety than panic. Interestingly, HAB mouse pups emit a higher number of isolation-induced USV^{39,52,53}, a behavior associated with anxiety⁵⁴ that could be reduced by treatment with diazepam³⁹.

We employed MEMRI to relate the increased disposition of HAB mice for emitting sonic calls due to increased basal anxiety levels to tonically increased neuronal activity. Mn²⁺ enters neurons through ion channels in an activity-dependent manner^{40,41}. Due to its paramagnetic characteristics, Mn²⁺ can be quantified *in vivo* using MRI. Voxel-wise comparisons of HAB and NAB mice revealed, among others, increased Mn²⁺ accumulation

in the septal-hippocampal complex, which has been suggested as a key circuit implicated in generalized anxiety⁵⁵. In addition, we observed increased Mn²⁺ levels within the PAG. Local muscimol infusion into the PAG completely abolished sonic vocalizations and significantly reduced anxiety-like behavior. The PAG has been established as a gating center for vocalization across many species³, including mice^{9,20}. Here we extend those observations by its role as an important hub for the coordination of anxiety-related vocalization.

The intraneuronal accumulation of Mn²⁺ is biased towards axon terminals⁴⁰. Therefore, we used retrograde tracing to identify brain structures which project to the PAG and may contribute to the increased Mn²⁺ accumulation observed at level of the PAG. Those structures included the mPFC, the lateral septum, the preoptic area, the VMH and the zona incerta. This is in line with previous findings^{56–58} (for review see Silva & McNaughton, 2019⁵⁹). Electrical stimulation of the prelimbic cortex in rats has been shown to trigger vocalizations⁴⁵. To prove a functional involvement of the mPFC-dIPAG projection in sonic vocalization in mice, we employed a double-viral chemogenetic approach to selectively inhibit this projection during tail suspension. While the intervention proved to be capable of modulating behavioral responses as seen by decreased avoidance behavior during the BMT, it was inefficient in affecting sonic vocalization. Even though this finding suggests that the mPFC-dIPAG projection is not essential for this behavior, technical reasons such as a restricted expression of the chemogenetic receptors may limit our conclusion.

Given that mice emit sonic calls in both interactions with conspecifics^{34,37} (wriggling, defeat) and during circa-strike attacks by predators³⁶, the question arises as to their ecological relevance. Mice mostly communicate in the ultrasonic range e.g., during courtship^{60,61}, in female-female interactions^{62,63} and in form of isolation-induced pup calls^{64,65} to attract mating partners, social partners or maternal care. Ultrasonic communication gives rodents an advantage in evading predator detection since many predators are unable to hear ultrasonic sounds, the sound waves are more directional, and attenuate rapidly compared to sounds in the sonic frequency range^{66,67}. So, why do mice then also emit squeaks and squeals audible to humans and predators? Sonic mouse vocalization has been described in the context of pain^{68,69}, when a non-receptive female is approached by a male mouse⁷⁰, wriggling sounds of pups⁷¹, or during defense³⁶. We have shown that mouse squeaks emitted when held by the tail or in a defeat situation have a fundamental frequency of 3800 Hz, which is in line with previous reports^{35,68}. Evaluation

of the spectral features revealed that some calls contain nonlinear features such as subharmonics and deterministic chaos⁷². These spectral elements have previously been described in calls of high arousal like alarm calls and screams across different species including humans^{72–75}. Nonlinearities make calls evocative and attract the listener's attention⁷⁴. Further, these features were found to prevent habituation to the sound^{76,77}. In particular, subharmonics present an interesting aspect that allow the animal to lower the pitch, a characteristic which receivers associate with larger body size and aggression of the vocalizing animal^{78,79}. This allows small animals to mimic the vocal frequency of a larger animal and potentially prevent a predator attack⁷².

To assess the impact of sonic calls on potential predators and conspecifics, we designed playback experiments, in which the animals could control the occurrence of sonic calls or control white noise sound by their own behavior. Playback of sonic calls attracted rats, however, only if combined with a stimulus mouse. The same has been the case for both HAB and NAB mice. In absence of a stimulus mouse, sonic calls lose their appetitive nature (NAB) or even turn into a repellent signal (HAB). The neural basis of this remarkable social contextualization remains to be shown in future studies.

In the desperate situation of being trapped or caught by a predator, attraction of a conspecific may distract predators and, thus, increase the likelihood to escape. However, while the best hearing frequency of *Mus musculus* is near 16 kHz, foxes and cats perceive best sounds of 4 kHz and 8 kHz, respectively^{46–48}. Intriguingly, hunters regularly use whistles that imitate distress calls in the range of 3 to 10 kHz to lure foxes or feral cats. Assuming that vocalizations are transmitting information, the sender should choose a frequency that triggers the highest responsiveness in the receiver. Under this premise, it is likely that the emission of 3.8 kHz calls by mice and the hearing range of predators have coevolved. Vocalizations addressing a predator have been observed across species and typically increase in rate with closer proximity of the threat (e.g., also a human experimenter). It is assumed that such calls inform the predator that the prey is prepared for defense actions and counter-attack⁸⁰. Further, the squeaks may startle the predator, offering the prey a chance to escape^{81–83}. On top, the screams of a struggling prey might attract a second predator expecting an easy meal. The subsequent fight between the two rival predators might offer the prey another chance to flee⁸². In support of these hypotheses, playback of avian distress calls was indeed shown to trigger approach and to startle predators

Taken together, our study provides insights into sonic mouse vocalization as a mean of communication under distress that has so far received little to no attention in neurobiological research. So, why do mice squeak? Because they are anxious, show increased activity of the PAG and to attract both conspecifics and predators to increase the likelihood to escape if trapped.

Acknowledgements

We thank Robert Neuner for technical support and Dr. Alice Hartmann for experimental assistance.

JR was supported by FAPESP-BAYLAT and the international Max Planck Research School for Translational Psychiatry (IMPRS-TP).

DEH was supported by the Federal Ministry of Education and Research (BMBF) and the Max Planck Society.

AC is the incumbent of the Vera and John Schwartz Professorial Chair in Neurobiology at the Weizmann Institute of Science; the Head of the Max Planck Society–Weizmann Institute of Science Laboratory for Experimental Neuropsychiatry and Behavioral Neurogenetics gratefully funded by the Max Planck Foundation; and the Head of Ruhman Family Laboratory for Research in the Neurobiology of Stress at the Weizmann Institute of Science. This work is supported by Bruno and Simone Licht (AC) and Roberto and Renata Ruhman.

Author Contributions

Conceptualization J.R., A.J.G., A.C. and C.T.W.; Formal Analysis J.R., A.J.G., S.F.K. and M.C.; Investigation J.R., A.J.G. and D.E.H.; Resources N.S.C.; Writing J.R. and C.T.W.; Visualization J.R. and A.J.G.; Supervision A.C. and C.T.W.; Funding Acquisition A.C. and C.T.W.

Declaration of Interest

The authors declare no competing interests.

Figure Titles and Legends

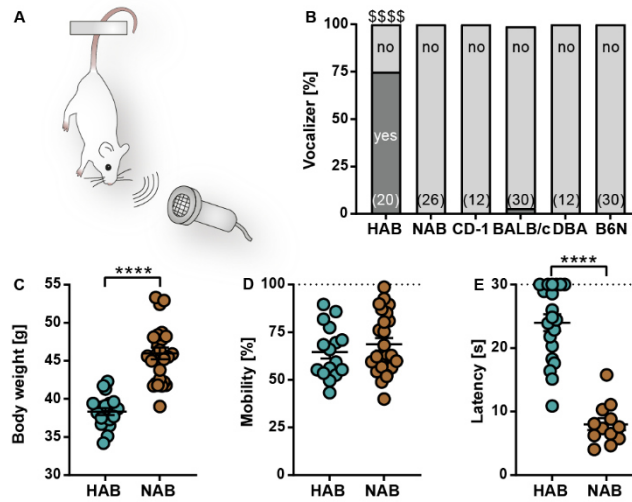


Figure 1: Mice bred for high anxiety-related behavior show a high disposition for sonic vocalization. (A) Sonic calls were triggered during a 5-min tail suspension and recorded using an ultrasound microphone. (B) Percentage of male mice of different mouse lines emitting sonic calls during tail suspension. HAB: High anxiety-related behavior, NAB; normal anxiety-related behavior, B6N: C57/Bl6. (C) Body weight of HAB (n=20) and NAB (n=26) mice. (D) Mobility behavior during the tail suspension. (E) Latency to hind paw flicks or licking during a hot plate test (n=20 HAB, n=12 NAB). Data are presented as percentage of total (B), individual data with mean \pm SEM (C-E). \$\$\$\$ $p < 0.0001$ (Chi square test), **** $p < 0.0001$ (unpaired t test).

Results

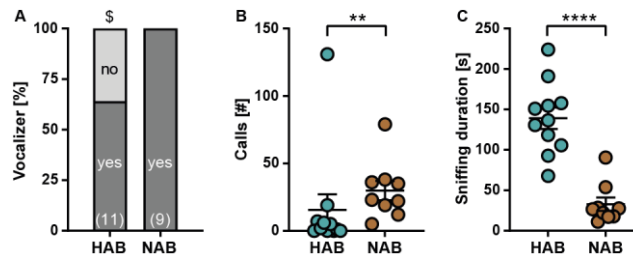


Figure 2: HAB mice produce less female-induced ultrasonic vocalization. (A) Percentage of male HAB (n = 11) and NAB (n = 9) mice emitting ultrasonic calls in the presence of a same-strain female. (B) Number of ultrasonic calls emitted during 10 min of interaction (not corrected for outliers). (C) Total duration of anogenital and facial sniffing by male mouse. Data are presented as percentage of total (A) individual data with mean \pm SEM (B-C). § $p < 0.05$ (Chi square test), ** $p < 0.01$, **** $p < 0.0001$ (unpaired t test).

Results

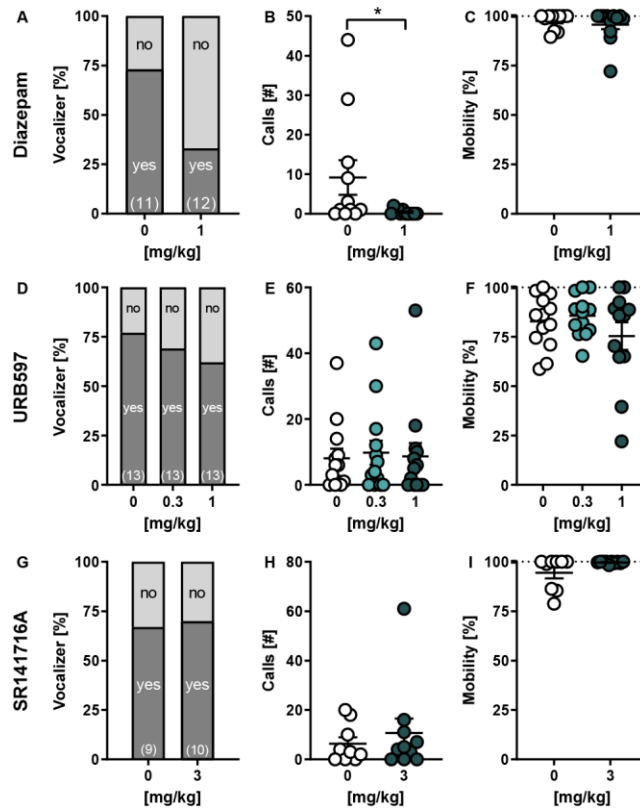


Figure 3: Sonic vocalization is sensitive to anxiolytics. Percentage of HAB mice emitting sonic calls (A, D, G), number of calls emitted per mouse (B, E, H), and mobility behavior (C, F, I) during tail suspension (2.5 min) 60 min after systemic treatment with diazepam (A-C), FAAH inhibitor URB597 (D-F), or CB1 receptor antagonist/inverse agonist SR141716A (G-I). Data are presented as percentage of total (A, D, G), individual data with mean \pm SEM (B-C, E-F, H-I). * $p < 0.05$ (Mann Whitney test for B).

Results

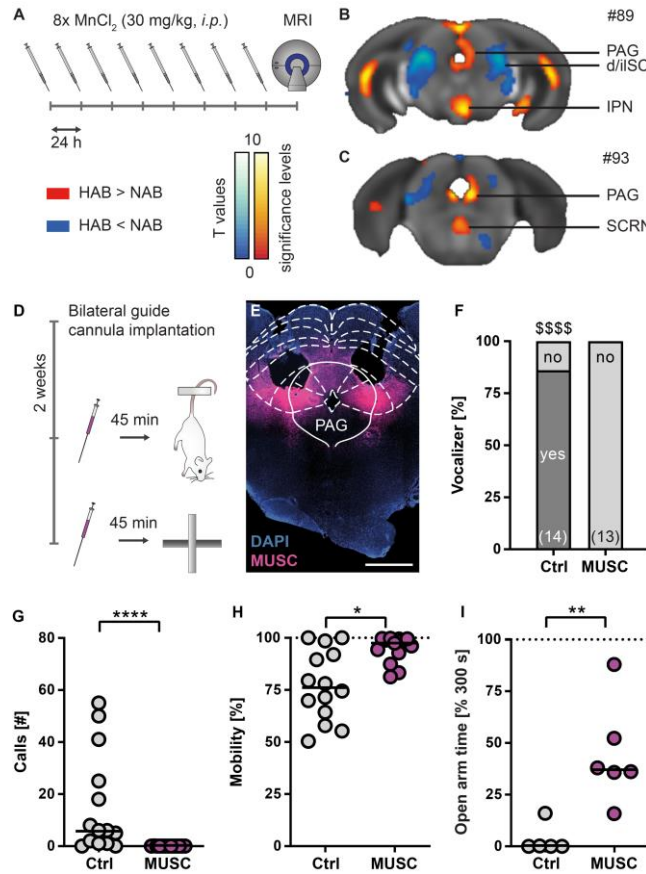


Figure 4: The dorsolateral periaqueductal grey controls sonic vocalization. (A-C) Manganese-enhanced MRI (MEMRI) comparing HAB vs. NAB mice. (A) HAB (n = 31) and NAB (n = 26) mice received daily systemic manganese injections (30 mg/kg) and underwent MRI scanning 24 hours after the last injection. (B-C) Increased tonic neuronal activity in the caudal periaqueductal grey (PAG) of HAB mice. d/ILSC: deep/intermediate layers of superior colliculus; IPN: interpedunclopontine nucleus. Numbers (#) indicate image numbers of corresponding reference images in the Allen Brain Atlas. (D-I) Local inhibition of the dlPAG using muscimol (MUSC). (D) MUSC was bilaterally injected via guide cannulas into the dlPAG 45 min prior to the TST and EMP (n = 14). (E) Representative image of the injection site. Scale bar: 1 mm. (F) Percentage of HAB mice emitting sonic calls, (G) the number of calls emitted per mouse, and (H) mobility behavior during the tail suspension (5 min). (I) Open arm time on the Elevated Plus Maze (EPM) during the first 5 min of the test. Data are presented as percentage of total (F) or individual data with median (G-I). \$\$\$\$p < 0.0001 (Chi square test), *p < 0.05, **p < 0.01, ****p < 0.0001 (Mann-Whitney test).

Results

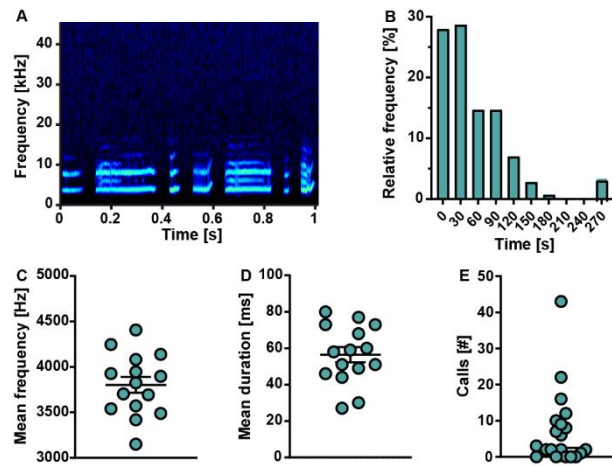


Figure 5: HAB mice emit sonic calls when caught by the tail. (A) Representative spectrogram displaying various HAB calls. (B) Relative frequency of calls emitted by HAB mice over the course of a 5-min tail suspension. (C) Mean fundamental frequency of HAB calls. (D) Mean duration of HAB calls. (E) Number of calls emitted per mouse during tail suspension. Data are presented as relative frequency (B), individual data with mean \pm SEM (C,D), or median (E).

Results

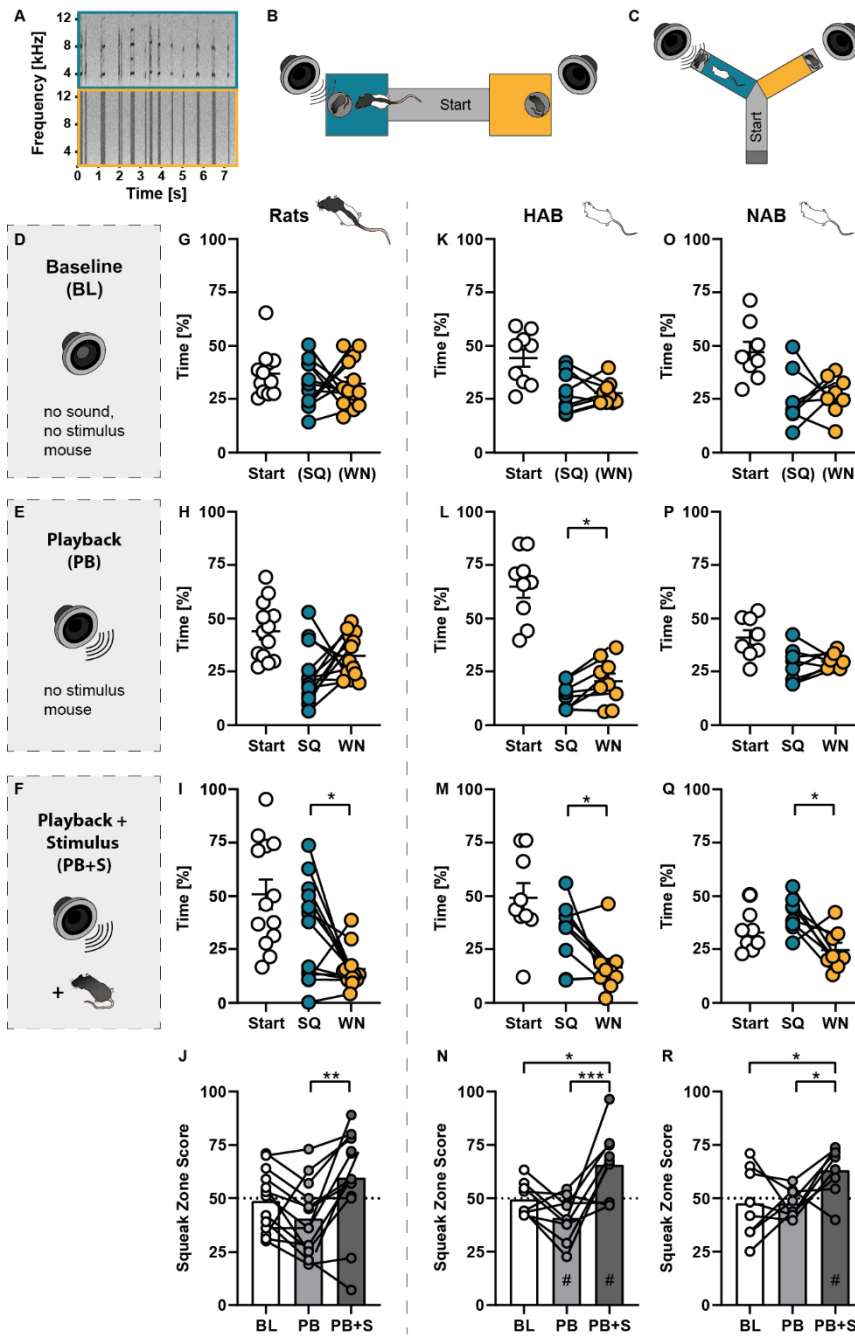


Figure 6: Sonic mouse calls are appetitive to rats and mice in the presence of a social stimulus. (A) HAB squeaks (SQ, upper spectrogram) or control time- and amplitude-matched white noise (WN, lower spectrogram) served as stimulus sounds. (B) Setup for rat ($n = 13$) playback experiment with two playback compartments and a connecting corridor. (C) Playback experiment with HAB ($n = 9$) and NAB ($n = 8$) mice were performed in a Y-maze with two playback compartments and a start arm where no sound was presented. (D) During the baseline stage (BL) animals could freely explore the maze without sound presentation or stimulus mouse. (E) Squeaks or white noise were played back once the animal has entered the respective zone during the playback stage (PB)

without additional stimulus mouse. (F) During the last stage (Playback + Stimulus, PB+S), the sounds were presented with an additional male stimulus mouse being present in each playback zone. Percentage of time spent in each zone is presented for rats (G-I), HAB (K-M), and NAB (O-Q). The squeak zone score for each stage of rats (J), HAB (N), and NAB (R). Data are presented as individual data with mean \pm SEM (G-I, K-M, O-Q) or individual data with mean (J, N, R). * $p < 0.05$, ** $p < 0.01$, *** $p < 0.001$ (paired t test for I, L, M, Q; RM 1-way ANOVA followed by Tukey's post-hoc test for J, N, R), # $p < 0.05$ (one sample t test for N,R).

STAR Methods

Resource availability

Lead contact

Further information and requests for resources and reagents should be directed to and will be fulfilled by the lead contact Dr. Carsten T. Wotjak (wotjak@psych.mpg.de).

Materials availability

This study did not generate new unique reagents.

Data and code availability

- All data reported in this paper will be shared by the lead contact upon request.
- Any additional information required to reanalyze the data reported.

Experimental model and subject details

Adult male C57BL/6NCr1 (B6N; n = 38, 6 months age), BALB/cAnNCr1 (BALB/c; n = 30, 5 months age), and DBA/2NCr1 (DBA, n = 12, 4 months age) mice were purchased from Charles River Laboratories (Sulzfeld, Germany). High-anxiety-related behavior (HAB; male n = 235, 2-9 months age; female n = 36, 2-4 months age), normal-anxiety-related behavior (NAB; male n = 91, 4-7 months age; female n = 8, 4 months age), both originating from a selective breeding approach which started with CD-1 outbred mice³⁹ and male CD-1 mice (n = 12, 4 months age) were bred in the vivarium of the Max Planck Institute of Biochemistry (Martinsried, Germany). After admission at the Max Planck Institute of Psychiatry, mice were permitted a recovery period of at least 10 days before starting with the experiments. Due to changes in the animal facility of the Max Planck Institute of Psychiatry, over time mice had to be housed under different conditions. All animals were group-housed under standard housing conditions (20-22 °C room temperature, 50-60 % humidity) in either Makrolon type II cages or Green Line IVC mouse cages with food and water *ad libitum*. Mice were kept under SPF conditions which were confirmed by biannual health monitoring using sentinel mice. A 12/12-hour normal or inverse light/dark cycle (6 am – 6 pm) was maintained. For within-strain comparisons, littermates of the same sex were randomly assigned to experimental groups. All mouse experiments were performed according to the European Community Council Directive 2010/63/EEC and approved by the local government of Upper Bavaria (55.2-1-54-2531: 44-09, 188-12, 142-12, 133-06, 08-16; 55.2-2532.Vet_02-17-223). All efforts were made to reduce the number of experimental subjects and to minimize any suffering.

Adult male Long Evans rats (n = 13, 2 months age) were group-housed under standard housing conditions at the Institute of Biomedical Sciences of the University of São Paulo, São Paulo, Brazil. Rats were kept in open cages with food and water *ad libitum* and maintained in a 12/12-hour normal light/dark cycle (lights on at 6 am).

Method details

Drugs

URB597 (0.3 or 1 mg/kg; Sigma-Aldrich, St. Louis, MO, USA) and SR141716A (3 mg/kg; Sigma-Aldrich) were dissolved in 15 % dimethylsulfoxide, 4.25 % polyethylene glycol, 4.25 % Tween 80, and 76.5 % saline. Diazepam (DZP, 1 mg/kg; Ratiopharm, Ulm, Germany) was dissolved in physiological saline. The drugs were injected intraperitoneally (*i.p.* at 10 ml/kg) 1 h prior to the behavioral paradigm. To activate DREADDs, clozapine *N*-oxide (CNO; Tocris, Bristol, Great Britain) dissolved in physiological saline was injected *i.p.* at 10 mg/kg and 10 ml/kg 45 min before exposure to the behavioral test.

Muscimol (MUSC; Sigma-Aldrich) and fluorescently-labeled MUSC (fMUSCL; BODIPY™ TMR-X conj., Thermo Fisher Scientific, Waltham, MA, USA) were dissolved in artificial cerebrospinal fluid (aCSF) and injected locally via guide cannulas 45 min prior to behavioral testing at 0.1 ng/nl. Vocalization experiments were conducted using fMUSC in a crossover design whereby half of the animals received fMUSC and the other half vehicle (aCSF). On the next day, the treatment was switched. For the elevated plus maze (EPM) experiment mice received MUSC or vehicle.

Stereotaxic Injections and Implantations

For all stereotaxic surgeries, mice were deeply anesthetized and then maintained at surgical tolerance with isoflurane (CP-Pharma, Burgdorf, Germany) in oxygen-enriched air. Pre-surgery analgesia was provided via subcutaneous (*s.c.*) injections of 5 mg/kg meloxicam (Metacam, Boehringer Ingelheim, Ingelheim am Rhein, Germany) and 200 mg/kg metamizole (Vetalgin®, MSD Animal Health). Post-surgery the animals were checked on daily and treated with 5 mg/kg meloxicam *s.c.* if needed for 3 days. Stereotaxic injections were delivered using a glass syringe connected to a micropump system (UMP3 and Micro4™, World Precision Instruments, Sarasota, FL, USA). All coordinates were validated and adapted to the CD-1 strain. For targeting the dlPAG the following

coordinates were used: AP -4.38 mm, ML \pm 0.3 mm, DV -2.20 mm. Fluoro-Gold (FG, 4 %, 350 nl; Fluorochrome, Denver, CO, USA) was injected unilaterally while all adeno-associated virus (AAV) injections were performed bilaterally. For double-viral targeting, 300 μ l AAVrg-pmSyn-EBFP-Cre (#51507, Addgene, Watertown, MA, USA) were injected at a titer of 7.6×10^9 gc/ μ l into the dlPAG. One week later, AAV1/2-hSyn-DIO-hM4D-mCherry (titer: 5×10^9 gc/ μ l) or AAV2-eSyn-EGFP (titer: 7.6×10^9 gc/ μ l; #VB1107, Vector Biolabs, Malvern, PA, USA) were injected into the medial prefrontal cortex (mPFC, AP +1.20 mm, ML \pm 0.3 mm) at two dorsoventral positions (DV -1.80 and -2.40 mm), 250 nl respectively. Animals were allowed 3 weeks recovery before subjected to behavioral testing.

For local MUSC injections, guide cannulas (L3 mm, 26 gauge; World Precision Instruments) were implanted bilaterally at AP -4.25 mm, ML \pm 1.02 mm, DV -1.55 mm with an angle of $\pm 25^\circ$. With an injection needle of 4 mm length, the target injection site was at AP -4.25 mm, ML \pm 0.6 mm, DV -2.45 mm. The cannulas were fixed to the skull with skull screws positioned above the hippocampus and dental cement (Paladur®; Kulzer, Hanau, Germany). To prevent clogging, dummy injection needles (L3.5 mm) with a dust cap were inserted into the guide cannulas. After allowing at least 2 weeks of recovery, the animals were slightly anesthetized (2-2.5 % of isoflurane) to inject 100 nl of MUSC or vehicle at 100 nl/min bilaterally via the guide cannulas.

Behavioral Tests

Tail Suspension Test (TST) and Sound Recording

Mice were attached to a vertical metal rod with lightly adhesive tape at a height of about 45 cm above ground. Light conditions were at 80-100 lx. A CM16/CMPA ultrasound microphone (Avisoft Bioacoustics, Glienicke, Germany) connected to an UltraSoundGate 116 (Avisoft Bioacoustics) was placed in 25 cm distance from the mouse. Sound was recorded using Avisoft RECORDER (Version 2.9) and mice were videotaped using ANY-maze tracking software (Stoelting Co., Dublin, Ireland) to allow for scoring of mobility behavior by a trained observer. The test lasted for 2.5 or 5 min.

Hot Plate Test

To test for thermal pain sensitivity, mice were placed on a warm metal surface (53 ± 0.1 °C) surrounded by a cubic Plexiglas wall (Ugo Basile, Gemonio, Italy). The latency to hind paw flicks or licks was measured with a stopwatch. If no reaction was observed, the test was stopped after 30 s.

Social Defeat

Male HAB or B6N mice were placed into the open top home cages of male single-housed CD-1 resident mice. Vocalization was recorded using a CM16/CMPA ultrasound microphone. The test was aborted, and the intruder mouse removed once approximately 15 calls were recorded, the attacks accumulated to avoid wounding or after 10 min of testing.

Social Interaction with Female Mice

Male mice were placed into a square cage with transparent Plexiglas walls and an open top (L40 x W40 x H35 cm) without bedding (to avoid background noise). After a habituation period of 5 min, a female mouse of the same strain was inserted, and the mice could freely interact for 10 min. To record ultrasonic vocalization, a CM16/CMPA ultrasound microphone was positioned approximately 25 cm above ground hanging through the open top of the cage. The session was videotaped and the time the male mouse spent sniffing on the female mouse (anogenital and facial sniffing) was scored. The cage was cleaned with soap and water in between each trial.

Elevated Plus Maze (EPM)

The maze was an elevated (32 cm above ground) plus-shaped platform consisting of two opposite arms enclosed by opaque Plexiglas walls (L27 x W5 x H14 cm) and two opposite arms without walls (L30 x W5 cm, surrounded by a small rim of 0.5 cm height), connected by a central zone (L5 x W5 cm). Mice were placed in the end of one of the closed arms facing the wall. They were allowed to freely explore the maze for 15 min. The experiment was video-recorded, and the time spent in the closed arms was determined. The maze was cleaned with soap and water after each trial.

Beetle Mania Task (BMT)

To test for defensive reactions, the BMT was performed as described previously⁴². In brief: Mice were inserted in one end of a rectangular arena (L100 × W15 × H37 cm) made of gray polyethylene. After a 5-min habitation phase, an erratically moving robo-beetle (Hexbug Nano, Innovation First Labs Inc., Greenville, TX, USA; L4.5 × W1.5 × H1.8 cm) was inserted far most distant from the mouse. During the 10-min test period, avoidance behavior upon contact with the robo-beetle (whereby the mouse withdrew from the robo-beetle with accelerated speed) was scored. The maze was cleaned with soap and water after each trial.

Playback Experiments

The sounds played back were sonic calls recorded from male HAB mice during a TST. Using Audacity® open-source software, a time- and amplitude-matched white noise sound was created as a control stimulus. The recordings were of 21 s length and were seamlessly repeated if needed.

The playback (PB) experiment with mice was performed in a Y-shaped grey polyethylene maze (arm dimensions: W9.5 x L30 x H10 cm). Two arms were equipped with speakers over each end, the start arm was not. Each rear end of the arms was segregated by a fence. The test animal was placed into the start arm and was automatically tracked using EthoVision XT 14 (Noldus Information Technology, Wageningen, the Netherlands). During the first stage of the test, the baseline (BL) stage, the animal could freely explore the maze without sound presentation for 3 min. In the second stage (PB, 3 min), the squeak sound was automatically presented whenever the animal entered the left arm and continued playing until the animal left the arm. In the same manner, the control sound was played whenever the animal was positioned in the right arm of the maze. No sound was presented in the start arm. In the last stage (PB+S, 3 min) male B6N stimulus mice were constrained to the rear end of the two playback arms, allowing visual, auditory, and olfactory but no physical contact with the test animal. The sounds were presented in the same manner as in the PB stage. The maze was cleaned with soap and water after each trial.

The setup for rats consisted of two transparent Plexiglas boxes (L25 x W25 x H25 cm) connected by a corridor of 100 cm length (W12.5 x H26 cm). The speakers were installed above the two boxes. Transparent plastic containers with holes were fixed in the rear ends

of the boxes for stimulus mice. Rats were habituated to the setup on 3 consecutive days, allowing 10 min of free exploration without sound presentation. The playback experiment was performed on the fourth day analogous to the mouse playback experiment. A 3-min BL stage without sound presentation was followed by a 4-min PB stage. The squeaks were played whenever the rat entered the left box and the control sound was presented when it was positioned in the right box. No sound was presented when the rat was in the corridor. During the PB+S stage (4 min), male B6N mice were placed into the containers and the sounds were played back in same manner as in the PB stage. The setup was cleaned with 70 % ethanol after each trial.

For both experiments, the time spent in each zone was determined. The Squeak Zone Score was calculated as $time\ in\ squeak\ zone / (time\ in\ squeak\ zone + time\ in\ white\ noise\ zone)$.

Sound Analysis

The number of calls and the call duration were analyzed manually in Raven Pro (Interactive Sound Analysis Software Version 1.5; The Cornell Lab of Ornithology, Ithaca, NY, USA). For analysis of the fundamental frequency of sonic calls, a custom-written Python 2.7 script was used.

Histology

To verify injection and implantation sites, sections of either freshly frozen or perfused brains were analyzed. For both cases mice were overdosed with isoflurane. To obtain fresh tissue, the brain was dissected from the skull and shortly placed into ice-cold methylbutane. Brains were then stored at -80 °C until sectioned using a cryostat. 20 µm sections were mounted directly onto microscopy slides (SuperFrost Plus™, Thermo Fisher Scientific) and stored at -20 °C. Transcardial perfusion was performed after respiratory arrest had been confirmed. Cold phosphate buffered saline (PBS) was supplied followed by 4 % paraformaldehyde (PFA) in PBS. The brain was dissected from the skull, incubated at 4 °C in 4 % PFA overnight and subsequently transferred into 30 % sucrose in PBS solution. Perfused brains were vibratome-sectioned at 30 µm slice thickness. The slices were stored in cryoprotectant solution at -20 °C.

Mice that had received fMUSC injections were perfused 1-3 days after injection. To visualize FG labeling, mice were perfused 1 week after surgery. Brains were freshly frozen from animals of the double-viral experiment 5 weeks after the first viral injection.

To visualize the infection of the tissue with AAVrg-pmSyn-Cre-EBFP and AAV1/2-hSyn-DIO-hM4D-mCherry, their fluorophores were enhanced via immunohistochemistry. The microscope slides were thawed and dried and the sections were fixed with 4 % PFA for 30 min. After washing three times with PBS, they were incubated for 1 h in Mouse IgG Blocking Reagent of the M.O.M.® Immunodetection Kit Basic (Vector Laboratories, Burlingame, California, USA). Subsequently, they were washed twice for 2 min in PBS and then incubated for 15 min in M.O.M. Diluent. The primary antibody solution containing the two primary antibodies, M.O.M. Diluent and 0.1 % Triton X-100 was applied for overnight incubation. After two times 4 min washes in PBS, the slices were incubated for 2 h in the secondary antibodies diluted in 1.5 % normal goat serum, 0.1 % Triton X-100 and PBS. After the final washing steps (three times 5 min in PBS), the slides were dried, mounted with mounting medium (DAPI Fluoromount-G®, SouthernBiotech, Birmingham, AL, USA) and covered with a glass slide. The primary and secondary antibodies used were mouse anti-EBFP (1:50, ab32791; Abcam, Cambridge, Great Britain) and anti-mCherry (1:250, ab167453; Abcam), Alexa Fluor® 594 goat anti-mouse (1:250, A-11032; Thermo Fisher Scientific), Alexa Fluor® 488 goat anti-rabbit (1:250, A-11034; Thermo Fisher Scientific).

Immunofluorescence imaging was done using a Axioplan 2 Imaging fluorescence microscope (Zeiss, Oberkochen, Germany).

Manganese-enhanced magnetic resonance imaging (MEMRI)

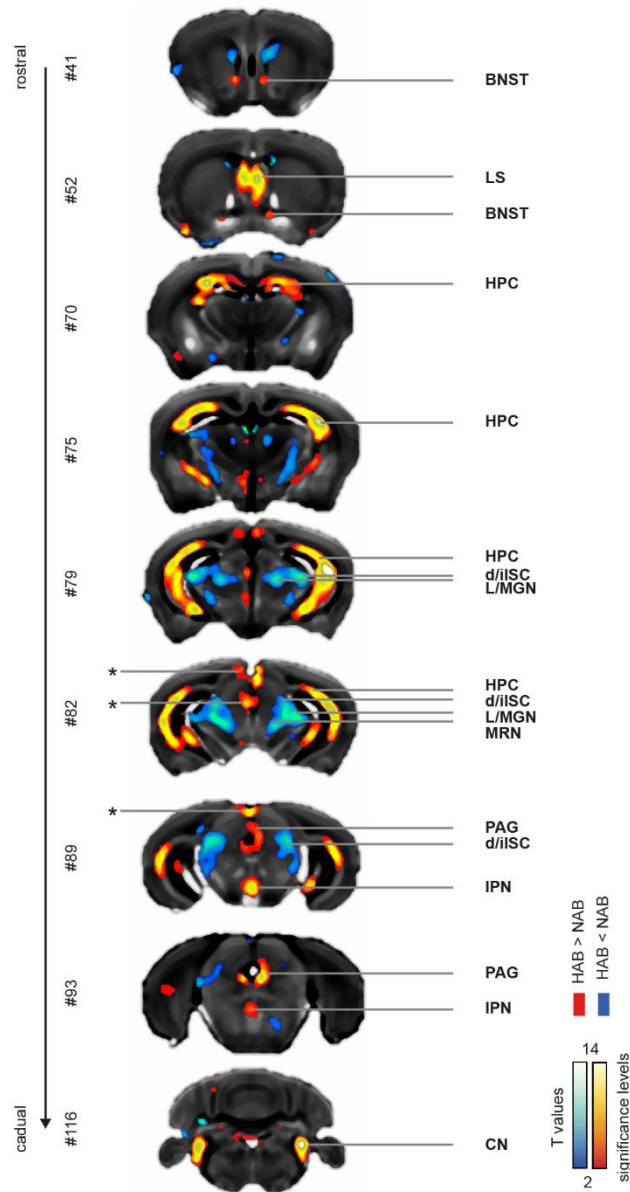
For detailed description of the procedure and analysis see Grünecker et al., 2010⁸⁴. Male HAB and NAB mice received *i.p.* injections of 30 mg/kg manganese ($\text{MnCl}_2 \cdot 4\text{H}_2\text{O}$, Sigma-Aldrich) in saline for eight consecutive days. 24 hours after the last injection, the MRI experiments were performed in a 7T MRI scanner (Avance Biospec 70/30, Bruker BioSpin, Ettlingen, Germany). The animals were anesthetized with isoflurane (1.5-1.7 % in oxygenated air) and body temperature was constantly monitored and kept at 36-37 °C throughout the procedure using a water flow heating pad (Haake S 5P, Thermo Fisher Scientific, Waltham, United States). T1-weighted images were acquired using a 3D gradient echo pulse sequence (repetition time TE = 50 ms, echo time TE = 3.2 ms). A

matrix of $128 \times 128 \times 128$ at a field of view of $16 \times 16 \times 18 \text{ mm}^3$ yielding a final resolution of $125 \times 125 \times 140.6 \text{ }\mu\text{m}^3$ was used and each voxel was imaged 10 times for averaging. Additionally, 3D T2-weighted images were acquired using a rapid acquisition relaxation enhanced (RARE) pulse sequence (TR = 1 s, TE = 10 ms). The same spatial resolution as for T1-weighted images was acquired, imaging two averages. The reconstructed images (Paravision, Bruker BioSpin, Ettlingen, Germany) were further analyzed using the statistical parametric mapping package SPM5 (using the spm mouse toolbox) and SPM8 (using the segment option for bias correction) (www.fil.ion.ucl.ac.uk/spm/). The acquired images of all animals were segmented exploiting mouse specific tissue probability maps, to obtain bias corrected images. Subsequently, the images were spatially normalized in several steps: 1. Normalization of all images (including brain and extracranial tissue) to a representative single animal image and calculation of the mean normalized image. 2. Creation of a brain mask on the mean normalized image. Brain extraction in native space using the back-transformed mean brain mask. 3. Normalization of the brain extracted images to the group template. Finally, images were smoothed using a Gaussian kernel of eight times the image resolution. Differential manganese accumulation was revealed by pairwise voxel-based comparison between HAB vs. NAB (FDR $p < 0.001$, cluster extent >20).

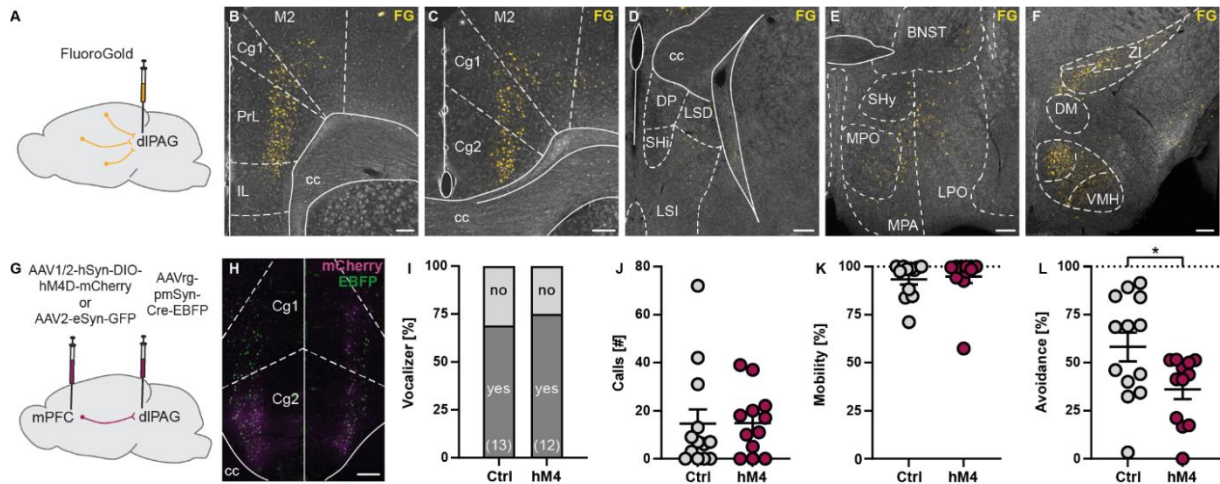
Quantification and statistical analysis

Data is presented as mean values \pm standard error (SEM), if appropriate. Statistical details such as the number of animals used can be found in the respective figures and/or figure legends. For normal distribution, paired and unpaired t tests and one-way analysis of variance (ANOVA) followed by Tukey's post-hoc test were performed. In case of not normally distributed data, we applied non-parametric statistics (Kruskal-Wallis or Mann-Whitney U-tests), and for contingency analyses Chi square test. Statistically significant differences were accepted if $p < 0.05$. Statistical analysis was performed using GraphPad Prism 9.1.

SUPPLEMENTAL INFORMATION



Supplemental Figure 1: Complete MEMRI data set showing differences in tonic neuronal activity in HAB vs. NAB mice. BNST: bed nucleus of the stria terminalis, CN: cochlear nucleus, d/iISC: deep/intermediate layers of the superior colliculus, HPC: hippocampus proper, IPN: interpedunclopontine nucleus, LS: lateral septal nucleus, L/MGM: lateral/medial geniculate, MRN: midbrain reticular nucleus, PAG: periaqueductal gray, nucleus. Numbers (#) indicate image numbers of corresponding reference images in the Allen Brain Atlas. Asterisks indicate potential artifacts which have been observed to occur close to the brain surface or the ventricular system.



Supplemental Figure 2: The mPFC-dIPAG projections decreases avoidance but does not control sonic vocalization. (A-F) Retrograde FluoroGold (FG) tracing. (A) Schematic illustration. FG was unilaterally injected into the dlPAG. (B-F) Afferent structures labeled by FG. BNST: bed nucleus of stria terminalis, cc: corpus callosum, Cg1: cingulate cortex area 1, Cg2: cingulate cortex area 2, DM: dorsomedial hypothalamic nucleus, DP: dorsal peduncular cortex, IL: infralimbic cortex, LPO: lateral preoptic area, LSD: lateral septal nucleus, dorsal part, LSI: lateral septal nucleus, intermediate part, M2: secondary motor cortex, MPA: medial preoptic area, MPO: medial preoptic nucleus, PrL: prelimbic cortex, SHi: septohippocampal nucleus, SHy: septohypothalamic nucleus, VMH: ventromedial hypothalamic nucleus, ZI: zona incerta. Scale bars: 200 μm . (G-L) Chemogenetic inhibition of mPFC-dIPAG projection. (G) Experimental schematic. (H) Representative image of mPFC. Scale bar: 200 μm . (I) Percentage of HAB mice emitting sonic calls, (J) the number of calls emitted per mouse, and (K) mobility behavior during the tail suspension (2.5 min). (L) Avoidance behavior during the Beetle Mania Task (BMT; mouse withdrew from the robo-beetle with accelerated speed). Data are presented as percentage of total (I) or individual data with mean \pm SEM (I-L). * $p < 0.05$ (unpaired t test).

References

1. Wetzel, D.M., Kelley, D.B., and Campbell, B.A. (1980). Central control of ultrasonic vocalizations in neonatal rats: I. Brain stem motor nuclei. *J. Comp. Physiol. Psychol.* 94, 596–605.
2. Fitch, T. (2006). Production of Vocalizations in Mammals. In *Encyclopedia of Language & Linguistics* (Elsevier), pp. 115–121.
3. Jürgens, U. (2009). The Neural Control of Vocalization in Mammals: A Review. *J. Voice* 23, 1–10.
4. Holstege, G., and Subramanian, H.H. (2016). Two different motor systems are needed to generate human speech. *J. Comp. Neurol.* 524, 1558–1577.
5. Hernandez-Miranda, L.R., Ruffault, P.L., Bouvier, J.C., Murray, A.J., Morin-Surun, M.P., Zampieri, N., Cholewa-Waclaw, J.B., Ey, E., Brunet, J.F., Champagnat, J., et al. (2017). Genetic identification of a hindbrain nucleus essential for innate vocalization. *Proc. Natl. Acad. Sci. U. S. A.* 114, 8095–8100.
6. Fenzl, T., and Schuller, G. (2002). Periaqueductal gray and the region of the paralemniscal area have different functions in the control of vocalization in the neotropical bat, *Phyllostomus discolor*. *Eur. J. Neurosci.* 16, 1974–1986.
7. Kittelberger, J.M., Land, B.R., and Bass, A.H. (2006). Midbrain periaqueductal gray and vocal patterning in a teleost fish. *J. Neurophysiol.* 96, 71–85.
8. Green, D.B., Shackleton, T.M., Grimsley, J.M.S., Zobay, O., Palmer, A.R., and Wallace, M.N. (2018). Communication calls produced by electrical stimulation of four structures in the Guinea pig brain. *PLoS One* 13, 1–28.
9. Tschida, K., Michael, V., Takato, J., Han, B.X., Zhao, S., Sakurai, K., Mooney, R., and Wang, F. (2019). A Specialized Neural Circuit Gates Social Vocalizations in the Mouse. *Neuron* 103, 459-472.e4.
10. Magoun, H.W., Atlas, D., Ingersoll, E.H., and Ranson, S.W. (1937). Associated facial, vocal and respiratory components of emotional expression: An experimental study. *J. Neurol. Neurosurg. Psychiatry* S1-17, 241–255.
11. Adamez, J., and O’Leary, J.L. (1959). Experimental mutism resulting from periaqueductal lesions in cats. *Neurology* 9, 636–636.
12. Skultety, F.M. (1962). Experimental Mutism in Dogs. *Arch. Neurol.* 6, 235–241.
13. Jürgens, U. (1994). The role of the periaqueductal grey in vocal behaviour. *Behav. Brain Res.* 62, 107–117.
14. Shipley, M.T., Ennis, M., Rizvi, T.A., and Behbehani, M.M. (1991). Topographical Specificity of Forebrain Inputs to the Midbrain Periaqueductal Gray: Evidence for Discrete Longitudinally Organized Input Columns. In *The Midbrain Periaqueductal Gray Matter*, A. Depaulis and R. Bandler, eds. (Springer US), pp. 417–448.
15. Zhang, S.P., Davis, P.J., Bandler, R., and Carrive, P. (1994). Brain stem integration of vocalization: role of the midbrain periaqueductal gray. *J. Neurophysiol.* 72, 1337–1356.
16. Kyuhou, S.I., and Gemba, H. (1998). Two vocalization-related subregions in the midbrain periaqueductal gray of the guinea pig. *Neuroreport* 9, 1607–1610.

17. Esposito, A., Demeurisse, G., Alberti, B., and Fabbro, F. (1999). Complete mutism after midbrain periaqueductal gray lesion. *Neuroreport* 10, 681–685.
18. Gao, S.C., Wei, Y.C., Wang, S.R., and Xu, X.H. (2019). Medial Preoptic Area Modulates Courtship Ultrasonic Vocalization in Adult Male Mice. *Neurosci. Bull.* 35, 697–708.
19. Michael, V., Goffinet, J., Pearson, J., Wang, F., Tschida, K., and Mooney, R. (2020). Circuit and synaptic organization of forebrain-to-midbrain pathways that promote and suppress vocalization. *Elife* 9, 1–29.
20. Chen, J., Markowitz, J.E., Lilascharoen, V., Taylor, S., Sheurpukdi, P., Keller, J.A., Jensen, J.R., Lim, B.K., Datta, S.R., and Stowers, L. (2021). Flexible scaling and persistence of social vocal communication. *Nature* 593, 108–113.
21. Holy, T.E., and Guo, Z. (2005). Ultrasonic songs of male mice. *PLoS Biol.* 3, 1–10.
22. Portfors, C. V. (2007). Types and functions of ultrasonic vocalizations in laboratory rats and mice. *J. Am. Assoc. Lab. Anim. Sci.* 46, 28–34.
23. Lahvis, G.P., Alleva, E., and Scattoni, M.L. (2011). Translating mouse vocalizations: Prosody and frequency modulation. *Genes, Brain Behav.* 10, 4–16.
24. Sangiamo, D.T., Warren, M.R., and Neunuebel, J.P. (2020). Ultrasonic signals associated with different types of social behavior of mice. *Nat. Neurosci.* 23, 411–422.
25. Fischer, J., and Hammerschmidt, K. (2011). Ultrasonic vocalizations in mouse models for speech and socio-cognitive disorders: Insights into the evolution of vocal communication. *Genes, Brain Behav.* 10, 17–27.
26. Scearce-Levie, K., Roberson, E.D., Gerstein, H., Cholfin, J.A., Mandiyan, V.S., Shah, N.M., Rubenstein, J.L.R., and Mucke, L. (2008). Abnormal social behaviors in mice lacking Fgf17. *Genes, Brain Behav.* 7, 344–354.
27. Scattoni, M.L., Crawley, J., and Ricceri, L. (2009). Ultrasonic vocalizations: A tool for behavioural phenotyping of mouse models of neurodevelopmental disorders. *Neurosci. Biobehav. Rev.* 33, 508–515.
28. Malkesman, O., Scattoni, M.L., Paredes, D., Tragon, T., Pearson, B., Shaltiel, G., Chen, G., Crawley, J.N., and Manji, H.K. (2009). The Female Urine Sniffing Test : A Novel Approach for Assessing Reward-Seeking Behavior in Rodents. *BPS* 67, 864–871.
29. Scattoni, M.L., Ricceri, L., and Crawley, J.N. (2011). Unusual repertoire of vocalizations in adult BTBR T+tf/J mice during three types of social encounters. *Genes, Brain Behav.* 10, 44–56.
30. Wöhr, M., and Schwarting, R.K.W. (2013). Affective communication in rodents: Ultrasonic vocalizations as a tool for research on emotion and motivation. *Cell Tissue Res.* 354, 81–97.
31. Coburn, C.A. (1912). Singing mice. *J. Anim. Behav.* 2, 364–366.
32. Dice, L.R. (1932). The Songs of Mice. *J. Mammal.* 13, 187.
33. Scott, J.P. (1946). Incomplete adjustment caused by frustration of untrained fighting mice. *J. Comp. Psychol.* 39, 379–390.
34. Ehret, G. (1974). Schallsignale Der Hausmaus (*Mus Musculus*). *Behaviour* 52, 38–56.
35. Houseknecht, C.R. (1968). Sonographic Analysis of Vocalizations of Three Species of Mice. *J. Mammal.* 49, 555.

36. Blanchard, R.J., Hebert, M.A., Ferrari, P., Palanza, P., Figueira, R., Blanchard, D.C., and Parmigiani, S. (1998). Defensive behaviors in wild and laboratory (Swiss) mice: The mouse defense test battery. *Physiol. Behav.* 65, 201–209.
37. Gourbal, B.E.F., Barthelemy, M., Petit, G., and Gabrion, C. (2004). Spectrographic analysis of the ultrasonic vocalisations of adult male and female BALB/c mice. *Naturwissenschaften* 91, 381–385.
38. Yang, M., Farrokhi, C., Vasconcellos, A., Blanchard, R.J., and Blanchard, D.C. (2006). Central infusion of ovine CRF (oCRF) potentiates defensive behaviors in CD-1 mice in the Mouse Defense Test Battery (MDTB). *Behav. Brain Res.* 171, 1–8.
39. Krömer, S.A., Keßler, M.S., Milfay, D., Birg, I.N., Bunck, M., Czibere, L., Panhuysen, M., Pütz, B., Deussing, J.M., Holsboer, F., et al. (2005). Identification of glyoxalase-I as a protein marker in a mouse model of extremes in trait anxiety. *J. Neurosci.* 25, 4375–4384.
40. Bedenk, B.T., Almeida-Corrêa, S., Jurik, A., Dedic, N., Grünecker, B., Genewsky, A.J., Kaltwasser, S.F., Riebe, C.J., Deussing, J.M., Czisch, M., et al. (2018). Mn²⁺ dynamics in manganese-enhanced MRI (MEMRI): Cav1.2 channel-mediated uptake and preferential accumulation in projection terminals. *Neuroimage* 169, 374–382.
41. Almeida-Corrêa, S., Czisch, M., and Wotjak, C.T. (2018). In Vivo Visualization of Active Polysynaptic Circuits With Longitudinal Manganese-Enhanced MRI (MEMRI). *Front. Neural Circuits* 12.
42. Heinz, D.E., Genewsky, A., and Wotjak, C.T. (2017). Enhanced anandamide signaling reduces flight behavior elicited by an approaching robo-beetle. *Neuropharmacology* 126, 233–241.
43. Sutton, D., Larson, C., and Lindeman, R.C. (1974). Neocortical and limbic lesion effects on primate phonation. *Brain Res.* 71, 61–75.
44. Jürgens, U., and von Cramon, D. (1982). On the role of the anterior cingulate cortex in phonation: A case report. *Brain Lang.* 15, 234–248.
45. Bennett, P.J.G., Maier, E., and Brecht, M. (2019). Involvement of rat posterior prelimbic and cingulate area 2 in vocalization control. *Eur. J. Neurosci.* 50, 3164–3180.
46. Heffner, H., and Masterton, B. (1980). Hearing in Glires: Domestic rabbit, cotton rat, feral house mouse, and kangaroo rat. *J. Acoust. Soc. Am.* 68, 1584–1599.
47. Heffner, R.S., and Heffner, H.E. (1985). Hearing range of the domestic cat. *Hear. Res.* 19, 85–88.
48. Malkemper, E.P., Topinka, V., and Burda, H. (2015). A behavioral audiogram of the red fox (*Vulpes vulpes*). *Hear. Res.* 320, 30–37.
49. Kelly, J.B., and Masterton, B. (1977). Auditory sensitivity of the albino rat. *J. Comp. Physiol. Psychol.* 91, 930–936.
50. Heffner, H.E., and Heffner, R.S. (2007). Hearing ranges of laboratory animals. *J. Am. Assoc. Lab. Anim. Sci.* 46, 20–22.
51. Fanselow, M.S., and Lester, L.S. (1988). A functional behavioristic approach to aversively motivated behavior: Predatory imminence as a determinant of the topography of defensive behavior. In *Evolution and learning*. (Lawrence Erlbaum Associates, Inc), pp. 185–212.
52. Frank, E., Kessler, M.S., Filiou, M.D., Zhang, Y., Maccarrone, G., Reckow, S., Bunck, M., Heumann, H., Turck, C.W., and Landgraf, R. (2009). Stable Isotope Metabolic Labeling

- with a Novel N-Enriched Bacteria Diet for Improved Proteomic Analyses of Mouse Models for Psychopathologies. 4.
53. Kessler, M.S., Bosch, O.J., Bunck, M., Landgraf, R., Neumann, D., Kessler, M.S., Bosch, O.J., Bunck, M., Landgraf, R., Kessler, M.S., et al. (2011). Maternal care differs in mice bred for high vs . low trait anxiety : Impact of brain vasopressin and Maternal care differs in mice bred for high vs . low trait anxiety : Impact of brain vasopressin and cross-fostering. 0919.
 54. Fish, E.W., Sekinda, M., Ferrari, P.F., Dirks, A., and Miczek, K.A. (2000). Distress vocalizations in maternally separated mouse pups: Modulation via 5-HT1(A), 5-HT1(B) and GABA(A) receptors. *Psychopharmacology (Berl)*. 149, 277–285.
 55. Gray, J.A., and McNaughton, N. *The Neuropsychology of Anxiety : Reprise*.
 56. Beart, P.M., Summers, R.J., Stephenson, J.A., and Christie, M.J. (1994). Excitatory amino acid projections to the nucleus of the solitary tract in the rat: a retrograde transport study utilizing d-[3H]aspartate and [3H]GABA. *J. Auton. Nerv. Syst.* 50, 109–122.
 57. Beitz, A.J. (1989). Possible origin of glutamatergic projections to the midbrain periaqueductal gray and deep layer of the superior colliculus of the rat. *Brain Res. Bull.* 23, 25–35.
 58. Tovote, P., Esposito, M.S., Botta, P., Chaudun, F., Fadok, J.P., Markovic, M., Wolff, S.B.E., Ramakrishnan, C., Fenno, L., Deisseroth, K., et al. (2016). Midbrain circuits for defensive behaviour. *Nature* 534, 206–212.
 59. Silva, C., and McNaughton, N. (2019). Are periaqueductal gray and dorsal raphe the foundation of appetitive and aversive control? A comprehensive review. *Prog. Neurobiol.* 177, 33–72.
 60. Whitney, G., Alpern, M., Dizinno, G., and Horowitz, G. (1974). Female odors evoke ultrasounds from male mice. *Anim. Learn. Behav.* 2, 13–18.
 61. Nyby, J., Dizinno, G.A., and Whitney, G. (1976). Social status and ultrasonic vocalizations of male mice. *Behav. Biol.* 18, 285–289.
 62. Maggio, J.C., and Whitney, G. (1985). Ultrasonic vocalizing by adult female mice (*Mus musculus*). *J. Comp. Psychol.* 99, 420–436.
 63. Warren, M.R., Clein, R.S., Spurrier, M.S., Roth, E.D., and Neunuebel, J.P. (2020). Ultrashort-range, high-frequency communication by female mice shapes social interactions. *Sci. Rep.* 10, 1–14.
 64. Zippelius, H.M., and Schleidt, W.M. (1956). Ultraschall-Laute bei jungen Mäusen. *Naturwissenschaften* 43, 502.
 65. Sewell, G.D. (1970). Ultrasonic Communication in Rodents. *Nature* 227, 410–410.
 66. Brudzynski, S.M. (2009). *Communication of Adult Rats by Ultrasonic Vocalization: Biological, Sociobiological, and Neuroscience Approaches.* 50.
 67. Brudzynski, S.M., and Fletcher, N.H. (2010). *Rat ultrasonic vocalization : short-range communication (Elsevier B.V.)*.
 68. Ehret, G. (1974). Schallsignale Der Hausmaus (*Mus Musculus*). *Behaviour* 52, 38–56.
 69. Scott, J.P., and Jackson, R.B. (1946). Incomplete adjustment caused by frustration of untrained fighting mice. 1946.

70. Sales, G. (1972). Ultrasound and mating behaviour in rodents with some observations on other behavioural situations. *J. Zool.* 168, 149–164.
71. Ehret, G., and Bernecker, C. (1986). Low-frequency sound communication by mouse pups (*Mus musculus*): wriggling calls release maternal behaviour. *Anim. Behav.* 34, 821–830.
72. Fitch, T., Neubauer, J., and Herzel, H. (2002). Calls out of chaos: the adaptive significance of nonlinear phenomena in mammalian vocal production. *Anim. Behav.* 63, 407–418.
73. Blumstein, D.T., Richardson, D.T., Cooley, L., Winternitz, J., and Daniel, J.C. (2008). The structure, meaning and function of yellow-bellied marmot pup screams. *Anim. Behav.* 76, 1055–1064.
74. Arnal, L.H., Flinker, A., Kleinschmidt, A., Giraud, A.L., and Poeppel, D. (2015). Human Screams Occupy a Privileged Niche in the Communication Soundscape. *Curr. Biol.* 25, 2051–2056.
75. Schwartz, J.W., Engelberg, J.W.M., and Gouzoules, H. (2020). Was That a Scream? Listener Agreement and Major Distinguishing Acoustic Features. *J. Nonverbal Behav.* 44, 233–252.
76. Blumstein, D.T., and Récapet, C. (2009). The sound of arousal: The addition of novel nonlinearities increases responsiveness in marmot alarm calls. *Ethology* 115, 1074–1081.
77. Karp, D., Manser, M.B., Wiley, E.M., and Townsend, S.W. (2014). Nonlinearities in Meerkat Alarm Calls Prevent Receivers from Habituating. *Ethology* 120, 189–196.
78. Morton, E.S. (1977). On the Occurrence and Significance of Motivation-Structural Rules in Some Bird and Mammal Sounds Author (s): Eugene S. Morton Published by: The University of Chicago Press for The American Society of Naturalists Stable URL: <https://www.jstor.org/stab.111>, 855–869.
79. Anikin, A., Pisanski, K., Massenet, M., and Reby, D. (2021). Harsh is large: nonlinear vocal phenomena lower voice pitch and exaggerate body size.
80. Litvin, Y., Blanchard, D.C., and Blanchard, R.J. (2007). Rat 22 kHz ultrasonic vocalizations as alarm cries. *Behav. Brain Res.* 182, 166–172.
81. Driver, P.M., and Humphries, D.A. (1969). The significance of the high-intensity alarm call in captured passerines. *Ibis (Lond. 1859)*. 111, 243–244.
82. Hogstedt, G. (1983). Adaptation Unto Death: Function of Fear Screams. *Am. Nat.* 121, 562–570.
83. Wise, K., Conover, M., and Knowlton, F. (1999). Response of coyotes to avian distress calls: testing the startle-predator and predator-attraction hypotheses. *Behaviour* 136, 935–949.
84. Grünecker, B., Kaltwasser, S.F., Peterse, Y., Sämann, P.G., Schmidt, M. V., Wotjak, C.T., and Czisch, M. (2010). Fractionated manganese injections: effects on MRI contrast enhancement and physiological measures in C57BL/6 mice. *NMR Biomed.* 23, 913–921.

3. DISCUSSION

In this thesis, different aspects of defensive behaviors and threat responding along with the underlying neuronal circuits and neuromodulatory systems have been considered. In the following, I will summarize the results and give an overview about research questions that arise from the studies. However, the main focus of this general discussion will lie on principles and concepts of the design and analysis of behavioral testing. Study-specific aspects are mainly discussed in the respective manuscripts.

Innate defensive behaviors can be triggered by threats of different sensory modalities such as olfactory, auditory, visual, tactile, or composite cues. In the three studies of this thesis, different behavioral paradigms have been used that involved such threats to induce and investigate defensive behaviors in mice. Considering the model of the predator imminence continuum, the stimuli presented were of different intensity and induced defensive behaviors depending on the perceived distance of the threat. The visual stimuli of the VTT mimic both, a distant threat in the form of a cruising aerial predator (sweeping dot stimulus; De Franceschi et al., 2016) and a more proximal threat imitating a rapidly approaching aerial predator (looming disk stimulus; Yilmaz and Meister, 2013; De Franceschi et al., 2016). In both cases, the animals had a chance to escape to a shelter at any time. The auditory stimuli presented during the ASR paradigm range in the medial distance. However, the animals did not have the possibility to evade the threat as they were confined to the apparatus. In case of the BMT (Heinz et al., 2017), physical contact with the multi-sensory robo-beetle was established, thereby presenting a more proximal threat but offering the animal a chance to escape within the arena. The extreme end of the spectrum is reached in the TST where the animal was caught and trapped by the tail without a chance to escape. The use of these threats allowed me to study the brain regions and circuits as well as the neuromodulatory systems involved in threat responding.

Translational psychiatric research can be designed by applying top-down or bottom-up approaches. The former investigates a phenotype to elucidate the underlying mechanisms (e.g., genes involved), while with the latter candidate genes are mutated and the resulting phenotypes are studied. Both approaches have been presented in this thesis.

In the first study, a bottom-up design has been employed to investigate the interaction of the eCB and the CRF system using behavioral tests for threat responding as well as for anxiety measures. To study the interplay of CRF and the CB1 receptor, we generated a

new conditional knockout mouse line that selectively lacked CB1 in CRF-positive neurons. Employing double *in situ* hybridization on wild-type brains, we found an overall low level of co-localization of CRF and CB1 in the brain. While there were no differences in fear and anxiety-related behaviors under basal conditions and after exposure to a traumatic experience, the startle amplitude of male knockout mice was significantly increased. This corroborates previous findings which demonstrated increases in the startle response by intracerebroventricular administration of CRFR1 agonists (Devigny et al., 2011) or CRF (Swerdlow et al., 1986; Liang et al., 1992) and CRF overexpression (Dirks et al., 2002; Toth et al., 2014; Flandreau et al., 2015). The limited phenotypic differences observed between knockout and wild-type animals could on the one hand be explained by the circuits and projections involved in the different tasks. On the other hand, it might have to do with the level of activation of those circuits. As described earlier, the eCB system needs to be triggered above a certain threshold such as by a strong threat to exert its actions (Kamprath et al., 2009). The repeated exposure to a sudden loud noise as it was the case in the ASR paradigm could lead to such an above-threshold activation. Interestingly, an increased ASR was only observed in male, but not female knockout mice. This could be attributed to sex dimorphisms of the CRF system, as has been demonstrated in terms of behavior, HPA axis function, and gene expression (Toth et al., 2014, for reviews see Bangasser and Valentino, 2014 and Brivio et al., 2020). Such sex differences highlight the importance to study both sexes.

The remarkable confinement to the hyperarousal phenotype of the knockout mouse line should be further investigated and confirmed in future studies. Such experiments could involve the systemic injection of CRFR1 or CRFR2 antagonists before exposing the conditional knockout mice to the startle response paradigm. This will also shine light onto the question whether CRF or the co-transmission of neurotransmitters like GABA or glutamate mediate the behavioral effect observed. Also, the co-localization and co-expression of CRF and CB1 should be examined further using additional and potentially more sensitive methods like RNAscope or the analysis of single-cell sequencing data (e.g., from data repositories). The resulting candidate brain regions could then be targeted locally via guide cannulas with CRFR1 antagonists to study the effect on arousal. Given the co-localization of CRF and CB1 in the piriform cortex, exposure of the animals to olfactory threatening cues such as 2,5-dihydro-2,4,5-trimethylthiazoline (TMT), a component of the fox feces odor could be worthwhile exploring.

Next, I employed a screening approach with a multi-factorial design (genotype, sex, and traumatic experience). In order to capture potential differences between the groups across the negative valence and arousal systems, the mice were exposed to a battery of behavioral and physiological tests. Test batteries for mice and rats are a commonly used approach in both top-down and bottom-up studies (Crawley and Paylor, 1997; Rogers et al., 1999; Hatcher et al., 2001; Wolf et al., 2016). Since psychiatric disorders are complex and might involve several physiological and behavioral systems, it is challenging and might be insufficient to capture those in a single classical test. In a typical test battery, the animals are assessed in a series of different paradigms measuring various behavioral or physiological aspects, as has been done in the first study. Test batteries come with several advantages. Compared to simply performing a single test or using a new batch of animals for each test, a test battery allows for within-subject measurements, it has the power of picking up subtle differences that might be missed in a single test, and it can demonstrate a true positive phenotype that is confirmed across several paradigms. But most importantly, testing animals in a series of paradigms drastically reduces the number of animals needed. On the one hand, this reduces costs and effort to obtain a sufficient number of animals e.g., with targeted mutations like in the case of the $CB1^{cKO-CRF}$ mouse line. On the other hand, reducing the number of animals going into experimental research is an crucial factor from an ethical perspective, following the principle of the 3Rs: Replace, Reduce, Refine (Russell and Burch, 1959). However, the use of test batteries also comes with limitations and considerations that need to be taken into account. When testing animals in a series of paradigms, each test might pose a stressor to the animal and the animal's experiences accumulate. Studies have shown that the extensive handling and experience of a mouse alters its behavior compared to naïve mice, e.g., shown by reduced locomotor activity (McIlwain et al., 2001; Voikar et al., 2004). Therefore, results from a series of tests should ideally not be directly compared to the results obtained by a naïve group of animals exposed only to a single test (McIlwain et al., 2001). Comparisons of results obtained in a test battery with those acquired by naïve mice should be interpreted with care and should be replicated before final conclusions are drawn. Further, stressful experiences can impair cognitive function and learning (Moreira et al., 2016). Therefore, the order of testing is important. Classically, the more stressful and invasive tests are performed at the end of the battery to reduce potential carry-over effects. This rule has also been applied in the first study by starting the test battery with an OFT and ending it with the more challenging BMT.

Beside technical considerations, also the analysis of test battery data comes with challenges. Video analysis, novel tracking software, and machine learning tools like DeepLabCut (Mathis et al., 2018) allow to determine countless measures for behavioral paradigms. In a single open field test, classic parameters like the total distance moved or the time spent in the inner or outer zone can be measured but using elaborate tracking tools, additional measures such as speed, angular velocity, head turnings, rotations, rearing, jumping, elongation, grooming, the distance to objects, and many more can be assessed. In this fashion, dozens of parameters and values might be collected for each animal by the end of a test battery and are possibly combined with further results from physiological or molecular measures. However, statistical analysis is often performed by separate comparisons for each parameter and each test, such as via Student's t-tests or 1-way ANOVA for parametric data. Subsequently, individual significantly differing variables are often presented without correction for multiple testing thus increasing the risk of false positive findings. Applying correction for multiple testing in turn requires a rather large sample size to grant sufficient power and to reflect significant results. Increasing the sample size of a mouse cohort comes with the beforementioned ethical issue and contradicts the aim to reduce the number of animals used. Further, a large sample size might reveal statistically significant differences that are yet not biologically significant. In order to increase the possibility to draw general conclusions from the test battery results, different means of data analysis have been suggested that include multivariate comparisons and reductions of dimensionality (Feyissa et al., 2017; Stukalin and Einat, 2019). Performing principal component or factor analysis allows to reduce a large number of complex variables to a few components that mirror the behavioral phenotypes measured and highlight important variables by high loadings (Feyissa et al., 2017; Kielar et al., 2018; Heinz et al., 2021). Similarly, logistic regression analysis and z-scores reduce the dimensionality of the behavioral data and help to gain an overall conclusion from the measurements obtained by a test battery (Guilloux et al., 2011; Stukalin and Einat, 2019). Alternatively, screening approaches with a limited number of animals can be performed by first exposing an exploration sample to a test battery. After correction for multiple testing, the behavioral test that revealed a significant difference e.g., between the genotypes tested is then repeated with a naïve cohort of animals. With this approach, the result can be replicated without further stringent multiple testing correction and a robust overall conclusion regarding the group difference can be drawn. This approach as well as measures for dimensionality reduction have been applied in study two.

In the second study, the consequences of trauma exposure on grey matter volume were investigated and correlated with the severity of hyperarousal symptoms. Using a well-powered exploration sample, we assessed the behavioral consequences of the exposure to an inescapable foot shock after an incubation time of four weeks. The animals were thereby exposed to a short test battery which included exposure to threatening stimuli of different sensory modalities. To reduce the dimensionality of the data, we calculated the Hyperarousal Score using logistic regression analysis. The variables included were contained to the arousal domain of PTSD symptoms. Although trauma-related changes in memory are an important characteristic of the disease phenotype, the limited variability of the memory-related data did not provide a basis to include those variables in the logistic regression analysis. The Hyperarousal Score therefore combines behavioral readouts measured in response to threats of different sensory modalities (auditory, visual, and multi-sensory) and allowed us to clearly distinguish shocked animals and non-shocked controls. Using a naïve cohort of mice as a replication sample, we could replicate those behavioral results and subject the animals to longitudinal measurements of brain morphometry using whole-brain MRI scans. A cross-sectional design revealed a volume decrease of the dorsal hippocampus and an increase of the reticular nucleus in shocked mice compared to non-shocked controls. With the longitudinal within-subject design, a reduction of grey matter volume of the globus pallidus could be correlated with high symptom severity as revealed by regression with the Hyperarousal Score. This finding highlights the power of the design of the study since the globus pallidus was a largely non-considered brain structure in PTSD-related neuronal circuits. Further, using the validated Hyperarousal Score as regressor allowed us to rely on the smaller replication cohort for grey matter volume measurements. Finally, this approach enabled us to assess relationships between dimensional rather than categorical trauma consequences on hyperarousal and grey matter volume changes.

Our descriptive study raises questions concerning the causes and mechanisms of the observed volume changes. The increases and decreases in grey matter volume could on the one hand be pathogenic and promote behavioral changes related to arousal, on the other hand they could be compensatory mechanisms, assuming that a reduction in synaptic contacts protects against over-excitation. To tackle this question, future experiments could chemogenetically target the brain areas of interest, such as the globus pallidus. Injections of a viral vector encoding for inhibitory Designer Receptors Exclusively Activated by Designer Drugs (DREADDs) and administration of clozapine N-oxide (CNO) before or directly after trauma exposure could highlight the involvement of this brain area in fear

memory and trauma-induced changes in behavior. To study the mechanistic basis of volume changes, histological analysis of the brain sections could be valuable. Labeling with bromodeoxyuridine as a marker for cell proliferation along with Nissl and Golgi stainings for the quantification of neurons, astrocytes, and oligodendrocytes as well as dendritic length and spine density measurements would give insights into the processes underlying the grey matter volume changes.

In the third study, a top-down approach was used. Based on the vocalization phenotype observed in an inbred mouse line, circa-strike behavior was studied (Perusini and Fanselow, 2015). I investigated the characteristics of sonic mouse vocalization, the underlying neuronal circuits, and its ecological function. Sonic calls were found to be emitted at high disposition by mice selectively bred for high anxiety-related behavior when caught by the tail but not by other commonly used laboratory mouse lines. Circa-strike threat responses like vocalization are described as panic-like behaviors. Yet, the panicolytic properties of enhanced AEA levels previously shown in the BMT with HAB mice (Heinz et al., 2017) had no effect on vocalization. The anxiolytic compound diazepam however reduced sonic vocalization. Also local muscimol injections into the dlPAG and the resulting abolishment of vocalization and which coincided with an increase in open arm time on the EPM speak for relation between anxiety but not panic and sonic vocalization.

Follow-up questions of this study would certainly concern the further dissection of the neuronal pathways involved in the control of sonic vocalization. Employing a retrograde tracing approach, I could identify several brain structures afferent to the dlPAG. Chemogenetic silencing of the medial prefrontal cortex to dlPAG projection had no effect on sonic vocalization. In order to identify which of the remaining dlPAG afferents play a functional role, they could be labeled via a retrograde virus encoding a fluorophore under an activity-sensitive E-SARE promoter injected into the dlPAG (Kawashima et al., 2013). The thereby identified projections could subsequently be stimulated optogenetically (terminal stimulation) to test for their functional involvement in vocalization. The dynamics of the afferent brain area and the dlPAG during vocalization could additionally be described using calcium imaging. The identified pathway could further be activated (e.g., optogenetically) in other mouse lines such as NAB or C57Bl/6 mice to assess whether sonic calls could be triggered. Such an experiment would show that the circuit is genuine but might be activated or disinhibited in HAB mice at a lower threshold compared to other mouse lines leading to the observed vocalization behavior. To further study the ecological relevance of the 4 kHz calls of HAB mice, the sound should be played back to other mouse

predators such as cats. Intriguingly, mouse predators have a best hearing frequency close to the fundamental frequency of the mouse calls (4 kHz for foxes, 8 kHz for cats), while the best hearing frequency of mice lies around 16 kHz (Masterton and Heffner, 1980; Heffner and Heffner, 1985; Malkemper et al., 2015) suggesting a predator-prey co-evolution.

The mouse lines used in study two and three such as the HAB, CD1, BALB/c or C57Bl/6 mice for top-down approaches are inbred mouse lines that are widely used in psychiatric and neuroscience research. These lines have been bred over generations of brother-sister mating to generate genetically homogeneous strains for research. However, the limitations in the sole use of inbred mouse lines should be considered (for reviews see Ishikawa, 2013; Zilkha et al., 2016). These mice have initially mostly been selected and bred to be easy to handle, to show low level of aggression and to be highly reproductive, generating mouse strains that differ profoundly from wild mice. While the use of inbred mouse lines and the myriad of transgenic mouse strains comes with clear benefits for scientists and increases reproducibility, the lack of genetic diversity also produces a lack of complex behaviors as has been highlighted when comparing inbred mice to wild-derived mice (Chalfin et al., 2014). Chalfin and colleagues further showed that backcrossing of wild-derived mice with an inbred mutant mouse line enriched the behavioral repertoire and yet allowed them to study the specific gene functions (Chalfin et al., 2014). Gene-of-interest manipulations can further be achieved using tools like CRISPR-Cas9 (Wang et al., 2013) or TALEN (Joung and Sander, 2013) for non-model organisms like wild-derived mice. The implementation of wild-derived mice into studies on threat responding offers opportunities to increase the complexity of behaviors that can be observed and studied. Regarding study three, the investigation of sonic vocalization behavior in wild-derived mice could reveal further insights into its ecological function and the anxiety versus panic component by using pharmacological tools.

Many studies do not only come with reduced genetic variability but also reductionist behavioral test situations. The classic behavioral paradigms for mice and rats that measure emotionality and threat responses take place in a very reduced, simple, and artificial environment for a short time period. Additionally, for the time of the test, the animals are separated from their cage mates. This approach permits a relatively high degree of standardization and the possibility to measure defined behaviors. Yet, these tests do not allow to observe more complex behaviors such as interactions of an individual within a group and changes of behavior over a longer time period. Early on, there have

been attempts to tackle these challenges and expose and observe mice in semi-natural environments (Calhoun, 1962; Poole and Morgan, 1976; Roper and Polioudakis, 1977). Recent technological advances facilitate such experiments both by providing the possibility to automatically track and distinguish animals in a group and by (semi)-automated analysis tools (Kimchi et al., 2007; Shemesh et al., 2013; Weissbrod et al., 2013; Pérez-Escudero et al., 2014). Such developments also allowed to record USV in groups of mice and identify the call emitting animal (Neunuebel et al., 2015; Sangiamo et al., 2020). This enables researchers to observe animals and their interactions in an undisturbed manner over hours, days, or weeks. Further, the experiments permit insights into complex behaviors that are ethologically relevant and provide understanding of the underlying circuitries when combined with circuit dissection tools and genetically targeted mice (Shemesh et al., 2016; Anpilov et al., 2020). Clearly, such long-term observations yield an enormous amount of data that requires high computational power to perform automated analyses. For screening approaches, such as the investigation of a new genetically targeted mouse line similar to study one, long-term observations might highlight additional behavioral phenotypic differences that are not captured in standard tests and increase the reliability of the data since results are based on large data sets.

In summary, in this thesis novel insights into defensive behaviors and the underlying mechanistic basis have been presented. In the discussion, difficulties and considerations to be taken into account when performing and analyzing behavioral tests have been highlighted. Some options are fairly simple to incorporate, such as adapting the statistical analysis of test batteries. Others, like the generation of new mouse lines by backcrossings with wild-derived mice, would require more efforts.

Declaration of Contribution as a Co-Author

Chapter 2.1

Ruat J, Hartmann A, Heinz DE, Nemcova P, Stoffel R, Deussing JM, Chen A, Wotjak CT (2021) CB1 receptors in corticotropin-releasing factor neurons selectively control the acoustic startle response in male mice. *Genes Brain Behav.* e12775

Julia Ruat performed and analyzed the single and double *in situ* hybridizations, did the re-genotyping, performed the baseline behavioral paradigms and the PTSD experiments together with Dr. Alice Hartmann and wrote the manuscript. Daniel E. Heinz and Paulina Nemcova assisted in the blood collection for CORT measurements. The radioimmunoassay was performed by Rainer Stoffel. Jan M. Deussing generated the conditional knockout mouse line. Andrea Ressle performed the initial genotyping of the mouse line. Dr. Carsten Wotjak and Prof. Alon Chen conceptualized and supervised the study and were involved in drafting the manuscript.

Chapter 2.2

Ruat, J, Heinz DE, Binder FP, Stark T, Neuner R, Hartmann A, Kaplick PM, Chen A, Czisch M, Wotjak CT (2021) Structural correlates of trauma-induced hyperarousal in mice. *Prog Neuro-Psychopharmacology Biol Psychiatry.* 111, 110404.

Julia Ruat performed the VTT and the ASR and wrote the manuscript. Daniel E. Heinz performed the foot shock experiments together Dr. Carsten T. Wotjak, the BMT of Experiment 1, and the MRI scans. The linear regression analysis was done by Florian Binder. The Python script for the VTT was written by Robert Neuner. He further assisted in the setup of the paradigm. Dr. Alice Hartmann performed the BMT of Experiment 2. The VTT videos of Experiment 1 were analyzed by Paul Kaplick. Prof. Alon Chen supervised the study. Dr. Michael Czisch and Tibor Stark analyzed the MRI data. Dr. Carsten Wotjak conceptualized and supervised the study and was involved in drafting the manuscript.

Chapter 2.3

Ruat J, Genewsky AJ, Heinz DE, Canteras NS, Czisch M, Chen A, Wotjak CT. Why do mice squeak?

Julia Ruat performed the baseline characterization of the sonic and ultrasonic vocalization, the line comparison, pain sensitivity measurements, the pharmacological treatments, the tracing and double-viral approach, the playback experiments and wrote the manuscript. The muscimol and the MEMRI experiments were performed by Dr. Andreas J. Genewsky (data has been presented in his PhD thesis; Genewsky, 2017). Daniel E. Heinz assisted with intraperitoneal injections in some of the experiments. Prof. Newton S. Canteras provided the experimental rats and access to his laboratory and equipment. The MEMRI analysis was performed by Dr. Michael Czisch. Dr. Carsten Wotjak and Prof. Alon Chen conceptualized and supervised the study and were involved in drafting the manuscript.

Hiermit bestätige ich die Richtigkeit der angegebenen Beiträge zu den einzelnen Publikationen.

München, 2021

.....

Julia Ruat

München, 2021

.....

PD Dr. Carsten T. Wotjak

Bibliography

- Adametz J, O'Leary JL (1959) Experimental mutism resulting from periaqueductal lesions in cats. *Neurology* 9:636–636.
- Aldenhoff JB, Gruol DL, Rivier J, Vale W, Siggins GR (1983) Corticotropin releasing factor decreases postburst hyperpolarizations and excites hippocampal neurons. *Science* 221:875–877.
- Allin JT, Banks EM (1972) Functional aspects of ultrasound production by infant albino rats (*Rattus norvegicus*). *Anim Behav* 20:175–185.
- Alon T, Zhou L, Pérez CA, Garfield AS, Friedman JM, Heisler LK (2009) Transgenic mice expressing green fluorescent protein under the control of the corticotropin-releasing hormone promoter. *Endocrinology* 150:5626–5632.
- American Psychiatric Association (1994) *Diagnostic and Statistical Manual of Mental Disorders*, 4th ed.
- American Psychiatric Association (2013) *Diagnostic and Statistical Manual of Mental Disorders*, 5th ed.
- Anpilov S, Shemesh Y, Eren N, Harony-Nicolas H, Benjamin A, Dine J, Oliveira VEM, Forkosh O, Karamihalev S, Hüttl R-E, Feldman N, Berger R, Dagan A, Chen G, Neumann ID, Wagner S, Yizhar O, Chen A (2020) Wireless Optogenetic Stimulation of Oxytocin Neurons in a Semi-natural Setup Dynamically Elevates Both Pro-social and Agonistic Behaviors. *Neuron* 107:644-655.e7.
- Arató M, Bánki CM, Bissette G, Nemeroff CB (1989) Elevated CSF CRF in suicide victims. *Biol Psychiatry* 25:355–359.
- Arnal LH, Flinker A, Kleinschmidt A, Giraud AL, Poeppel D (2015) Human Screams Occupy a Privileged Niche in the Communication Soundscape. *Curr Biol* 25:2051–2056.
- Arriaga G, Zhou EP, Jarvis ED (2012) Of Mice, Birds, and Men: The Mouse Ultrasonic Song System Has Some Features Similar to Humans and Song-Learning Birds. *PLoS One* 7.
- Baker DG, West SA, Nicholson WE, Ekhtator NN, Kasckow JW, Hill KK, Bruce AB, Orth DN, Geraciotti TD (1999) Serial CSF corticotropin-releasing hormone levels and adrenocortical activity in combat veterans with posttraumatic stress disorder. *Am J Psychiatry* 156:585–588.
- Bandler R, Carrive P, Depaulis A (1991) Emerging Principles of Organization of the Midbrain Periaqueductal Gray Matter. In: *The Midbrain Periaqueductal Gray Matter* (Depaulis A, Bandler R, eds), pp 1–8. Boston, MA: Springer US.
- Bandler R, Shipley MT (1994) Columnar organization in the midbrain periaqueductal gray: modules for emotional expression? *Trends Neurosci* 17:379–389.
- Bangasser DA, Valentino RJ (2014) Sex differences in stress-related psychiatric disorders: Neurobiological perspectives. *Front Neuroendocrinol* 35:303–319.
- Beckett SRG, Duxon MS, Aspley S, Marsden CA (1997) Central c-fos expression following 20kHz/ultrasound induced defence behaviour in the rat. *Brain Res Bull* 42:421–426.
- Besson J-M, Fardin V, Olivéras J-L (1991) Analgesia Produced by Stimulation of the Periaqueductal Gray Matter: True Antinoceptive Effects Versus Stress Effects. In: *The Midbrain Periaqueductal Gray Matter* (Depaulis A, Bandler R, eds), pp 121–138. Boston, MA: Springer US.
- Bisogno T, Howell F, Williams G, Minassi A, Cascio MG, Ligresti A, Matias I, Schiano-Moriello A, Paul P, Williams EJ, Gangadbaran U, Hobbs C, Di Marzo V, Doherty P (2003) Cloning of the first sn1-DAG lipases points to the spatial and temporal regulation of endocannabinoid signaling in the brain. *J Cell Biol* 163:463–468.
- Bissette G, Klimek V, Pan J, Stockmeier C, Ordway G (2003) Elevated concentrations of CRF in the locus coeruleus of depressed subjects. *Neuropsychopharmacology* 28:1328–1335.
- Bittencourt AS, Carobrez AP, Zamprogno LP, Tufik S, Schenberg LC (2004) Organization of single components of defensive behaviors within distinct columns of periaqueductal gray matter of the rat: Role of N-methyl-D-aspartic acid glutamate receptors. *Neuroscience* 125:71–89.

Bibliography

- Blanchard RJ, Blanchard DC (1990) An ethoexperimental analysis of defense, fear, and anxiety. In: N. McNaughton & G. Andrews Anxiety, pp 124–133. University of Otago Press.
- Blanchard RJ, Blanchard DC, Agullana R, Weiss SM (1991) Twenty-two kHz alarm cries to presentation of a predator, by laboratory rats living in visible burrow systems. *Physiol Behav* 50:967–972.
- Blanchard RJ, Hebert MA, Ferrari P, Palanza P, Figueira R, Blanchard DC, Parmigiani S (1998) Defensive behaviors in wild and laboratory (Swiss) mice: The mouse defense test battery. *Physiol Behav* 65:201–209.
- Blanchard RJ, Kleinschmidt CF, Fukunaga-Stinson C, Blanchard DC (1980) Defensive attack behavior in male and female rats. *Anim Learn Behav* 8:177–183.
- Blanchard RJ, Yudko EB, Rodgers RJ, Blanchard DC (1993) Defense system psychopharmacology: An ethological approach to the pharmacology of fear and anxiety. *Behav Brain Res* 58:155–165.
- Bluett RJ, Báldi R, Haymer A, Gaulden AD, Hartley ND, Parrish WP, Baechle J, Marcus DJ, Mardam-Bey R, Shonesy BC, Uddin MJ, Marnett LJ, Mackie K, Colbran RJ, Winder DG, Patel S (2017) Endocannabinoid signalling modulates susceptibility to traumatic stress exposure. *Nat Commun* 8:14782.
- Blumberg MS, Sokoloff G (2001) Do infant rats cry? *Psychol Rev* 108:83–95.
- Blumstein DT, Récapet C (2009) The sound of arousal: The addition of novel non-linearities increases responsiveness in marmot alarm calls. *Ethology* 115:1074–1081.
- Blumstein DT, Richardson DT, Cooley L, Winternitz J, Daniel JC (2008) The structure, meaning and function of yellow-bellied marmot pup screams. *Anim Behav* 76:1055–1064.
- Bosch-Bouju C, Larriue T, Linders L, Manzoni OJ, Layé S (2016) Endocannabinoid-Mediated Plasticity in Nucleus Accumbens Controls Vulnerability to Anxiety after Social Defeat Stress. *Cell Rep* 16:1237–1242.
- Branco T, Redgrave P (2020) The Neural Basis of Escape Behavior in Vertebrates. *Annu Rev Neurosci* 43:417–439.
- Brandão ML, Anseloni VZ, Pandóssio JE, De Araújo JE, Castilho VM (1999) Neurochemical mechanisms of the defensive behavior in the dorsal midbrain. *Neurosci Biobehav Rev* 23:863–875.
- Bremner JD, Licinio J, Darnell A, Krystal JH, Owens MJ, Southwick SM, Nemeroff CB, Charney DS (1997) Elevated CSF corticotropin-releasing factor concentrations in posttraumatic stress disorder. *Am J Psychiatry* 154:624–629.
- Britton DR, Koob GF, Rivier J, Vale M (1982) Intraventricular corticotropin-releasing factor enhances behavioral effects of novelty. *Life Sci* 31:363–367.
- Britton KT, Lee G, Dana R, Risch SC, Koob GF (1986) Activating and “anxiogenic” effects of corticotropin releasing factor are not inhibited by blockade of the pituitary-adrenal system with dexamethasone. *Life Sci* 39:1281–1286.
- Brivio E, Lopez JP, Chen A (2020) Sex differences: Transcriptional signatures of stress exposure in male and female brains. *Genes, Brain Behav* 19:1–22.
- Brown JS, Kalish HI, Farber IE (1951) Conditioned fear as revealed by magnitude of startle response to an auditory stimulus. *J Exp Psychol* 41:317–328.
- Brudzynski SM (2001) Pharmacological and behavioral characteristics of 22 kHz alarm calls in rats. *Neurosci Biobehav Rev* 25:611–617.
- Brudzynski SM (2009) Communication of adult rats by ultrasonic vocalization: Biological, sociobiological, and neuroscience approaches. *ILAR J* 50:43–50.
- Brudzynski SM, Fletcher NH (2010) Rat ultrasonic vocalization: short-range communication. In: *Handbook of Mammalian Vocalization. An Integrative Neuroscience Approach*, pp 69–76. Elsevier B.V.
- Brutus M, Shaikh MB, Siegel A (1985) Differential control of hypothalamically elicited flight behavior by the midbrain periaqueductal gray in the cat. *Behav Brain Res* 17:235–244.
- Buczynski MW, Parsons LH (2010) Quantification of brain endocannabinoid levels: Methods, interpretations and pitfalls. *Br J Pharmacol* 160:423–442.
- Burgdorf J, Knutson B, Panksepp J (2000) Anticipation of rewarding electrical brain stimulation evokes

Bibliography

- ultrasonic vocalization in rats. *Behav Neurosci* 114:320–327.
- Calhoun JB (1962) Population Density and Social Pathology. 206:139–149.
- Canteras NS (2002) The medial hypothalamic defensive system: Hodological organization and functional implications. *Pharmacol Biochem Behav* 71:481–491.
- Canteras NS, Chiavegatto S, Ribeiro Do Valle LE, Swanson LW (1997) Severe reduction of rat defensive behavior to a predator by discrete hypothalamic chemical lesions. *Brain Res Bull* 44:297–305.
- Canteras NS, Goto M (1999) Fos-like immunoreactivity in the periaqueductal gray of rats exposed to a natural predator. *Neuroreport* 10:413–418.
- Canteras NS, Simerly RB, Swanson LW (1994) Organization of projections from the ventromedial nucleus of the hypothalamus: A Phaseolus vulgaris-Leucoagglutinin study in the rat. *J Comp Neurol* 348:41–79.
- Carvalho AF, MacKie K, Van Bockstaele EJ (2010) Cannabinoid modulation of limbic forebrain noradrenergic circuitry. *Eur J Neurosci* 31:286–301.
- Cassella J V., Harty TP, Davis M (1986) Fear conditioning, pre-pulse inhibition and drug modulation of a short latency startle response measured electromyographically from neck muscles in the rat. *Physiol Behav* 36:1187–1191.
- Chalfin L, Dayan M, Levy DR, Austad SN, Miller RA, Iraqi FA, Dulac C, Kimchi T (2014) Mapping ecologically relevant social behaviours by gene knockout in wild mice. *Nat Commun* 5:4569.
- Charmandari E, Tsigos C, Chrousos G (2005) Endocrinology of the stress response. *Annu Rev Physiol* 67:259–284.
- Chen J, Markowitz JE, Lilascharoen V, Taylor S, Sheurpukdi P, Keller JA, Jensen JR, Lim BK, Datta SR, Stowers L (2021) Flexible scaling and persistence of social vocal communication. *Nature* 593:108–113.
- Chen Y, Andres AL, Frotscher M, Baram TZ (2012) Tuning synaptic transmission in the hippocampus by stress: The CRH system. *Front Cell Neurosci* 6:1–7.
- Coffey KR, Marx RG, Neumaier JF (2019) DeepSqueak: a deep learning-based system for detection and analysis of ultrasonic vocalizations. *Neuropsychopharmacology* 44:859–868.
- Comoli E, Ribeiro-Barbosa ER, Canteras NS (2003) Predatory hunting and exposure to a live predator induce opposite patterns of Fos immunoreactivity in the PAG. *Behav Brain Res* 138:17–28.
- Cox C, Harrion-Read PE, Steinberg H, Tomkiewicz M (1971) Lithium attenuates Drug-induced Hyperactivity in Rats. *Nature* 232:336–338.
- Cravatt BF, Giang DK, Mayfield SP, Boger DL, Lerner RA, Gilula NB (1996) Molecular characterization of an enzyme that degrades neuromodulatory fatty-acid amides. *Nature* 384:83–87.
- Crawley JN, Paylor R (1997) A Proposed Test Battery and Constellations of Specific Behavioral Paradigms to Investigate the Behavioral Phenotypes of Transgenic and Knockout Mice. *Horm Behav* 31:197–211.
- Cunningham ET, Sawchenko PE (2000) Oromotor Reflexes in the Rat : Implications for the Central Neural Control of Swallowing. *J Comp Neurol* 417:448–466.
- Cuomo V, Cagiano R, De Salvia MA, Maselli MA, Renna G, Racagni G (1988) Ultrasonic vocalization in response to unavoidable aversive stimuli in rats: Effects of benzodiazepines. *Life Sci* 43:485–491.
- Curti MW (1935) Native fear responses of white rats in the presence of cats. *Psychol Monogr* 46:78–98.
- Dabrowska J, Hazra R, Guo J-D, DeWitt S, Rainnie DG (2013) Central CRF neurons are not created equal: phenotypic differences in CRF-containing neurons of the rat paraventricular hypothalamus and the bed nucleus of the stria terminalis. *Front Neurosci* 7.
- Darwin C (1872) The expression of the emotions in man and animals. London: J. Murray.
- Davis M, Falls WA, Campeau S, Kim M (1993) Fear-potentiated startle: A neural and pharmacological analysis. *Behav Brain Res* 58:175–198.
- Davis M, Parisi T, Gendelman DS, Tischler M, Kehne JH (1982) Habituation and sensitization of startle reflexes elicited electrically from the brainstem. *Science* 218:688–690.

Bibliography

- De Franceschi G, Vivattanasarn T, Saleem AB, Solomon SG (2016) Vision Guides Selection of Freeze or Flight Defense Strategies in Mice. *Curr Biol* 26:2150–2154.
- Dedic N, Chen A, Deussing JM (2017) The CRF Family of Neuropeptides and their Receptors - Mediators of the Central Stress Response. *Curr Mol Pharmacol* 11:4–31.
- Degroot A, Köfalvi A, Wade MR, Davis RJ, Rodrigues RJ, Rebola N, Cunha RA, Nomikos GG (2006) CB1 receptor antagonism increases hippocampal acetylcholine release: Site and mechanism of action. *Mol Pharmacol* 70:1236–1245.
- Deussing JM, Chen A (2018) The corticotropin-releasing factor family: Physiology of the stress response. *Physiol Rev* 98:2225–2286.
- Devane WA, Hanuš L, Breuer A, Pertwee RG, Stevenson LA, Griffin G, Gibson D, Mandelbaum A, Etinger A, Mechoulam R (1992) Isolation and structure of a brain constituent that binds to the cannabinoid receptor. *Science* 258:1946–1949.
- Devigny C, Perez-Balderas F, Hoogeland B, Cuboni S, Wachtel R, Mauch CP, Webb KJ, Deussing JM, Hausch F (2011) Biomimetic screening of class-B G protein-coupled receptors. *J Am Chem Soc* 133:8927–8933.
- Di Marzo V, Bifulco M, De Petrocellis L (2004) The endocannabinoid system and its therapeutic exploitation. *Nat Rev Drug Discov* 3:771–784.
- Dielenberg RA, Hunt GE, McGregor IS (2001) “When a rat smells a cat”: The distribution of Fos immunoreactivity in rat brain following exposure to a predatory odor. *Neuroscience* 104:1085–1097.
- Dinh TP, Carpenter D, Leslie FM, Freund TF, Katona I, Sensi SL, Kathuria S, Piomelli D (2002) Brain monoglyceride lipase participating in endocannabinoid inactivation. *Proc Natl Acad Sci U S A* 99:10819–10824.
- Dirks A, Groenink L, Schipholt MI, Van Der Gugten J, Hijzen TH, Geyer MA, Olivier B (2002) Reduced startle reactivity and plasticity in transgenic mice overexpressing corticotropin-releasing hormone. *Biol Psychiatry* 51:583–590.
- Docherty NM (2005) Cognitive Impairments and Disordered Speech in Schizophrenia: Thought Disorder, Disorganization, and Communication Failure Perspectives. *J Abnorm Psychol* 114:269–278.
- Engelhardt KA, Fuchs E, Schwarting RKW, Wöhr M (2017) Effects of amphetamine on pro-social ultrasonic communication in juvenile rats: Implications for mania models. *Eur Neuropsychopharmacol* 27:261–273.
- Esposito A, Demeurisse G, Alberti B, Fabbro F (1999) Complete mutism after midbrain periaqueductal gray lesion. *Neuroreport* 10:681–685.
- Evans DA, Stempel AV, Vale R, Ruehle S, Lefler Y, Branco T (2018) A synaptic threshold mechanism for computing escape decisions. *Nature* 558:590–594.
- Fanselow MS, Lester LS (1988) A functional behavioristic approach to aversively motivated behavior: Predatory imminence as a determinant of the topography of defensive behavior. In: *Evolution and learning*, pp 185–212. Hillsdale, NJ, US: Lawrence Erlbaum Associates, Inc.
- Fardin V, Oliveras JL, Besson JM (1984) A reinvestigation of the analgesic effects induced by stimulation of the periaqueductal gray matter in the rat. II. Differential characteristics of the analgesia induced by ventral and dorsal PAG stimulation. *Brain Res* 306:125–139.
- Fendt M, Koch M, Schnitzler HU (1994) Lesions of the central gray block the sensitization of the acoustic startle response in rats. *Brain Res* 661:163–173.
- Feyissa DD, Aher YD, Engidawork E, Höger H, Lubec G, Korz V (2017) Individual Differences in Male Rats in a Behavioral Test Battery: A Multivariate Statistical Approach. *Front Behav Neurosci* 11.
- Fine J, Bartolucci G, Ginsberg G, Szatmari P (1991) The Use of Intonation to Communicate in Pervasive Developmental Disorders. *J Child Psychol Psychiatry* 32:771–782.
- Fish EW, Sekinda M, Ferrari PF, Dirks A, Miczek KA (2000) Distress vocalizations in maternally separated mouse pups: Modulation via 5-HT1(A), 5-HT1(B) and GABA(A) receptors. *Psychopharmacology (Berl)* 149:277–285.
- Fitch T (2006) Production of Vocalizations in Mammals. In: *Encyclopedia of Language & Linguistics*, pp 115–121. Elsevier.

Bibliography

- Fitch WT, Neubauer J, Herzel H (2002) Calls out of chaos: The adaptive significance of nonlinear phenomena in mammalian vocal production. *Anim Behav* 63:407–418.
- Flandreau E, Risbrough V, Lu A, Ableitner M, Geyer MA, Holsboer F, Deussing JM (2015) Cell type-specific modifications of corticotropin-releasing factor (CRF) and its type 1 receptor (CRF1) on startle behavior and sensorimotor gating. *Psychoneuroendocrinology* 53:16–28.
- Frühholz S, Dietziker J, Staib M, Trost W (2021) Neurocognitive processing efficiency for discriminating human non-alarm rather than alarm scream calls. *PLoS Biol* 19:1–30.
- Gao SC, Wei YC, Wang SR, Xu XH (2019) Medial Preoptic Area Modulates Courtship Ultrasonic Vocalization in Adult Male Mice. *Neurosci Bull* 35:697–708.
- Gaoni Y, Mechoulam R (1964) Isolation, Structure, and Partial Synthesis of an Active Constituent of Hashish. *J Am Chem Soc* 86:1646–1647.
- Genewsky AJ (2017) Ethobehavioral strategies for the study of fear in mice.
- Genewsky AJ, Wotjak CT (2017) The endocannabinoid system differentially regulates escape behavior in mice. *Front Behav Neurosci* 11:1–7.
- Gjerstad JK, Lightman SL, Spiga F (2018) Role of glucocorticoid negative feedback in the regulation of HPA axis pulsatility. *Stress* 21:403.
- Goetz RR, Klein DF, Gorman JM (1996) Symptoms essential to the experience of sodium lactate-induced panic. *Neuropsychopharmacology* 14:355–366.
- Gray JA, McNaughton N (1996) The neuropsychology of anxiety: reprise. *Nebr Symp Motiv* 43:61–134.
- Gross CT, Canteras NS (2012) The many paths to fear. *Nat Rev Neurosci* 13:651–658.
- Grossen NE, Kelley MJ (1972) Species-specific behavior and acquisition of avoidance behavior in rats. *J Comp Physiol Psychol* 81:307–310.
- Guilloux JP, Seney M, Edgar N, Sibille E (2011) Integrated behavioral z-scoring increases the sensitivity and reliability of behavioral phenotyping in mice: Relevance to emotionality and sex. *J Neurosci Methods* 197:21–31.
- Hage SR, Nieder A (2016) Dual Neural Network Model for the Evolution of Speech and Language. *Trends Neurosci* 39:813–829.
- Hammerschmidt K, Radyushkin K, Ehrenreich H, Fischer J (2009) Female mice respond to male ultrasonic “songs” with approach behaviour. *Biol Lett* 5:589–592.
- Hammerschmidt K, Whelan G, Eichele G, Fischer J (2015) Mice lacking the cerebral cortex develop normal song: Insights into the foundations of vocal learning. *Sci Rep* 5:1–7.
- Hammond S, O’Shea M (2007) Escape flight initiation in the fly. *J Comp Physiol A Neuroethol Sensory, Neural, Behav Physiol* 193:471–476.
- Handley SL, Mithani S (1984) Effects of alpha-adrenoceptor agonists and antagonists in a maze-exploration model of ‘fear’-motivated behaviour. *Naunyn Schmiedebergs Arch Pharmacol* 327:1–5.
- Häring M, Kaiser N, Monory K, Lutz B (2011) Circuit specific functions of cannabinoid CB1 receptor in the balance of investigatory drive and exploration. *PLoS One* 6:e26617.
- Häring M, Marsicano G, Lutz B, Monory K (2007) Identification of the cannabinoid receptor type 1 in serotonergic cells of raphe nuclei in mice. *Neuroscience* 146:1212–1219.
- Hatcher JP, Jones DNC, Rogers DC, Hatcher PD, Reavill C, Hagan JJ, Hunter AJ (2001) Development of SHIRPA to characterise the phenotype of gene-targeted mice. *Behav Brain Res* 125:43–47.
- Heckman JJ, Proville R, Heckman GJ, Azarfar A, Celikel T, Englitz B (2017) High-precision spatial localization of mouse vocalizations during social interaction. *Sci Rep* 7:1–16.
- Heffner RS, Heffner HE (1985) Hearing range of the domestic cat. *Hear Res* 19:85–88.
- Heinz DE, Genewsky A, Wotjak CT (2017) Enhanced anandamide signaling reduces flight behavior elicited by an approaching robo-beetle. *Neuropharmacology* 126:233–241.

Bibliography

- Heinz DE, Schöttle VA, Nemcova P, Binder FP, Ebert T, Domschke K, Wotjak CT (2021) Exploratory drive, fear, and anxiety are dissociable and independent components in foraging mice. *Transl Psychiatry* 11:318.
- Herkenham M, Lynn A, Johnson M, Melvin L, de Costa B, Rice K (1991) Characterization and localization of cannabinoid receptors in rat brain: a quantitative in vitro autoradiographic study. *J Neurosci* 11:563–583.
- Herkenham M, Lynn AB, Little MD, Johnson MR, Melvin LS, De Costa BR, Rice KC (1990) Cannabinoid receptor localization in brain. *Proc Natl Acad Sci U S A* 87:1932–1936.
- Hettema JM, Neale MC, Kendler KS (2001) A Review and Meta-Analysis of the Genetic Epidemiology of Anxiety Disorders. *Am J Psychiatry* 158:1568–1578.
- Hill MN, Bierer LM, Makotkine I, Golier JA, Galea S, McEwen BS, Hillard CJ, Yehuda R (2013) Reductions in circulating endocannabinoid levels in individuals with post-traumatic stress disorder following exposure to the world trade center attacks. *Psychoneuroendocrinology* 38:2952–2961.
- Hill MN, Campolongo P, Yehuda R, Patel S (2018) Integrating Endocannabinoid Signaling and Cannabinoids into the Biology and Treatment of Posttraumatic Stress Disorder. *Neuropsychopharmacology* 43:80–102.
- Hitchcock JM, Davis M (1991) Efferent Pathway of the Amygdala Involved in Conditioned Fear as Measured With the Fear-Potentiated Startle Paradigm. *Behav Neurosci* 105:826–842.
- Hofer MA, Shair H (1978) Ultrasonic vocalization during social interaction and isolation in 2-week-old rats. *Dev Psychobiol* 11:495–504.
- Hoffman HS, Ison JR (1980) Reflex modification in the domain of startle: I. Some empirical findings and their implications for how the nervous system processes sensory input. *Psychol Rev* 87:175–189.
- Holstege G, Subramanian HH (2016) Two different motor systems are needed to generate human speech. *J Comp Neurol* 524:1558–1577.
- Holy TE, Guo Z (2005) Ultrasonic songs of male mice. *PLoS Biol* 3:1–10.
- Hopkins DA, Holstege G (1978) Amygdaloid projections to the mesencephalon, pons and medulla oblongata in the cat. *Exp Brain Res* 32:529–547.
- Howlett AC, Barth F, Bonner TI, Cabral G, Casellas P, Devane WA, Felder CC, Herkenham M, Mackie K, Martin BR, Mechoulam R, Pertwee RG (2002) International Union of Pharmacology. XXVII. Classification of cannabinoid receptors. *Pharmacol Rev* 54:161–202.
- Hunsperger R (1963) Comportements affectifs provoqués par la stimulation électrique du tronc cérébral et du cerveau antérieur. *J Physiol* 55:45–97.
- Hunter DJ (2005) Gene–environment interactions in human diseases. *Nat Rev Genet* 6:287–298.
- Ishikawa A (2013) Wild mice as bountiful resources of novel genetic variants for quantitative traits. *Curr Genomics* 14:225–229.
- Jacob W, Yassouridis A, Marsicano G, Monory K, Lutz B, Wotjak CT (2009) Endocannabinoids render exploratory behaviour largely independent of the test aversiveness: Role of glutamatergic transmission. *Genes, Brain Behav* 8:685–698.
- Johnson AM, Ciucci MR, Russell JA, Hammer MJ, Connor NP (2010) Ultrasonic output from the excised rat larynx. *J Acoust Soc Am* 128:EL75–EL79.
- Joung JK, Sander JD (2013) TALENs: a widely applicable technology for targeted genome editing. *Nat Rev Mol Cell Biol* 14:49–55.
- Jürgens U (2002) Neural pathways underlying vocal control. *Neurosci Biobehav Rev* 26:235–258.
- Jürgens U (2009) The Neural Control of Vocalization in Mammals: A Review. *J Voice* 23:1–10.
- Jürgens U, Hage SR (2007) On the role of the reticular formation in vocal pattern generation. *Behav Brain Res* 182:308–314.
- Jürgens U, Pratt R (1979) Role of the periaqueductal grey in vocal expression of emotion. *Brain Res* 167:367–378.

Bibliography

- Kaltwasser MT (1990) Acoustic signaling in the black rat (*Rattus rattus*). *J Comp Psychol* 104:227–232.
- Kaltwasser MT (1991) Acoustic startle induced ultrasonic vocalization in the rat: a novel animal model of anxiety? *Behav Brain Res* 43:133–137.
- Kamprath K, Plendl W, Marsicano G, Deussing JM, Wurst W, Lutz B, Wotjak CT (2009) Endocannabinoids mediate acute fear adaptation via glutamatergic neurons independently of corticotropin-releasing hormone signaling. *Genes, Brain Behav* 8:203–211.
- Kathuria S, Gaetani S, Fegley D, Valiño F, Duranti A, Tontini A, Mor M, Tarzia G, La Rana G, Calignano A, Giustino A, Tattoli M, Palmery M, Cuomo V, Piomelli D (2003) Modulation of anxiety through blockade of anandamide hydrolysis. *Nat Med* 9:76–81.
- Katona I, Sperlách B, Sík A, Káfalvi A, Vizi ES, Mackie K, Freund TF (1999) Presynaptically located CB1 cannabinoid receptors regulate GABA release from axon terminals of specific hippocampal interneurons. *J Neurosci* 19:4544–4558.
- Katona I, Urbán GM, Wallace M, Ledent C, Jung KM, Piomelli D, Mackie K, Freund TF (2006) Molecular composition of the endocannabinoid system at glutamatergic synapses. *J Neurosci* 26:5628–5637.
- Kawashima T, Kitamura K, Suzuki K, Nonaka M, Kamijo S, Takemoto-Kimura S, Kano M, Okuno H, Ohki K, Bito H (2013) Functional labeling of neurons and their projections using the synthetic activity-dependent promoter E-SARE. *Nat Methods* 10:889–895.
- Keay KA, Bandler R (2001) Parallel circuits mediating distinct emotional coping reactions to different types of stress. *Neurosci Biobehav Rev* 25:669–678.
- Kielar A, Deschamps T, Jokel R, Meltzer JA (2018) Abnormal language-related oscillatory responses in primary progressive aphasia. *NeuroImage Clin* 18:560–574.
- Kimchi T, Xu J, Dulac C (2007) A functional circuit underlying male sexual behaviour in the female mouse brain. *Nature* 448:1009–1014.
- King SM, Dykeman C, Redgrave P, Dean P (1992) Use of a distracting task to obtain defensive head movements to looming visual stimuli by human adults in a laboratory setting. *Perception* 21:245–259.
- Knutson B, Burgdorf J, Panksepp J (1999) Anticipation of play elicits high-frequency ultrasonic vocalizations in young rats. *J Comp Psychol* 112:65–73.
- Koch M (1999) The neurobiology of startle. *Prog Neurobiol* 59:107–128.
- Koenen KC et al. (2017) Posttraumatic stress disorder in the World Mental Health Surveys. *Psychol Med* 47:2260–2274.
- Kono J, Konno K, Talukder AH, Fuse T, Abe M, Uchida K, Horio S, Sakimura K, Watanabe M, Itoi K (2017) Distribution of corticotropin-releasing factor neurons in the mouse brain: a study using corticotropin-releasing factor-modified yellow fluorescent protein knock-in mouse. *Brain Struct Funct* 222:1705–1732.
- Kreitzer AC, Regehr WG (2001) Retrograde inhibition of presynaptic calcium influx by endogenous cannabinoids at excitatory synapses onto Purkinje cells. *Neuron* 29:717–727.
- Krömer SA, Keßler MS, Milfay D, Birg IN, Bunck M, Czibere L, Panhuysen M, Pütz B, Deussing JM, Holsboer F, Landgraf R, Turck CW (2005) Identification of glyoxalase-I as a protein marker in a mouse model of extremes in trait anxiety. *J Neurosci* 25:4375–4384.
- Kubota Y, Shigematsu N, Karube F, Sekigawa A, Kato S, Yamaguchi N, Hirai Y, Morishima M, Kawaguchi Y (2011) Selective coexpression of multiple chemical markers defines discrete populations of neocortical gabaergic neurons. *Cereb Cortex* 21:1803–1817.
- Lafenêtre P, Chaouloff F, Marsicano G (2009) Bidirectional regulation of novelty-induced behavioral inhibition by the endocannabinoid system. *Neuropharmacology* 57:715–721.
- Lahvis GP, Allewa E, Scattoni ML (2011) Translating mouse vocalizations: Prosody and frequency modulation. *Genes, Brain Behav* 10:4–16.
- Lang PJ, Bradley MM, Cuthbert BN (1990) Emotion, Attention, and the Startle Reflex. *Psychol Rev* 97:377–395.
- Li Y, Zeng J, Zhang J, Yue C, Zhong W, Liu Z, Feng Q, Luo M (2018) Hypothalamic Circuits for Predation and Evasion. *Neuron* 97:911–924.e5.

Bibliography

- Liang KC, Melia KR, Miserendino MJD, Falls WA, Campeau S, Davis M (1992) Corticotropin-releasing factor: Long-lasting facilitation of the acoustic startle reflex. *J Neurosci* 12:2303–2312.
- Lingle S, Wyman MT, Kotrba R, Teichroeb LJ, Romanow CA (2012) What makes a cry a cry? A review of infant distress vocalizations. *Curr Zool* 58:698–726.
- Llorente-Berzal A, Terzian ALB, Di Marzo V, Micalle V, Viveros MP, Wotjak CT (2015) 2-AG promotes the expression of conditioned fear via cannabinoid receptor type 1 on GABAergic neurons. *Psychopharmacology (Berl)* 232:2811–2825.
- Long JZ, Li W, Booker L, Burston JJ, Kinsey SG, Schlosburg JE, Pavón FJ, Serrano AM, Selley DE, Parsons LH, Lichtman AH, Cravatt BF (2009) Selective blockade of 2-arachidonoylglycerol hydrolysis produces cannabinoid behavioral effects. *Nat Chem Biol* 5:37–44.
- Lu A, Steiner MA, Whittle N, Vogl AM, Walser SM, Ableitner M, Refojo D, Ekker M, Rubenstein JL, Stalla GK, Singewald N, Holsboer F, Wotjak CT, Wurst W, Deussing JM (2008) Conditional mouse mutants highlight mechanisms of corticotropin-releasing hormone effects on stress-coping behavior. *Mol Psychiatry* 13:1028–1042.
- Lutz B, Marsicano G, Maldonado R, Hillard CJ (2015) The endocannabinoid system in guarding against fear, anxiety and stress. *Nat Rev Neurosci* 16:705–718.
- Maejima T, Hashimoto K, Yoshida T, Aiba A, Kano M (2001) Presynaptic inhibition caused by retrograde signal from metabotropic glutamate to cannabinoid receptors. *Neuron* 31:463–475.
- Maggio JC, Whitney G (1985) Ultrasonic vocalizing by adult female mice (*Mus musculus*). *J Comp Psychol* 99:420–436.
- Mahrt E, Agarwal A, Perkel D, Portfors C, Elemans CPH (2016) Mice produce ultrasonic vocalizations by intra-laryngeal planar impinging jets. *Curr Biol* 26:R880–R881.
- Malkemper EP, Topinka V, Burda H (2015) A behavioral audiogram of the red fox (*Vulpes vulpes*). *Hear Res* 320:30–37.
- Marchand JE, Hagino N (1983) Afferents to the periaqueductal gray in the rat. A horseradish peroxidase study. *Neuroscience* 9:95–106.
- Marsicano G, Lutz B (1999) Expression of the cannabinoid receptor CB1 in distinct neuronal subpopulations in the adult mouse forebrain. *Eur J Neurosci* 11:4213–4225.
- Martinez RCR, Carvalho-Netto EF, Amaral VCS, Nunes-de-Souza RL, Canteras NS (2008) Investigation of the hypothalamic defensive system in the mouse. *Behav Brain Res* 192:185–190.
- Masterton B, Heffner H (1980) Hearing in Glires: Domestic rabbit, cotton rat, feral house mouse, and kangaroo rat. *J Acoust Soc Am* 68:1584–1599.
- Mathis A, Mamidanna P, Cury KM, Abe T, Murthy VN, Mathis MW, Bethge M (2018) DeepLabCut: markerless pose estimation of user-defined body parts with deep learning. *Nat Neurosci* 2018 219 21:1281–1289.
- Matsuda LA, Lolait SJ, Brownstein MJ, Young AC, Bonner TI (1990) Structure of a cannabinoid receptor and functional expression of the cloned cDNA. *Nature* 346:561–564.
- McIlwain KL, Merriweather MY, Yuva-Paylor LA, Paylor R (2001) The use of behavioral test batteries: Effects of training history. *Physiol Behav* 73:705–717.
- McNaughton N, Corr PJ (2004) A two-dimensional neuropsychology of defense: Fear/anxiety and defensive distance. *Neurosci Biobehav Rev* 28:285–305.
- McPartland JM, Agrawal J, Gleeson D, Heasman K, Glass M (2006) Cannabinoid receptors in invertebrates. *J Evol Biol* 19:366–373.
- Mechoulam R, Ben-Shabat S, Hanus L, Ligumsky M, Kaminski NE, Schatz AR, Gopher A, Almog S, Martin BR, Compton DR, Pertwee RG, Griffin G, Bayewitch M, Barg J, Vogel Z (1995) Identification of an endogenous 2-monoglyceride, present in canine gut, that binds to cannabinoid receptors. *Biochem Pharmacol* 50:83–90.
- Meier SM, Deckert J (2019) Genetics of Anxiety Disorders. *Curr Psychiatry Rep* 21:16.
- Merali Z, Du L, Hrdina P, Palkovits M, Faludi G, Poulter MO, Anisman H (2004) Dysregulation in the Suicide

Bibliography

- Brain: mRNA Expression of Corticotropin-Releasing Hormone Receptors and GABAA Receptor Subunits in Frontal Cortical Brain Region. *J Neurosci* 24:1478–1485.
- Merikangas KR, Swanson SA (2010) Comorbidity in Anxiety Disorders. In: Behavioral Neurobiology of Anxiety and Its Treatment (Stein MB, Steckler T, eds), pp 37–59. Berlin, Heidelberg: Springer Berlin Heidelberg.
- Metna-Laurent M, Soria-Gómez E, Verrier D, Conforzi M, Jégo P, Lafenêtre P, Marsicano G (2012) Bimodal control of fear-coping strategies by CB 1 cannabinoid receptors. *J Neurosci* 32:7109–7118.
- Micale V, Marzo V Di, Sulcova A, Wotjak CT, Drago F (2013) Endocannabinoid system and mood disorders: Priming a target for new therapies. *Pharmacol Ther* 138:18–37.
- Michael V, Goffinet J, Pearson J, Wang F, Tschida K, Mooney R (2020) Circuit and synaptic organization of forebrain-to-midbrain pathways that promote and suppress vocalization. *Elife* 9:1–29.
- Miczek KA, Van Der Poel AM (1991) Long Ultrasonic Calls in Male Rats Following Mating, Defeat and Aversive Stimulation: Frequency Modulation and Bout Structure. *Behaviour* 119:127–142.
- Mobbs D, Adolphs R, Fanselow MS, Barrett LF, LeDoux JE, Ressler K, Tye KM (2019) Viewpoints: Approaches to defining and investigating fear. *Nat Neurosci* 22:1205–1216.
- Mobbs D, Headley DB, Ding W, Dayan P (2020) Space, Time, and Fear: Survival Computations along Defensive Circuits. *Trends Cogn Sci* 24:228–241.
- Mobbs D, Marchant JL, Hassabis D, Seymour B, Tan G, Gray M, Petrovic P, Dolan RJ, Frith CD (2009) From threat to fear: The neural organization of defensive fear systems in humans. *J Neurosci* 29:12236–12243.
- Mobbs D, Petrovic P, Marchant JL, Hassabis D, Weiskopf N, Seymour B, Dolan RJ, Frith CD (2007) When fear is near: Threat imminence elicits prefrontal-periaqueductal gray shifts in humans. *Science* 317:1079–1083.
- Moles A, Costantini F, Garbugino L, Zanettini C, D'Amato FR (2007) Ultrasonic vocalizations emitted during dyadic interactions in female mice: A possible index of sociability? *Behav Brain Res* 182:223–230.
- Momose K, Inui A, Asakawa A, Ueno N, Nakajima M, Fujimiya M, Kasuga M (1999) Intracerebroventricularly administered corticotropin-releasing factor inhibits food intake and produces anxiety-like behaviour at very low doses in mice. *Diabetes, Obes Metab* 1:281–284.
- Moreira PS, Almeida PR, Leite-Almeida H, Sousa N, Costa P (2016) Impact of Chronic Stress Protocols in Learning and Memory in Rodents: Systematic Review and Meta-Analysis Pant AB, ed. *PLoS One* 11:e0163245.
- Munro S, Thomas KL, Abu-Shaar M (1993) Molecular characterization of a peripheral receptor for cannabinoids. *Nature* 365:61–65.
- Musolf K, Penn DJ (2012) Ultrasonic vocalizations in house mice: A cryptic mode of acoustic communication. *Evol House Mouse* 9780521760:253–277.
- Nashold BS, Wilson WP, Slaughter DG (1969) Sensations Evoked by Stimulation in the Midbrain of Man. *J Neurosurg* 30:14–24.
- Nemeroff CB, Owens MJ, Bissette G, Andorn AC, Stanley M (1988) Reduced Corticotropin Releasing Factor Binding Sites in the Frontal Cortex of Suicide Victims. *Arch Gen Psychiatry* 45:577–579.
- Nemeroff CB, Widerlöv E, Bissette G, Walléus H, Karlsson I, Eklund K, Kilts CD, Loosen PT, Vale W (1984) Elevated concentrations of CSF corticotropin-releasing factor-like immunoreactivity in depressed patients. *Science* 226:1342–1344.
- Neumeister A, Normandin MD, Pietrzak RH, Piomelli D, Zheng MQ, Gujarró-Anton A, Potenza MN, Bailey CR, Lin SF, Najafzadeh S, Ropchan J, Henry S, Corsi-Travali S, Carson RE, Huang Y (2013) Elevated brain cannabinoid CB 1 receptor availability in post-traumatic stress disorder: A positron emission tomography study. *Mol Psychiatry* 18:1034–1040.
- Neunuebel JP, Taylor AL, Arthur BJ, Roian Egnor SE (2015) Female mice ultrasonically interact with males during courtship displays. *Elife* 4:1–24.
- Nieder A, Mooney R (2020) The neurobiology of innate, volitional and learned vocalizations in mammals and birds. *Philos Trans R Soc B Biol Sci* 375.
- Nyby J (1983) Ultrasonic vocalizations during sex behavior of male house mice (*Mus musculus*): A description.

Bibliography

- Behav Neural Biol 39:128–134.
- Nyby J, Dizinno GA, Whitney G (1976) Social status and ultrasonic vocalizations of male mice. *Behav Biol* 18:285–289.
- Ohno-Shosaku T, Maejima T, Kano M (2001) Endogenous cannabinoids mediate retrograde signals from depolarized postsynaptic neurons to presynaptic terminals. *Neuron* 29:729–738.
- Okamoto Y, Morishita J, Tsuboi K, Tonai T, Ueda N (2004) Molecular Characterization of a Phospholipase D Generating Anandamide and Its Congeners. *J Biol Chem* 279:5298–5305.
- Otowa T et al. (2016) Meta-analysis of genome-wide association studies of anxiety disorders. *Mol Psychiatry* 21:1391–1399.
- Panksepp J, Burgdorf J (2000) 50-kHz chirping (laughter?) in response to conditioned and unconditioned tickle-induced reward in rats: Effects of social housing and genetic variables. *Behav Brain Res* 115:25–38.
- Panksepp JB, Jochman KA, Kim JU, Koy JJ, Wilson ED, Chen Q, Wilson CR, Lahvis GP (2007) Affiliative Behavior, Ultrasonic Communication and Social Reward Are Influenced by Genetic Variation in Adolescent Mice Crusio W, ed. *PLoS One* 2:e351.
- Peng J, Long B, Yuan J, Peng X, Ni H, Li X, Gong H, Luo Q, Li A (2017) A quantitative analysis of the distribution of CRH neurons in whole mouse brain. *Front Neuroanat* 11:1–12.
- Pereira AG, Moita MA (2016) Is there anybody out there? Neural circuits of threat detection in vertebrates. *Curr Opin Neurobiol* 41:179–187.
- Pérez-Escudero A, Vicente-Page J, Hinz RC, Arganda S, de Polavieja GG (2014) idTracker: tracking individuals in a group by automatic identification of unmarked animals. *Nat Methods* 2014 117 11:743–748.
- Perusini JN, Fanselow MS (2015) Neurobehavioral perspectives on the distinction between fear and anxiety. *Learn Mem* 22:417–425.
- Petrie GN, Nastase AS, Aukema RJ, Hill MN (2021) Endocannabinoids, cannabinoids and the regulation of anxiety. *Neuropharmacology* 195:108626.
- Pilz PK, Schnitzler HU, Menne D (1987) Acoustic startle threshold of the albino rat (*Rattus norvegicus*). *J Comp Psychol* 101:67–72.
- Pilz PKD, Caeser M, Ostwald J (1988) Comparative threshold studies of the acoustic pinna, jaw and startle reflex in the rat. *Physiol Behav* 43:411–415.
- Pomerantz SM, Nunez AA, Jay Bean N (1983) Female behavior is affected by male ultrasonic vocalizations in house mice. *Physiol Behav* 31:91–96.
- Poole TB, Morgan HDR (1976) Social and territorial behaviour of laboratory mice (*Mus musculus* L.) in small complex areas. *Anim Behav* 24:476–480.
- Portfors C V., Perkel DJ (2014) The role of ultrasonic vocalizations in mouse communication. *Curr Opin Neurobiol* 28:115–120.
- Purves KL, Coleman JRI, Meier SM, Rayner C, Davis KAS, Bækvad-hansen RCM, Børghlum AD, Cho SW, Deckert JJ, Gaspar HA, Bybjerg-grauholm J, Hettema JM, Hotopf M, Hougaard D, Hübel C, Kan C, Mcintosh AM, Mors O (2020) A major role for common genetic variation in anxiety disorders. *Mol Psychiatry*:3292–3303.
- Raadsheer C, Hoogendijk JG, Lucassen PJ, Tilders FJH, Ph D, Swaab DF (1995) Corticotropin-releasing hormone mRNA levels in the paraventricular nucleus of patients with Alzheimer's disease and depression. *Am J Psychiatry* 152:1372–1376.
- Rainnie DG, Fernhout BJH, Shinnick-Gallagher P (1992) Differential actions of corticotropin releasing factor on basolateral and central amygdaloid neurones, in vitro. *J Pharmacol Exp Ther* 263:846–858.
- Refojo D et al. (2011) Glutamatergic and dopaminergic neurons mediate anxiogenic and anxiolytic effects of CRHR1. *Science* 333:1903–1907.
- Rey AA, Purrio M, Viveros MP, Lutz B (2012) Biphasic effects of cannabinoids in anxiety responses: CB1 and GABA B receptors in the balance of gabaergic and glutamatergic neurotransmission.

Bibliography

- Neuropsychopharmacology 37:2624–2634.
- Riebe CJ, Pamplona F, Kamprath K, Wotjak CT (2012) Fear relief-toward a new conceptual frame work and what endocannabinoids gotta do with it. *Neuroscience* 204:159–185.
- Riede T, Borgard HL, Pasch B (2017) Laryngeal airway reconstruction indicates that rodent ultrasonic vocalizations are produced by an edge-tone mechanism. *R Soc Open Sci* 4.
- Rimpel J, Geyer D, Hopf HC (1982) Changes in the blink responses to combined trigeminal, acoustic and visual repetitive stimulation, studied in the human subject. *Electroencephalogr Clin Neurophysiol* 54:552–560.
- Rinaldi-Carmona M, Barth F, Héaulme M, Shire D, Calandra B, Congy C, Martinez S, Maruani J, Néliat G, Caput D, Ferrara P, Soubrié P, Brelière JC, Le Fur G (1994) SR141716A, a potent and selective antagonist of the brain cannabinoid receptor. *FEBS Lett* 350:240–244.
- Rizvi TA, Ennis M, Behbehani MM, Shipley MT (1991) Connections between the central nucleus of the amygdala and the midbrain periaqueductal gray: Topography and reciprocity. *J Comp Neurol* 303:121–131.
- Roberts LH (1975a) The rodent ultrasound production mechanism. *Ultrasonics* 13:83–88.
- Roberts LH (1975b) The functional anatomy of the rodent larynx in relation to audible and ultrasonic cry production. *Zool J Linn Soc* 56:255–264.
- Rogers DC, Jones DNC, Nelson PR, Jones CM, Quilter CA, Robinson TL, Hagan JJ (1999) Use of SHIRPA and discriminant analysis to characterise marked differences in the behavioural phenotype of six inbred mouse strains. *Behav Brain Res* 105:207–217.
- Roper TJ, Polioudakis E (1977) The Behaviour of Mongolian Gerbils in a Semi-Natural Environment, With Special Reference To Ventral Marking, Dominance and Sociability. *Behaviour* 61:207–236.
- Ruehle S, Remmers F, Romo-Parra H, Massa F, Wickert M, Wörtge S, Häring M, Kaiser N, Marsicano G, Pape HC, Lutz B (2013) Cannabinoid CB1 receptor in dorsal telencephalic glutamatergic neurons: Distinctive sufficiency for hippocampus-dependent and amygdala-dependent synaptic and behavioral functions. *J Neurosci* 33:10264–10277.
- Ruehle S, Rey AA, Remmers F, Lutz B (2012) The endocannabinoid system in anxiety, fear memory and habituation. *J Psychopharmacol* 26:23–39.
- Russell WMS, Burch RL (1959) *The Principles of Humane Experimental Technique*. Methuen.
- Sadananda M, Wöhr M, Schwarting RKW (2008) Playback of 22-kHz and 50-kHz ultrasonic vocalizations induces differential c-fos expression in rat brain. *Neurosci Lett* 435:17–23.
- Sangiamo DT, Warren MR, Neunuebel JP (2020) Ultrasonic signals associated with different types of social behavior of mice. *Nat Neurosci* 23:411–422.
- Scattoni ML, Gandhi SU, Ricceri L, Crawley JN (2008) Unusual repertoire of vocalizations in the BTBR T+tf/J mouse model of autism. *PLoS One* 3:48–52.
- Schenberg LC, Bittencourt AS, Sudré ECM, Vargas LC (2001) Modeling panic attacks. *Neurosci Biobehav Rev* 25:647–659.
- Schiff W, Caviness JA, Gibson JJ (1962) Persistent fear responses in rhesus monkeys to the optical stimulus of “looming.” *Science* 136:982–983.
- Schwartz JW, Engelberg JWM, Gouzoules H (2020) Was That a Scream? Listener Agreement and Major Distinguishing Acoustic Features. *J Nonverbal Behav* 44:233–252.
- Sewell GD (1970) Ultrasonic Communication in Rodents. *Nature* 227:410–410.
- Sharma S, Powers A, Bradley B, Ressler KJ (2016) Gene × Environment Determinants of Stress- and Anxiety-Related Disorders. *Annu Rev Psychol* 67:239–261.
- Shemesh Y et al. (2016) Ucn3 and CRF-R2 in the medial amygdala regulate complex social dynamics. *Nat Neurosci* 19:1489–1496.
- Shemesh Y, Sztainberg Y, Forkosh O, Shlapobersky T, Chen A, Schneidman E (2013) High-order social interactions in groups of mice. *Elife* 2013:1–19.

Bibliography

- Shen M, Piser TM, Seybold VS, Thayer SA (1996) Cannabinoid receptor agonists inhibit glutamatergic synaptic transmission in rat hippocampal cultures. *J Neurosci* 16:4322–4334.
- Shriberg LD, Paul R, McSweeney JL, Klin A, Cohen DJ, Volkmar FR (2001) Speech and Prosody Characteristics of Adolescents and Adults With High-Functioning Autism and Asperger Syndrome. *J Speech, Lang Hear Res* 44:1097–1115.
- Silva BA, Gross CT, Gräff J (2016) The neural circuits of innate fear: Detection, integration, action, and memorization. *Learn Mem* 23:544–555.
- Silva BA, Mattucci C, Krzywkowski P, Murana E, Illarionova A, Grinevich V, Canteras NS, Ragozzino D, Gross CT (2013) Independent hypothalamic circuits for social and predator fear. *Nat Neurosci* 16:1731–1733.
- Silva C, McNaughton N (2019) Are periaqueductal gray and dorsal raphe the foundation of appetitive and aversive control? A comprehensive review. *Prog Neurobiol* 177:33–72.
- Skultety FM (1962) Experimental Mutism in Dogs. *Arch Neurol* 6:235–241.
- Stenzel-Poore MP, Heinrichs SC, Rivest S, Koob GF, Vale WW (1994) Overproduction of corticotropin-releasing factor in transgenic mice: A genetic model of anxiogenic behavior. *J Neurosci* 14:2579–2584.
- Stukalin Y, Einat H (2019) Analyzing test batteries in animal models of psychopathology with multivariate analysis of variance (MANOVA): One possible approach to increase external validity. *Pharmacol Biochem Behav* 178:51–55.
- Sugiura T, Kondo S, Sukagawa A, Nakane S, Shinoda A, Itoh K, Yamashita A, Waku K (1995) 2-arachidonoylglycerol: A possible endogenous cannabinoid receptor ligand in brain. *Biochem Biophys Res Commun* 215:89–97.
- Swerdlow NR, Geyer MA, Vale WW, Koob GF (1986) Corticotropin-releasing factor potentiates acoustic startle in rats: Blockade by chlordiazepoxide. *Psychopharmacology (Berl)* 88:147–152.
- Takahashi A, Yap JJ, Bohager DZ, Faccidomo S, Clayton T, Cook JM, Miczek KA (2009) Glutamatergic and GABAergic modulations of ultrasonic vocalizations during maternal separation distress in mouse pups. *Psychopharmacology (Berl)* 204:61–71.
- Temizer I, Donovan JC, Baier H, Semmelhack JL (2015) A Visual Pathway for Looming-Evoked Escape in Larval Zebrafish. *Curr Biol* 25:1823–1834.
- Thomas DA, Barfield RJ (1985) Ultrasonic vocalization of the female rat (*Rattus norvegicus*) during mating. *Anim Behav* 33:720–725.
- Toth M, Gresack JE, Bangasser DA, Plona Z, Valentino RJ, Flandreau EI, Mansuy IM, Merlo-Pich E, Geyer MA, Risbrough VB (2014) Forebrain-specific CRF overproduction during development is sufficient to induce enduring anxiety and startle abnormalities in adult mice. *Neuropsychopharmacology* 39:1409–1419.
- Tovote P, Esposito MS, Botta P, Chaudun F, Fadok JP, Markovic M, Wolff SBE, Ramakrishnan C, Fenno L, Deisseroth K, Herry C, Arber S, Lüthi A (2016) Midbrain circuits for defensive behaviour. *Nature* 534:206–212.
- Traynor K (2007) Torisel approved for advanced kidney cancer. *Am J Heal Pharm* 64:1460.
- Tschida K, Michael V, Takatoh J, Han BX, Zhao S, Sakurai K, Mooney R, Wang F (2019) A Specialized Neural Circuit Gates Social Vocalizations in the Mouse. *Neuron* 103:459-472.e4.
- Vale R, Evans DA, Branco T (2017) Rapid Spatial Learning Controls Instinctive Defensive Behavior in Mice. *Curr Biol* 27:1342–1349.
- Vale W, Spiess J, Rivier C, Rivier J (1982) Characterization of a 41-residue ovine hypothalamic peptide that stimulates secretion of corticotropin and β -endorphin. *Obstet Gynecol Surv* 37:334.
- Van Daele DJ, Cassell MD (2009) Multiple forebrain systems converge on motor neurons innervating the thyroarytenoid muscle. *Neuroscience* 162:501–524.
- Van Segbroeck M, Knoll AT, Levitt P, Narayanan S (2017) MUPET—Mouse Ultrasonic Profile ExTraction: A Signal Processing Tool for Rapid and Unsupervised Analysis of Ultrasonic Vocalizations. *Neuron* 94:465-485.e5.

Bibliography

- Vivian JA, Farrell WJ, Sapperstein SB, Miczek KA (1994) Diazepam withdrawal: effects of diazepam and gepirone on acoustic startle-induced 22 kHz ultrasonic vocalizations. *Psychopharmacology (Berl)* 114:101–108.
- Vogel AP, Tsanas A, Scattoni ML (2019) Quantifying ultrasonic mouse vocalizations using acoustic analysis in a supervised statistical machine learning framework. *Sci Rep* 9:8100.
- Voikar V, Vasar E, Rauvala H (2004) Behavioral alterations induced by repeated testing in C57BL/6J and 129S2/Sv mice: implications for phenotyping screens. *Genes, Brain Behav* 3:27–38.
- Vrana SR, Spence EL, Lang PJ (1988) The Startle Probe Response: A New Measure of Emotion? *J Abnorm Psychol* 97:487–491.
- Walker DL, Davis M (1997) Anxiogenic effects of high illumination levels assessed with the acoustic startle response in rats. *Biol Psychiatry* 42:461–471.
- Wang H, Yang H, Shivalila CS, Dawlaty MM, Cheng AW, Zhang F, Jaenisch R (2013) One-Step Generation of Mice Carrying Mutations in Multiple Genes by CRISPR/Cas-Mediated Genome Engineering. *Cell* 153:910–918.
- Wang L, Chen IZ, Lin D (2015) Collateral Pathways from the Ventromedial Hypothalamus Mediate Defensive Behaviors. *Neuron* 85:1344–1358.
- Wang W, Schuette PJ, Nagai J, Tobias BC, Fernando FM, Ji S, de Lima MAX, La-Vu MQ, Maesta-Pereira S, Chakerian M, Leonard SJ, Lin L, Severino AL, Cahill CM, Canteras NS, Khakh BS, Kao JC, Adhikari A (2021) Coordination of escape and spatial navigation circuits orchestrates versatile flight from threats. *Neuron* 109:1848-1860.e8.
- Warren MR, Clein RS, Spurrier MS, Roth ED, Neunuebel JP (2020) Ultrashort-range, high-frequency communication by female mice shapes social interactions. *Sci Rep* 10:1–14.
- Weissbrod A, Shapiro A, Vasserman G, Edry L, Dayan M, Yitzhaky A, Hertzberg L, Feinerman O, Kimchi T (2013) Automated long-term tracking and social behavioural phenotyping of animal colonies within a semi-natural environment. *Nat Commun* 2013 41 4:1–10.
- White NR, Cagiano R, Moises AU, Barfield RJ (1990) Changes in mating vocalizations over the ejaculatory series in rats (*Rattus norvegicus*). *J Comp Psychol* 104:255–262.
- Whitney G, Alpern M, Dizinno G, Horowitz G (1974) Female odors evoke ultrasounds from male mice. *Anim Learn Behav* 2:13–18.
- Wilson RI, Nicoll RA (2001) Endogenous cannabinoids mediate retrograde signalling at hippocampal synapses. *Nature* 410:588–592.
- Wittchen HU, Jacobi F, Rehm J, Gustavsson A, Svensson M, Jönsson B, Olesen J, Allgulander C, Alonso J, Faravelli C, Fratiglioni L, Jennum P, Lieb R, Maercker A, Os J Van, Preisig M, Salvador-carulla L (2011) The size and burden of mental disorders and other disorders of the brain in Europe 2010. *Eur Neuropsychopharmacol* 21:655–679.
- Wöhr M (2014) Ultrasonic vocalizations in Shank mouse models for autism spectrum disorders: Detailed spectrographic analyses and developmental profiles. *Neurosci Biobehav Rev* 43:199–212.
- Wöhr M (2021) Measuring mania-like elevated mood through amphetamine-induced 50-kHz ultrasonic vocalizations in rats. *Br J Pharmacol*:1–19.
- Wöhr M, Schwarting RKW (2007) Ultrasonic communication in rats: Can playback of 50-kHz calls induce approach behavior? *PLoS One* 2.
- Wöhr M, Schwarting RKW (2008) Ultrasonic calling during fear conditioning in the rat: no evidence for an audience effect. *Anim Behav* 76:749–760.
- Wöhr M, Schwarting RKW (2013) Affective communication in rodents: Ultrasonic vocalizations as a tool for research on emotion and motivation. *Cell Tissue Res* 354:81–97.
- Wolf A, Bauer B, Abner EL, Ashkenazy-Frolinger T, Hartz AMS (2016) A Comprehensive Behavioral Test Battery to Assess Learning and Memory in 129S6/Tg2576 Mice. *PLoS One* 11:e0147733.
- World Health Organization (1992) *The ICD-10 Classification of Mental and Behavioural Disorders: Clinical Descriptions And Diagnostic Guidelines*, 10th ed. Geneva: World Health Organization.

Bibliography

- Wu LQ, Niu YQ, Yang J, Wang SR (2005) Tectal neurons signal impending collision of looming objects in the pigeon. *Eur J Neurosci* 22:2325–2331.
- Xiong XR, Liang F, Zingg B, Ji XY, Ibrahim LA, Tao HW, Zhang LI (2015) Auditory cortex controls sound-driven innate defense behaviour through corticofugal projections to inferior colliculus. *Nat Commun* 6:1–12.
- Ydenberg RC, Dill LM (1986) The Economics of Fleeing from Predators. In: *Advances in the Study of Behavior*, pp 229–249.
- Yeomans JS, Frankland PW (1995) The acoustic startle reflex: neurons and connections. *Brain Res Rev* 21:301–314.
- Yilmaz M, Meister M (2013) Rapid innate defensive responses of mice to looming visual stimuli. *Curr Biol* 23:2011–2015.
- Zhang SP, Bandler R, Carrive P (1990) Flight and immobility evoked by excitatory amino acid microinjection within distinct parts of the subtentorial midbrain periaqueductal gray of the cat. *Brain Res* 520:73–82.
- Zilkha N, Sofer Y, Beny Y, Kimchi T (2016) From classic ethology to modern neuroethology: overcoming the three biases in social behavior research. *Curr Opin Neurobiol* 38:96–108.
- Zippelius HM, Schleidt WM (1956) Ultraschall-Laute bei jungen Mäusen. *Naturwissenschaften* 43:502.
- Zuberbühler K (2000) Causal knowledge of predators' behaviour in wild Diana monkeys. *Anim Behav* 59:209–220.

Acknowledgements

The past years have been an exciting journey and I have sincerely enjoyed my time at the Max Planck Institute of Psychiatry.

First of all, I would like to thank my two supervisors PD Dr. Carsten T. Wotjak and Prof. Alon Chen. They gave me the opportunity to pursue my interests, allowed me to work independently yet provided guidance and support throughout all the years. I am very grateful for everything I learned from you.

I would like to thank Prof. Laura Busse and Dr. Jan M. Deussing for being part of my Thesis Advisory Committee. Thank you for joining the meetings and for your support.

In addition, I want to thank my former and present colleagues of the research groups of Neuronal Plasticity and the MPS & WIS Laboratory for Experimental Neuropsychiatry and Behavioral Neurogenetics. Working together, sharing an office, enjoying retreats far and near made long days seem shorter and brought lots of joy throughout the years. I am particularly grateful for working together with Daniel on whose support I could always rely on and who never hesitated to help.

I would like to thank the lab technicians, especially Andrea Ressle, Andrea Parl, and Claudia Kühne who patiently helped with all my questions.

For countless lunch breaks that covered any topic but science, I want to thank my friend Lea. Thank you for always listening and cheering me up in times of struggle.

Most importantly, I owe my deepest gratitude to my loving parents who always believed in me, supported me unconditionally at all times and made me a decent person. I am deeply grateful to my husband Benoît for his encouragement, contagious calmness, and his love. Thank you for always being by my side.